Dynamic modelling of charges for thermostatic expansion valves

Langmaack, Lasse Nicolai

Publication date:
2007

Document Version
Publisher's PDF, also known as Version of record

Dynamic modelling of charges for thermostatic expansion valves

Ph.D.-Thesis

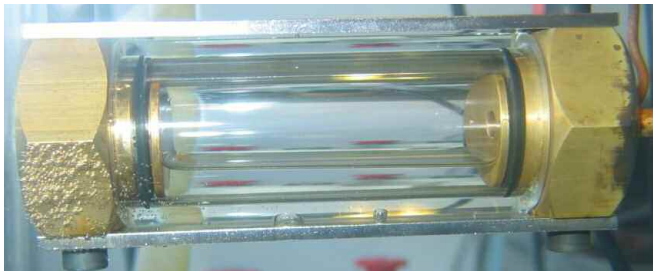

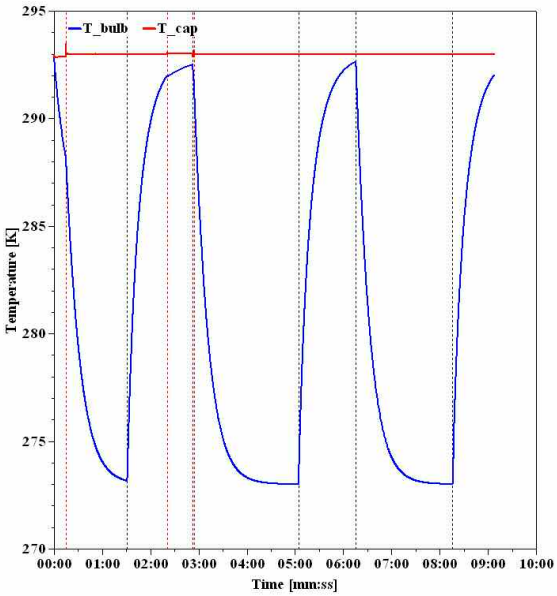

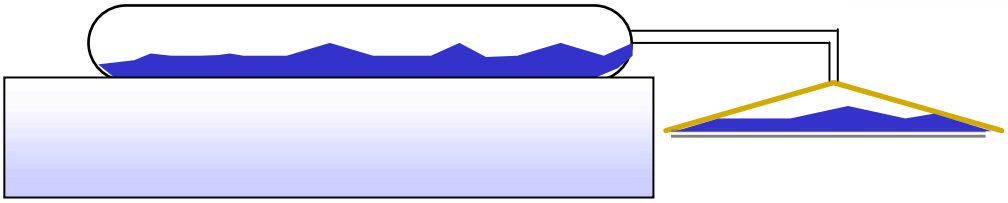

by

Lasse Nicolai Langmaack

December 2006

Department of Mechanical Engineering,
Technical University of Denmark

Automatic Controls laboratories,
Danfoss A/S

Preface

The work presented in this thesis has been carried out under the Industrial Ph.D. program supported by the Danish Ministry of Science and Technology. The thesis is submitted as a partial fulfilment of the requirements for the Ph.D. degree at DTU, Technical University of Denmark.

The study was carried out at the Department of Mechanical Engineering at DTU and the Automatic controls laboratories at Danfoss A/S.

Associate professor Ph.D. Hans Jørgen Høgaard Knudsen, Professor Ph.D. Henrik Carlsen, Ph.D. Arne Jakobsen, senior director of R&D Ph.D. Torben Funder-Kristensen, Consultant B.Sc. Jørgen Trelle Pedersen and Research engineer M.Sc. Lars Mou Jessen have supervised the work.

Besides the group of supervisors, I would also like to thank Consultant Ph.D. Peter Johannesen and Laboratory manager M.Sc. Jesper Schmidt Hansen and the rest of the AC-RL department for their input and ideas.

Especially, I want to thank Refrigeration specialist Ph.D. Bjarne Dindler Rasmussen for his valuable help and support in all phases of the project.

Lasse Nicolai Langmaack
Nordborg, December 2006

Abstract

The subject for this Ph.D. thesis is the dynamic modelling of charges for thermostatic expansion valves. This type of valve has been used to reduce energy consumption for refrigeration and air conditioning systems for many years.
With rising energy prices and increasing focus on environmental issues, a wider use of products that decrease energy consumption is expected. Traditionally, Danfoss has delivered thermostatic expansion valves for the installer market. In that market the products are as universal as possible, and preferably they have an adjustment option that makes it possible to customize the valve for the specific application. In the recent years, Danfoss has entered the OEM (Original Equipment Manufacturer) market. The costumers in that market are the manufacturers of mass produced systems. For Danfoss this means that the application of the valve is already known upon production. This opens the possibility of optimizing the valve for the application together with the customer. In order to get full benefit of this optimization, it is important to understand the valve in every detail.
This thesis covers two critical issues about charges for thermostatic expansion valves. One issue is the heat transfer between the evaporator outlet and the bulb. The other issue is the concentration of a condensable charge media and a non-condensable gas in the capsule and bulb respectively. In the thesis the phenomena are described physically and modelled. The model is verified by experimental results.
The thermal contact between the bulb and the evaporator outlet is crucial for the dynamics of the thermostatic expansion valve. In the simulation model the geometry and material parameters for evaporator outlet, bulb and the strap have to be input. By giving the parts in the model initial temperatures, the heat fluxes and the final temperatures can be evaluated over time. The model uses also thermal contact resistances as input. They have been evaluated by a combination of experimental tests and a finite element model which is also described in the thesis.
In the type of charges that consists of both condensable charge media and a non-condensable gas it is relevant to look at the concentrations of these in the capsule and in the bulb under different temperature conditions. It has been shown experimentally that a reorganization of the concentrations can result in different pressures at the same temperatures. The simulation model calculates the system consisting of capsule, bulb and capillary tube as two volumes where the capillary tube allows a mass transport in between. The simulation model results correlate well with experimental results and gives a physical explanation of the phenomena seen in tests made prior to this project.
The two models are merged into one model for the dynamic simulation of charges for thermostatic expansion valves.
This model can be used in the R&D department of Danfoss Automatic Controls for evaluating different charges and designs of capsule and bulb. The perspective is to implement the model in a full valve model which again can be implemented in a model for a refrigeration system. This would give the possibility to optimize the system even before prototyping.

Resume (dansk)

Emnet for denne Ph.D. afhandling er dynamisk modellering af fyldninger til termostatiske ekspansionsventiler. Denne type ventil har været brugt til at energioptimere køle- og airconditionanlæg i mange år. Set i lyset af stigende energipriser og øget fokus på miljø forventes, at endnu flere anlæg vil anvende produkter, der bidrager til energibesparelser. Traditionelt set har Danfoss leveret termostatiske ekspansionsventiler til grossister, der så igen har solgt dem videre til installatører. På det marked skal produkterne være så universelle som muligt og gerne have en indstillingsmulighed, så det kan tilpasses den aktuelle applikation. I de senere år har Danfoss fået del i OEM (Original Equipment Manufacturer) markedet. Her er kunderne producenter af masseproducerede anlæg. Det betyder, at Danfoss allerede ved produktion af ventilen kender applikationen den skal indgå i. Dette åbner muligheden for, sammen med kunden, at optimere ventilen til den pågældende applikation. For at få fuldt udbytte af denne optimering er det nødvendigt at forstå alle detaljer i ventilen.

Denne afhandling tager nogle kendte problemområder omkring fyldningen til termostatiske ekspansionsventiler i behandling. Områderne er dels varmeovergangen mellem føler og fordamper og dels den indre koncentrationsfordeling af fyldemedie og en ikke kondenserbar gas mellem kapsel og føler. I afhandlingen kortlægges hvilke fænomener der optræder. Disse beskrives og modelleres, og simuleringsmodellen verificeres ved eksperimentelle forsøg.

Følerens kontakt med fordamperen er afgørende for ventilens dynamik. I simuleringsmodellen opgives geometri og materialeparametre for både afgangsrør af fordamper, føler og det spændebånd, føleren er monteret med. Ved så at angive starttemperaturer for alle dele, kan varmestrømme og dermed sluttemperaturer bestemmes over tid. I modellen indgår også termiske kontaktmodstande der er blevet fundet ved hjælp af forsøg og en finite element model, der også er beskrevet i afhandlingen.

I den type fyldninger, hvor der både er et kondenserbart fyldemedie og en ikke-kondenserbar gas tilstede, er det relevant at se på fordelingen af disse i henholdsvis kapsel og føler under forskellige temperaturpåvirkninger. Det har været vist eksperimentelt, at en omfordeling vil kunne give anledning til et forskelligt trykniveau ved given temperaturpåvirkning. Simuleringsmodellen beregner systemet bestående af kapsel, føler og kapillarrør som to beholdere, hvor kapillarrøret tillader massetransport imellem de to. Simuleringsmodellen korrelerer med eksperimentelle forsøg og giver en fysisk forklaring på de fænomener, der blev set i forsøg før projektet startede.

De to modeller er blevet samlet til en samlet model til dynamisk simulering af fyldninger til termostatiske ekspansionsventiler.

Modellen kan bruges i Danfoss' udviklingsafdeling til udvælgelse af forskellige fyldninger og kapsel/føler design. På sigt skal modellen implementeres i en samlet ventilmodel som så igen vil kunne indgå i en model for hele kølekredsen for derved at kunne optimere køleanlæg allerede før prototypestadiet.

Nomenclature

Abbreviations

COP	Coefficient of performance
EXV	Electronic expansion valve
MOP	Maximum operating pressure
SEER	Seasonal energy efficiency ratio
TXV	Thermostatic expansion valve
UNI charge	Universal charge

Symbols

The symbols are listed in alphabetic order:

A	Diaphragm area	$[m^2]$
a	Area of nozzle seat	$[m^2]$
a,b,c	Constants in (A-1)	
$A_{b\_free\_amb}$	Part of bulb surface that is free to ambient	$[m^2]$
A_{b_i}	Inner area of bulb	$[m^2]$
A_{b_strap}	Contact area between strap and bulb	$[m^2]$
$A_{capillary}$	Inner Area of capillary tube	$[m^2]$
A_{et_i}	Inner area of evaporator tube	$[m^2]$
A_{et_strap}	Contact area between strap and evaporator tube	$[m^2]$
A_{strap_cross}	Cross sectional area of strap	$[m^2]$
B	$\frac{b \cdot P_c}{R \cdot T_c}$	
c_p	Heat capacity at constant pressure	[kJ/kg/K]
c_v	Heat capacity at constant volume	[kJ/kg/K]
c	Flow coefficient	[-]
fg	Liquid phase volume ratio	[-]
F_s	Spring force	[N]
F	Paramter required in (A-8)	
f	Fugacity	[Pa]
H	Enthalpy	[KJ]
h	specific enthalpy	[kJ/kg]
h_{air}	Heat transfer coefficient between air and bulb/strap	$[W/m^2/K]$
h_{charge}	Heat transfer coefficient between charge and bulb	$[W/m^2/K]$

h_{ref}	Heat transfer coefficient between refrigerant and evaporator tube	[W/m^2/K]
l_{bulb}	length of the cylindrical part of the bulb	[m]
L_{strap_free}	Length of free strap	[m]
L_{t_strap}	thickness of strap	[m]
M	Parameter for fin calculation	
m	Mass	[kg]
$\dot{m}$	Mass flux	[kg/s]
P	Power supplied to the compressor	[W]
P	Pressure	[kPa]
P_b	Bulb pressure	[Pa]
$P_{cross;MOP}$	Pressure of cross MOP charge	[kPa]
$P_{cross;UNI}$	Pressure of cross UNI charge	[kPa]
P_e	Evaporator pressure	[Pa]
P_{MOP}	Pressure of MOP charge	[kPa]
$P_{parallel;UNI}$	Pressure of parallel UNI charge	[kPa]
P_{pd}	Pressure drop across the valve (Pe-Pc)	[Pa]
P_{sat}	Saturation pressure of refrigerant	[kPa]
P_{strap}	Perimeter of strap	[m]
P_{sum}	Pressure of refrigerant side of diaphragm (Psat+Fs/A)	[kPa]
P_{sum}	Pressure of refrigerant side of diaphragm (Psat+Fs/A)	[kPa]
r_b,	Outer radius of the bulb	[m]
r_{b_i}	Inner radius of the bulb	[m]
$R_{c\_2\text{-}3}$	Contact resistance between evaporator tube /strap	[W/K]
$R_{c\_2\text{-}6}$	Contact resistance between evaporator tube/bulb	[W/K]
$R_{c\_5\text{-}6}$	Contact resistance between strap/bulb	[W/K]
r_{et}	Outer radius of the evaporator tube	[m]
r_{et_i}	Inner radius of the evaporator tube	[m]
R_{uni}	Universal gas constant	[kJ/kmol/K]
S	Entropy	[KJ]
$strap_{width}$	width of strap	[m]
t	Time	[sec]

t	Thickness of interface layer	[m]
T	Temperature	[K]
U	Internal energy	[kJ]
u	Specific internal energy	[kJ/kg]
V	Volume	[m^3]
v	Specific volume	[m^3/kg]
v	Specific volume	[m^3/kmol]
x	Mass fraction (Quality)	[-]
y	Response	
ρ	Density	[kg/m^3]
$\dot{Q}_e$	Heat transfer rate in the evaporator	[W]
$\dot{Q}_c$	Heat transfer rate in the condenser	[W]
$\dot{W}$	Work done by the compressor	[W]
$\dot{Q}$	Heat flux	[W]
Z	Compressibility $\frac{P \cdot v}{R \cdot T}$	[-]

Greek letters

α	Temperature function (A-8)	
β	angle used for calculations	[deg]
ζ_c	Paramter required in (A-5)-(A-7)	
λ_{strap}	Heat conductivity of strap	[W/K/m]
ξ	Binary interaction coefficient	[-]
τ	Time constant	[sec]
Ω_a, Ω_b, Ω_c	Constants used in (A-2)-(A-4)	

Subscripts:

Bulb	bulb
Cap	capsule
GAS	Gas/vapour
GASMIX	Mix of nitrogen and vapour
LIQ	Liquid
N2	Nitrogen
ref	Reference
ref	Refrigerant
Tot	Total

If there is more than one subscript, they are divided by an underscore (_).
Ex: h_{cap_GASMIX}: Specific enthalpy of the mixture of Nitrogen and vapour in the capsule.

How to read this thesis

The thesis is build up in three main parts.

Chapter 1 to chapter 5 introduces thermostatic expansion valves and the different charges for them. Readers who are familiar with the details of thermostatic expansion valves can skip chapters 2, 3 and 4 and jump right to the summation in chapter 5.
Chapter 6 to chapter 9 contain the description of the models developed through this work.
Chapter 10 sums up the conclusions and states some ideas for further work on this subject.

Appendix A gives a description of how the calculation of properties of mixture charges can be implemented.

The source code for the model can be found in the enclosure

References are stated in the text in the format [X], where X refers to the number in the reference list on page 74.

Contents

Preface……...……...……..……....i
Abstract……...……...……..…ii
Resume (dansk)……..……..…iii
Nomenclature……..…….……..…..iv
How to read this thesis……...…….....……..…..vii

1 Introduction **1**
1.1 Motivation 1
1.2 Process of the work 2
1.3 Prior work 2
1.4 Contribution of this work 3
2 The vapour compression refrigeration cycle **4**
2.1 The expansion device 6
2.2 The expansion valve 7
2.3 The thermostatic expansion valve 8
3 The dynamics of thermostatic expansion valves **11**
3.1 The time constant 11
4 Charges for thermostatic expansion valves **13**
4.1 Categorization of condensable gas charges 14
4.2 Type of charge media 15
4.3 Amount of charge 16
4.4 Thermal ballast brick 17
4.5 Nitrogen 18
4.6 Tolerances on the charge pressure 18
5 Charges for thermostatic expansion valves **20**
6 Dynamic model for charges for TXV's **21**
6.1 Strategy of modeling 21
6.2 Purpose of the model 21
7 Heat transfer from refrigerant to charge **24**
7.1 Modelling 24
7.2 Determination of thermal contact resistances 31
7.3 Experimental measurements 31
7.4 Experimental evaluation of the temperature distribution in empty bulb 33
7.5 Test series: 33
7.6 The Finite element model 34
7.7 Test on charged bulbs 40
7.8 The analytical model 42
7.9 Conclusion on the model for the heat transfer from the system refrigerant to the charge 46
8 Charge model **47**
8.1 Basic two-bulb system 47
8.2 The static model 48
8.3 The dynamic model 51
8.4 New test setup 57
8.5 Dynamic behaviour of charges in cyclic tests 59

8.6 Explanation of observations 61
8.7 Discussion on the use of the model 68
9 The merged model 70
9.1 Using the merged model 71
10 Conclusions and suggestions for future work 73
10.1 Suggestions for future work 73
11 References 74

Appendix:

A. Mixture charge……..……...……..75

Enclosure:

Printed source code for WinDali model

1 Introduction

1.1 Motivation

Thermostatic expansion valves have been used for refrigeration for more than 60 years. Today's designs are somewhat different than the early designs. Nevertheless, the main principle of the way the valve works has not been changed. The sudden need for a better model of this rather mature product has to be found in a shift of market situation for Danfoss.

The costumers of Danfoss have traditionally been wholesalers who deliver parts for the installers. Given the fact that the exact application for the valve is not known upon production, the products need to be as universal as possible. For TXV's this means that they need to be applicable for a large temperature range and that they need adjustment screws that make it possible for the installer to get a satisfactory plant efficiency and stability.
In the recent years, Danfoss has also entered the OEM (Original Equipment Manufacturer) market. Delivering components (TXV's) to this marked differs significantly from the above described situation. OEM costumers are the manufactures of refrigeration and air conditioning systems. They produce standard systems on a large scale and Danfoss becomes a sub supplier for their production.
Because all valves delivered are mounted on similar systems, the valves do not need to be universal anymore. They need to be customised for the specific system. The customization covers a large range of aspects. Part of this customization is also an optimization of the valve on the system where the optimum setting of the valve is found. And due to the high degree of optimization on these systems only small variations in setting are tolerated.

The measure for the energy consumption for Air conditioning systems for residential households in the USA is expressed as the Seasonal energy efficiency ratio (SEER) according to ARI standard [2].

The test procedure required to calculate SEER implies four tests, where three of them are steady state tests under different conditions while one of them is a cyclic on/off test. Therefore the air conditioning system and thereby also the TXV has to have the right dynamics.

Effectively January 1st 2006, the legal requirement for American residential air conditioning systems was changed from SEER 10 to SEER 13. This implies that the same cooling capacity now has to be generated with only 75 % energy consumption.

The reason for starting this project was the realization that some behaviours of the valve that have been shown experimentally cannot be explained by static calculations. It was the firm belief that a dynamic model would be able to answer some of these questions.

In order to investigate these phenomena a dynamic model had to be set up.

The short formulation of the motivation:

Motivation:
In order to meet the costumers demand for smaller tolerances on the factory setting of TXV's, a dynamic model which takes even small variations in the bulb pressure into account is needed.

1.2 Process of the work

When this work started three years ago, the problem description was to model the charge of the TXV dynamically. The problem was that strange observations had been made during various tests. These observations correlated somehow with problems observed on refrigeration systems. Therefore it was interesting to clarify the physics behind the observations. There were of course some hypothesises, but the different physical phenomena still remained unnamed and unquantified.

Therefore this work has been a constantly iterating process like shown in Figure 1-1.

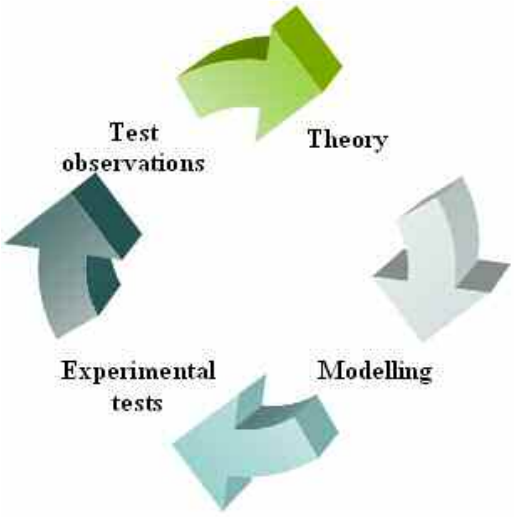

Figure 1-1: Cycle of work progress

The process was started with some observations made during experimental tests that originally were made to obtain other results. Next step was to analyze what was observed and try to make some simple models in order to see whether this could explain the observations or not. If not, there were several possibilities. One could be that the model was not good enough. Another reason could be that the theory behind the model did not describe the observations i.e. the hypothesis could be rejected and a new had to be stated. A third reason could be that more phenomena and their interaction had to be included. Any of these reasons invite for more tests, where the tests get more and more specific in order to capture the phenomena.

Once having a breakthrough with correlation between isolated phenomena and specific models, these need to be combined and interactions need to be taken into account. The results in this thesis reflect a lot of iterations and more could be made in order to improve the model even further.

1.3 Prior work

Although thermostatic expansion valves have been used in refrigeration for more than 60 years, only little focus has been on the modelling and simulation of them. The thermostatic expansion valve is normally described in a very simple way which also works for most cases. However there have been several attempts to model the thermostatic expansion valve in more detail [1], [9] and [3]. Most of the work has been focused on the mechanics and the flow part of the valve. All of them have assumed that

the bulb pressure is given by the saturation pressure corresponding to temperature at the evaporator outlet, which is also a good approximation for the static situation.

James & James [6] investigated the dynamic temperature response of the charge for a TXV. They developed a mathematical model for a TXV. Part of that model describes the dynamics of the charge. Unfortunately they did not take the strap with which the bulb is mounted into account.
Conde & Suter [3] made an interesting observation during their test of TXV's. They experienced something they call a hysteresis in the charge. Their oberservations correlate well with the observations made in this work. The model presented in this thesis will clarify the physics behind this phenomenon.

1.4 Contribution of this work

The work presented in this thesis deals only with the charge of the thermostatic expansion valve. All publications known to the author have assumed the charge pressure to be given by the saturation pressure at the temperature of the charge, which in most cases also was the main idea. However, years of experience have taught Danfoss that this correlation can be disorganized by different phenomena inside the charged part of the valve.
This work presents a dynamic model for the charge of a thermostatic expansion valve that takes these phenomena into account.

2 The vapour compression refrigeration cycle

The TXV is a component used in the vapour compression cycle. The purpose of the vapour- compression cycle is basically to move heat from a low temperature to a high temperature.
The cycle is based on the fact that fluids absorb heat while they evaporate and reject heat while they condense.
Therefore the vapour- compression cycle contains two heat exchangers, one for the evaporation (evaporator) and one for the condensation (condenser). Figure 2-1 shows how the components of the cycle are connected, while Figure 2-2 shows the cycle in the logP-h diagram. The numbers with circle around indicate state points that will be referred to in the following text.

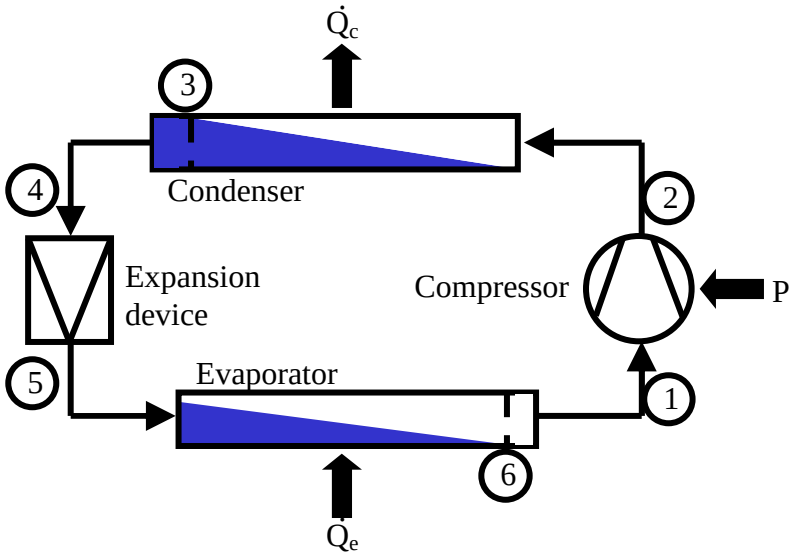

Figure 2-1: The basic vapour- compression cycle (components)

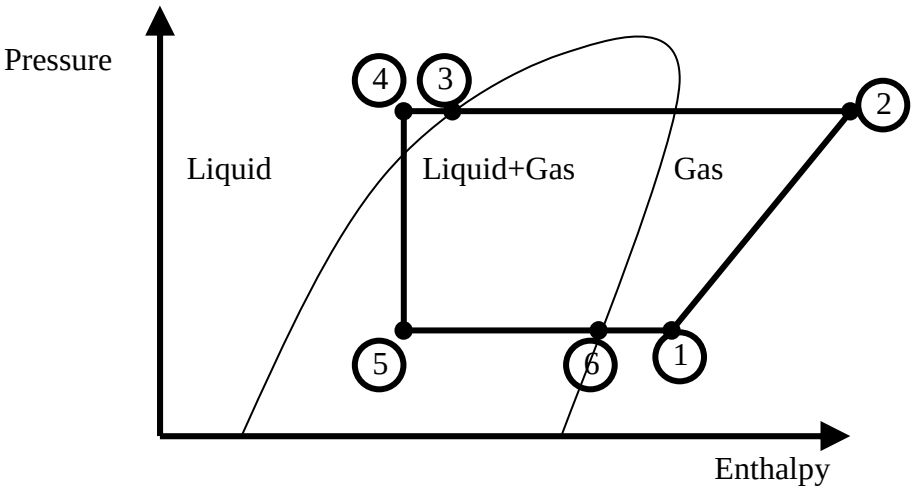

Figure 2-2: The basic vapour- compression cycle (logP-h diagram)

For heat pumps the main idea is to use the heat rejected in the condenser ($\dot{Q}_c$). For refrigeration applications the focus is on the heat transferred to the evaporator ($\dot{Q}_e$). In order to compress gas, work has to be done. The energy for thos work comes from the power supplied to the compressor (P).

In order to establish a heat transfer rate into the evaporator, the evaporation temperature has to be lower than its surroundings. In the same way, the condensation temperature has to be higher than its surroundings. This means that the temperature of the condenser has to be higher than the temperature of the evaporator.
The temperatures at which gasses condense (dew point) and liquids evaporate (bubble point) are substance specific and depend solely on the pressure. Therefore the temperature of the evaporator and the condenser can be controlled by controlling the pressure in the evaporator and condenser. In order to maintain a higher pressure in the condenser than in the evaporator, two more components are needed. The compressor is placed at the outlet of the evaporator, while an expansion device is placed at the inlet of the evaporator. These four components form the basic vapour compression cycle. The following will explain the purpose of each of them.

Compressor:
Starting at the state point 1 in Figure 2-1 the refrigerant just left the evaporator in the state of a slightly superheated gas at low pressure. The compressor takes in the gas, compresses it, and discharges it at a higher pressure. In the ideal case the compression is an reversible and adiabatic process. The work done by the compressor therefore becomes

$$\dot{W} = \dot{m} \cdot (h_2 - h_1) \qquad \textbf{(2-1)}$$

Where $\dot{m}$ is the mass flow rate and h1 and h2 are the specific enthalpies at state point 1 and 2, respectively.
The function of the compressor ensures a constant flow of refrigerant through the system. The compressor is also the part of the system where energy has to be applied/ converted.

Condenser:
After compression, the refrigerant has a high pressure (State point 2) and is pushed through the condenser. While it is flowing trough the condenser, the refrigerant rejects heat $\dot{Q}_c$ to the surroundings and condenses.

$$\dot{Q}_c = \dot{m} \cdot (h_2 - h_4) \qquad \textbf{(2-2)}$$

The last part of the condenser (State point 3-4) is used for subcooling i.e. cooling the liquid below its bubble point temperature. The subcooling ensures that no vapour will leave the condenser. Vapour flowing to the expansion valve will disturb the flow through the expansion device and thereby decrease the flow rate through the evaporator.

Expansion device:
When reaching the expansion device the refrigerant is a liquid at high pressure (State point 4). While it flows through the expansion device, the pressure is dropped from the

condensing pressure to the evaporation pressure. This pressure drop causes the refrigerant to start evaporating.

Evaporator:
Right after the expansion device (State point 5) the refrigerant enters the evaporator, where the evaporation takes place. The heat needed for evaporation is taken from the evaporators surroundings.

$$\dot{Q}_e = \dot{m} \cdot (h_1 - h_6) \quad \textbf{(2-3)}$$

The last part of the evaporator (State point 6-1) is used for superheating i.e. heating the vapour above the dew point temperature. The superheating ensures that no liquid will leave the evaporator and thereby enter the compressor where it can cause damage. On important point here is that the heat transfer coefficient is smaller for gas than for liquid. Therefore efficiency decreases with increasing superheat. A balance has to be found between evaporator stability (high superheat) and system efficiency (low superheat) and the compressor needs to be protected against liquid in the inlet (high superheat).
The superheated gas at low pressure is now ready for compression again and the cycle repeats itself.
The challenge using this cycle is to get the needed refrigeration capacity (refrigeration system) or heating capacity (heat pump) using a minimum of power.

Coefficient of performance (COP):
A measure for the energy efficiency of a refrigeration cycle is the COP. For a cooling system the COP can be expressed as

$$COP = \frac{\dot{Q}_e}{\dot{W}} \quad \textbf{(2-4)}$$

Improving COP implies therefore either increase cooling capacity or decrease the compression work.

2.1 The expansion device

After presenting the basic vapour compression cycle, focus will now be on the expansion device in the vapour compression cycle used for refrigeration.
It becomes clear that the function of the expansion device is to create a pressure drop to initiate the evaporation. Another important point is that, given the pressure drop across it, the flow area of the expansion device determines the mass flow into the evaporator.
Depending on application more or less complex expansion devices can be used. Using one or the other becomes a question of operating cost and production cost. For very small systems like household refrigerators the expansion device is a capillary tube, whereas for larger systems an expansion valve is preferred.
The difference is that the capillary tube has a fixed area for refrigerant flow, while the expansion valve can vary the opening area.
For energy efficient systems the flow into the evaporator has to be adjusted in such way that the leaving vapour has the desired degree of superheat. Increasing the flow rate will decrease the superheat and thereby increase the risk of getting liquid in the compressor and decrease the stability of the evaporator. Decreasing the flow rate will increase

superheat and decrease the efficiency. Having a fixed flow rate during variable load will cause a varying superheat and thereby varying efficiency. This loss of efficiency has to be held against the lower production price of the refrigeration system.

2.2 The expansion valve

Having made the choice to use an expansion valve, the next choice is right ahead. Expansion valves can either be operated manually, electronically (EXV) or thermostatic (TXV). The input signals are the same for all of them, namely the evaporation pressure and the temperature of the vapour leaving the evaporator. In order to operate the manual valve, someone has to read the temperature and the pressure on gauges and change the setting of the valve by turning a handle. The EXV gets the input from sensors, calculates an opening degree and uses a small motor to adjust the opening area of the valve. The TXV converts the temperature signal to a pressure and the opening degree of the valve is determined by equilibrium of pressures. The working principle of the thermostatic expansion valve will be explained in every detail in the following chapters.
The choice between TXV and EXV has to be made from application to application. In general it can be mentioned that a TXV solution is cheaper than the EXV solution. On the other hand the EXV is more flexible regarding changing of characteristics. EXV solutions are common on large systems whereas TXV solutions are more common on small systems.
On many systems TXV and EXV will perform equal, which does not justify the rather expensive EXV solution. Nevertheless there are systems where EXV's perform better than TXV's and the extra cost can be justified. But for the time being, there are no indicators that the market will turn its back on TXV's. From today's point of view there are reasons to believe that TXV's will stay in the market on a large scale.

The model presented in this thesis covers the temperature-pressure converter of the TXV.

2.3 The thermostatic expansion valve

The basic components of the TXV are shown on Figure 2-3.

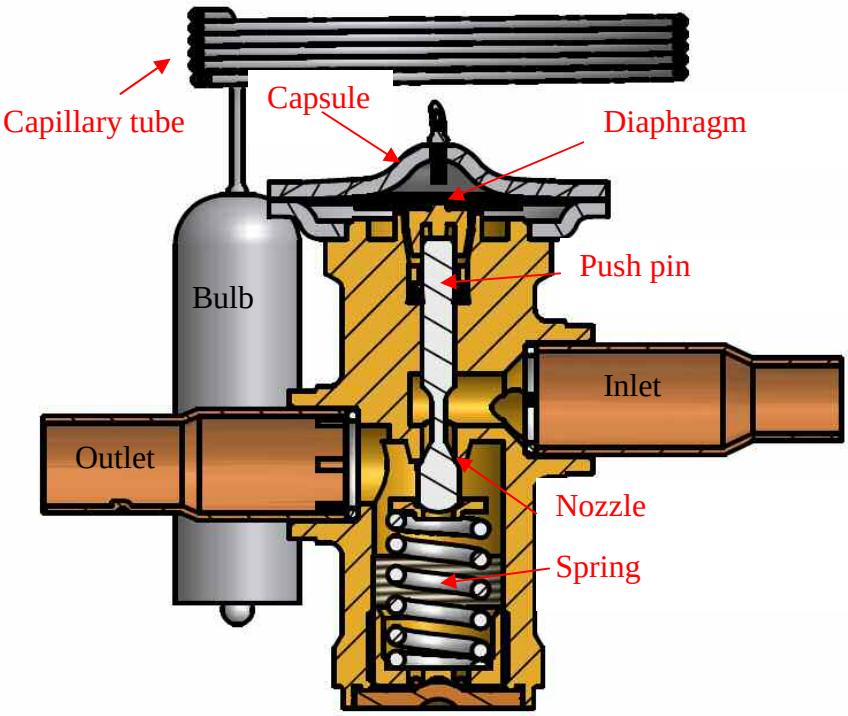

Figure 2-3: Basic components of the TXV (Model: Danfoss TR 6)

The refrigerant flows into the inlet, through the nozzle and out of the outlet. The opening of the nozzle depends on the vertical position of the push pin which again depends on the deflection of the diaphragm. Generally the valve can be divided into two parts divided by the diaphragm. The upper part is the charged system, and the lower part is the mechanical part of the valve.

2.3.1 The charged system

The charged system is the bulb, capillary tube and capsule. The bulb is mounted on the evaporator's outlet to make sure that it has the same temperature as the out flowing refrigerant. The bulb is a temperature-pressure converter. It senses a temperature and produces a pressure according to physical relations. The widest used charge is a condensable gas. This gas will condense and evaporate in the system according to the temperature of the bulb. Since it is a closed system, the pressure will vary with the temperature. The pressure in the capsule adjusts to the pressure in the bulb, because the two volumes are connected through the capillary tube. Therefore the pressure in the capsule will increase with increasing temperature of the bulb and decrease with decreasing temperature of the bulb. Further considerations on this and other systems will follow in later chapters.

2.3.2 The mechanical part

The main mechanical parts in the valve are the diaphragm, needle, spring and of course the nozzle. Many other parts like extra springs, o-rings, gaskets etc. can be necessary to secure a proper function, but they will not be discussed here, because it will be different for each type of valve.
As mentioned, the opening area of the valve is determined by the position of the diaphragm, which depends on the forces above versus the forces underneath.

2.3.3 Free body diagram of the diaphragm

Figure 2-4 shows a free body diagram of the diaphragm.

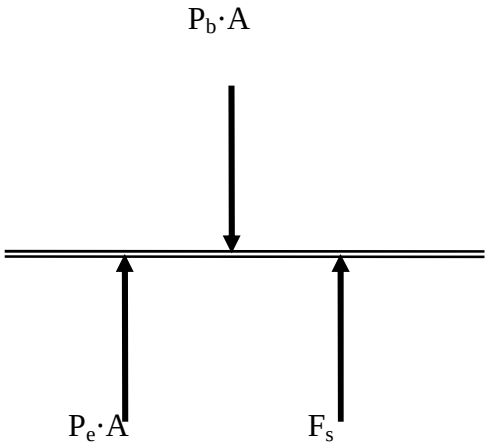

Figure 2-4: Force balance diaphragm

The following equation describes the diaphragm equilibrium.

$$P_b \cdot A = P_e \cdot A + F_s \quad \textbf{(2-5)}$$

(2-5) is only true, if the flow through the nozzle is considered not to contribute to the equilibrium. This may also (to some extend) be true for the so called balanced port versions. But for other valves the flow forces need to be considered. Therefore (2-5) becomes:

$$P_b \cdot A = P_e \cdot A + F_s \pm P_{pd} \cdot a \quad \textbf{(2-6)}$$

Whether this contribution needs to be added or subtracted in (2-6) depends on the design of the valve. In some designs the flow forces help closing the valve while they help opening the valve in other designs. The stiffness of the diaphragm can also contribute to the force balance, but for simplicity it is left out of this description.

With increasing temperature at the evaporator outlet, Pb becomes greater while Pe and Fs remain unchanged. Thus the diaphragm will move downwards, and more refrigerant will be led to the evaporator. The greater amount of refrigerant in the evaporator will decrease the temperature of the bulb and the valve will begin closing again.

3 The dynamics of thermostatic expansion valves

The dynamics of the thermostatic expansion valve lies mostly in the dynamics of the charge. As soon as the temperature of the evaporator changes the new evaporation pressure builds up underneath the diaphragm. But the temperature change of the charge, and thereby the pressure change inside the bulb does take some time. For simplicity the system is considered as a first order system. The response can be expressed with a time constant.

3.1 The time constant

The response of a first order system to a unit step change is described by

$$y(t) = 1 - e^{\frac{-t}{\tau}} \qquad \textbf{(3-1)}$$

Where
y : Response
t : time
ι : Time constant

(3-1) shows that for $y(\tau) = 1 - e^{-1} = 0{,}632$ i.e. the time constant is the time after which the value reaches 63,2 % of its new set point. This is also shown graphically in Figure 3-1.

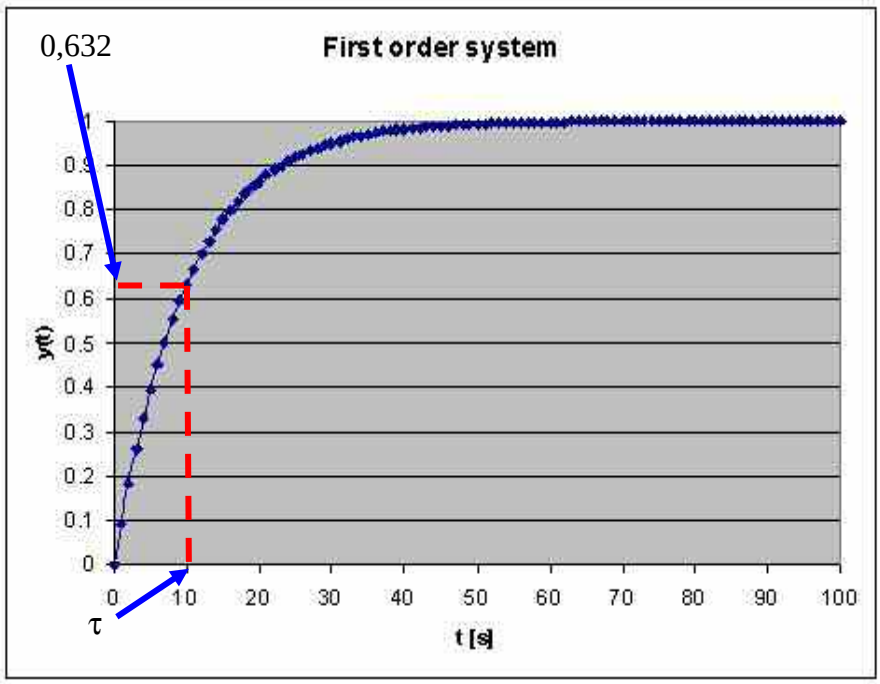

Figure 3-1: First order system

Experience has shown that depending on application long or short time constants are desired. Therefore there is no reason to try to eliminate these time constants, but rather to be able to predict and modify them.
In general it is an advantage to have a rather short time constant for decreasing temperature to ensure that the valve closes quickly and thereby minimize the risk to get liquid into the compressor. In the same way it is of advantage to have a rather long time constant for increasing temperatures in order to eliminate unnecessary fluctuations, and thereby prevent the valve from hunting. Hunting is a phenomenon where the valve fluctuates between full open and closed. Hunting is often seen when the superheat becomes very low and/or if the TXV is oversized.

The dynamics of the valve as whole is mostly determined by the dynamics of the charge.

4 Charges for thermostatic expansion valves

Basically the charged system can be considered as a temperature to force converter. There are several methods to construct a device which can convert temperature to force, and most of them have been applied to TXV's with more ore less success.
One method is the adsorption charge. A solid adsorbent and a gas is put into the bulb. The lower the temperature of the solid, the more gas it adsorbs and the gas pressure decreases. This method is used for some applications.
However, the absolutely most used principle is to have a closed system with some amount of gas which will condense/ evaporate according to temperature changes. This phase change will change the pressure of the closed system. This pressure will cause the deformation of a diaphragm which then pushes a pushrod with a force. The pushrod again determines the opening area of valve. Figure 4-1 shows how the temperature of the bulb affects the valve opening. One of the main advantages of this system is that the sensing bulb can be located somewhere else than the diaphragm as long as they have a pressure equalization connection (Normally a capillary tube).

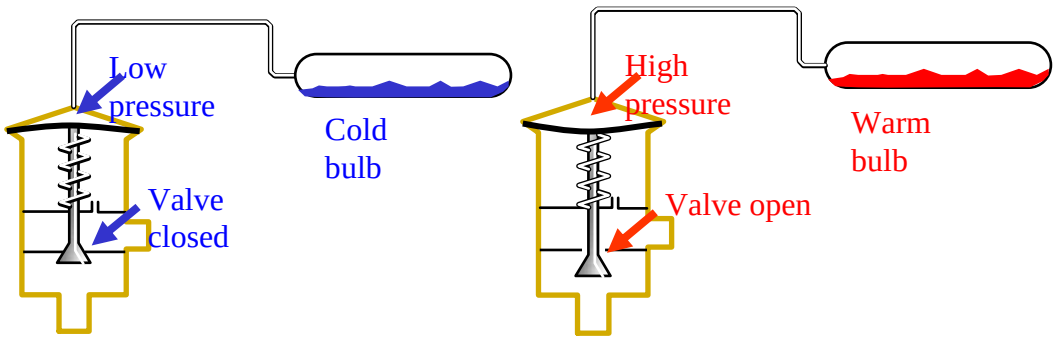

Figure 4-1: Valve opening for cold and warm bulb

The substance in the charged system is called the charge.
The charge can be a pure gas or a mixture of two or more gasses. Development of a charge for a given valve in a given application starts by defining the required temperature/ pressure correlation within the specified temperature range. In a balanced valve this correlation can be calculated by determination of Pb in (2-5) page 9. The pressure Pe can be calculated using the equation of state for the refrigerant.

4.1 Categorization of condensable gas charges

The categorization of a charge is determined by two parameters and two possible additional choices.

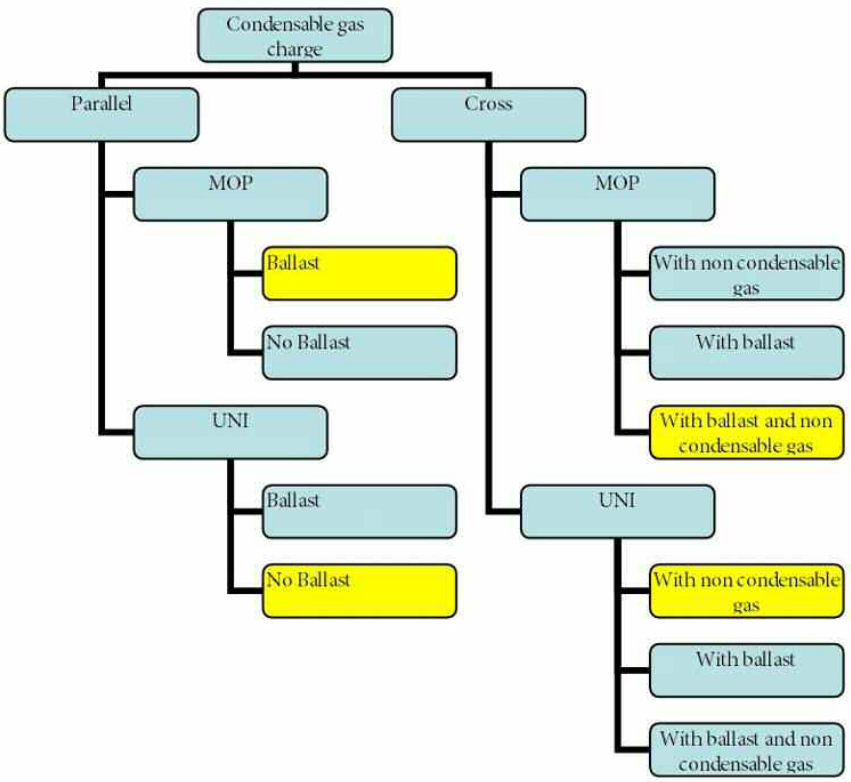

Figure 4-2: Charge categorization diagram

1. Type of media:
    a. Parallel charge
    b. Cross charge
2. Amount of charge
    a. Universal charge
    b. MOP charge

Additional choices

a. Thermal ballast
b. Nitrogen

The choice either a or b for the one parameter does not limit the choice of the other parameter. This means the combination of the choices for the two parameters gives four different types of charges. The additional choices although do not apply to all four combinations. Figure 4-2 shows the different combinations of charges. The ones marked with yellow are the most common. In the following the different types will be explained in more detail.

4.2 Type of charge media

The range of possible charge media is wide. By categorization the only question is if the charge media is the same chemical substance as the refrigerant of the system.
If the bulb is charged with the same refrigerant as the system refrigerant, the charge is called a parallel charge else it is called a cross charge. As an example the temperature/ pressure curves for system and bulb both charged with R134a looks like Figure 4-3. The system pressure is somewhat higher than the bulb pressure because of the spring force.

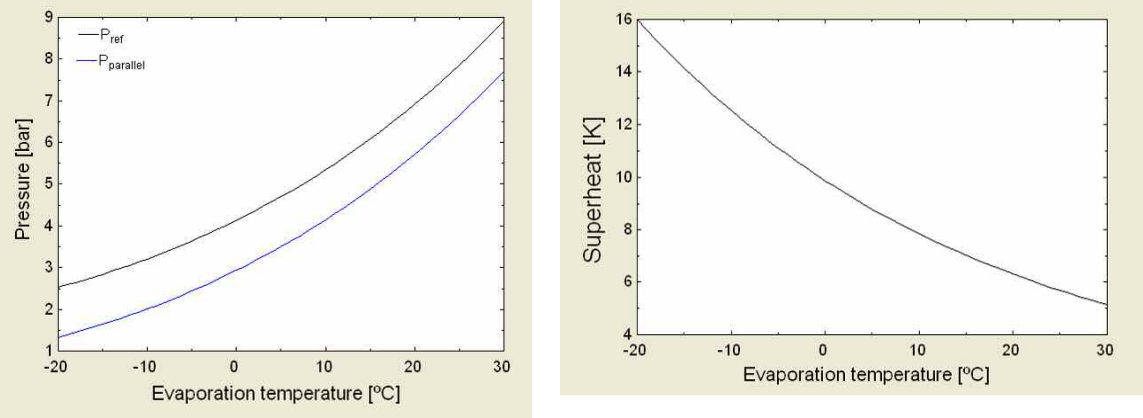

Figure 4-3: Parallel charge

Figure 4-3 shows that the superheat is increasing for decreasing temperature throughout the temperature range of the valve. This means that a greater part of the evaporator is used for superheating and thereby becoming less efficient. To avoid this phenomenon, the temperature/ pressure curve for the charge should be more flat.

By looking at different substances, it becomes clear, that a flatter curve will also lie on a lower pressure level. Figure 4-4 shows the example of R134a as refrigerant and R152a as charge. Thus it is necessary to raise the pressure level without changing the slope of the curve. This can be done mechanically by adding a compression spring on top of the diaphragm or a tension spring under the diaphragm. It can also be done by adding a non condensable gas to the charge, and thereby increase the pressure level. Due to the simplicity at production, Danfoss has chosen the latter solution for their cross charges. The non condensable gas used is mainly nitrogen (N2). This option will be treated in more detail in section 4.5.

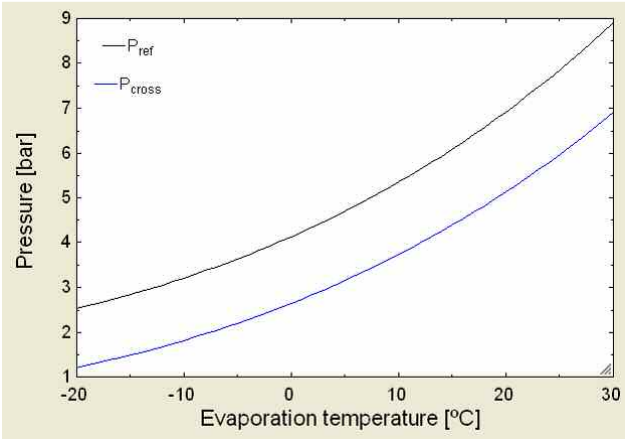

Figure 4-4: Cross charge without nitrogen

Figure 4-5 shows the curves for a cross charge. Here the system refrigerant is R134a and the charge is R152a and a partial pressure of nitrogen. Here the superheat is more constant throughout the temperature range.

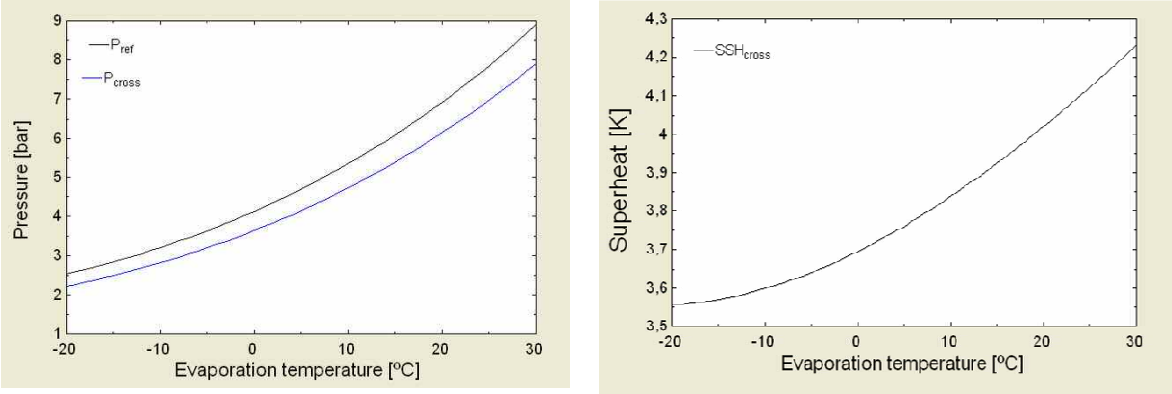

Figure 4-5: Cross charge with nitrogen

4.3 Amount of charge

The amount of charge is a very important parameter for the operation of the valve.
The amount of liquid in an universal charge has a lower limit and an upper limit. The lower is important when the capsule temperature is lower than the bulb temperature. In that case there shall be liquid enough to fill the capsule and the capillary tube with liquid and still keep some liquid in the bulb as well.
If the capsule, on the other hand, gets warmer than bulb, the bulb shall be able to contain all the liquid and still have some free volume.
The limits are valid within a specified temperature range. The advantage of the universal charge is that there will always be a liquid surface in the bulb. Thereby the pressure in the charged system will always be the saturation pressure at bulb temperature. As the name indicates the universal charge can be used for most applications without taking the capsule temperature into consideration.

However, for some applications it can be beneficial to limit the amount of charge considerably below the lower limit for the universal charge. This limitation is because of the compressor. In some applications an evaporation pressure above a certain limit is not accepted.
This limitation is controlled by the amount of charge. A sufficiently small amount of charge will at a given heat input be totally evaporated and the pressure in the bulb will almost remain constant (Only pressure increase is that of a gas heating up). Any further temperature increase of the bulb will not cause the valve to open more. This will ensure that the suction pressure cannot go above a certain value.
Charges limited for that reason are called Maximum Operating Pressure (MOP) charges. The MOP is the pressure of the refrigerant at the point where the last drop of charge just evaporated. Figure 4-6 shows the definition of the MOP.

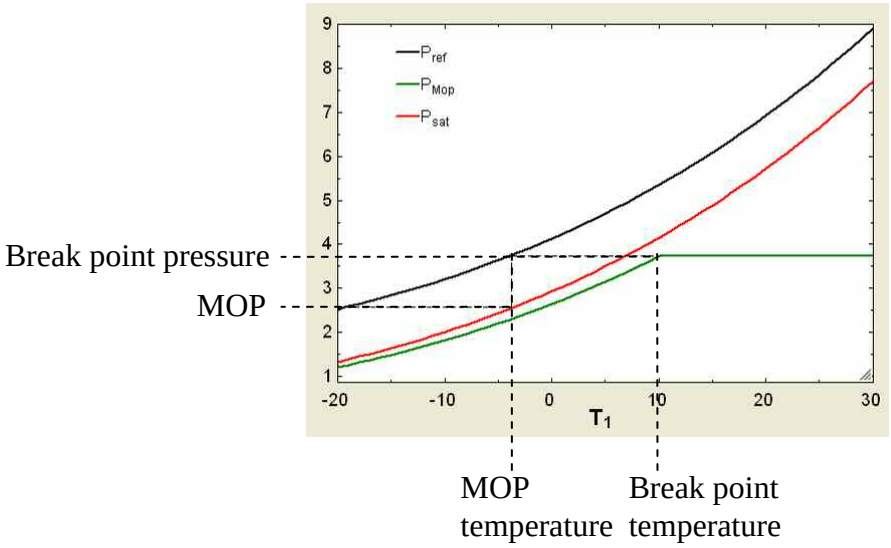

Figure 4-6: MOP definition

In Figure 4-6 the black curve is the pressure acting underneath the diaphragm. The green curve is the pressure in the bulb, while the red curve is the saturation curve of the refrigerant. The MOP is defined as the maximum pressure in the evaporator. The maximum pressure of the bulb is called the break point pressure.

There are two main problems with MOP charges. One problem is a phenomenon called charge migration. When the bulb is warmer than the capsule, liquid will evaporate in the bulb and condense in the capsule. After some time there will be no more liquid in the bulb, and the pressure in the charged system is now determined by the temperature of the capsule and not the temperature of the bulb. The only solution is to make the bulb colder than the capsule by cooling the bulb or warming up the capsule in order to move the liquid back.
The other problem with MOP charges is the very fast dynamic response, i.e. short time constants, because of the decreased thermal mass of the charge. This problem can be overcome by placing a so called thermal ballast brick in the bulb. The background and function of the thermal ballast brick will be explained in the following.

4.4 Thermal ballast brick

Because of the reduced amount of liquid and thereby thermal mass, the MOP charges have relatively short time constants compared to universal charges.
This problem can be overcome in different ways. The one used by Danfoss at this time is putting a solid brick of porous material into the bulb. The porous brick will give a longer time constant. But the time constant for increasing temperature will be longer then the one for decreasing temperature. The explanation is that the brick sucks the liquid phase. By increasing the temperature, the whole brick has to be warmed up to evaporate some charge. As the temperature decreases, the condensation can start as soon as there is a cold surface at the bulb wall. The brick material can be chosen according to the desired time constants.

4.5 Nitrogen

As mentioned in the description of cross charges it is usually necessary to raise the pressure level of the bulb at all temperatures. This is currently done by adding a partial pressure of nitrogen. This partial pressure will only change slightly with temperature, and thereby not change the slope of the saturation curve considerably. Figure 4-7 shows the saturation curve for R 410A and a temperature/pressure curve for R 410A and a partial pressure of nitrogen (1 bar at 25ºC). The latter has been corrected for temperature and volume changes.

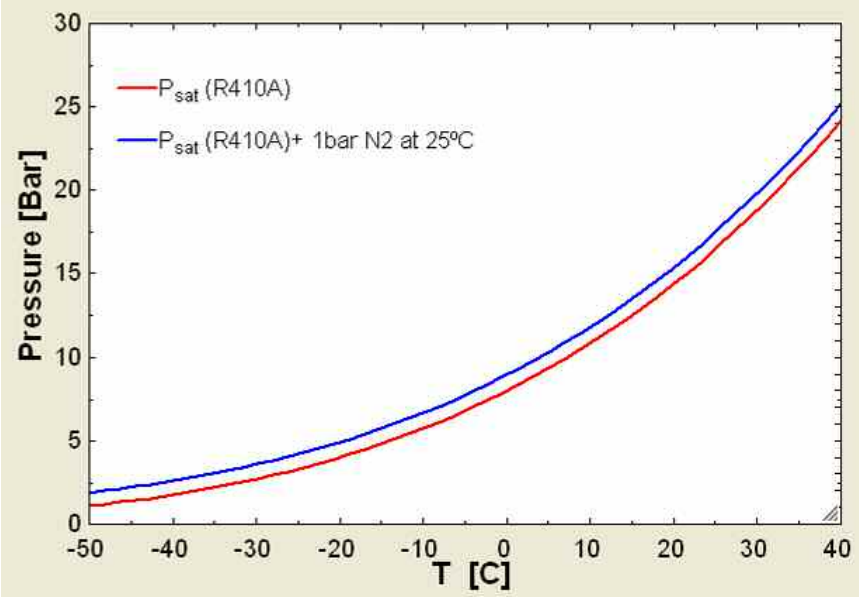

Figure 4-7: Temperature/ pressure relationship with and without nitrogen

4.6 Tolerances on the charge pressure

Looking at the TXV as a whole the charge pressure is only one of the four pressures acting on the valve diaphragm (Equation (2-6)). In this chapter the charge pressure will be seen in a broader perspective.

The costumer buying the TXV does not measure the charge pressure, but does only see the overall performance of the valve. What the costumer sees is the ability to uphold a stable superheat at the expected value under certain conditions When the TXV leaves Danfoss it is adjusted at a so called factory setting. The factory setting is a superheat at a certain value for certain standard conditions of the refrigeration or air conditioning system. If the conditions for the valve in the system differ from standard conditions the value of the superheat changes and an adjustment might be necessary. In the special case of sale to OEM costumers the valve is set to a specific value taken the real conditions in the particular refrigeration or air conditioning system of the costumer into account. This procedure ensures that no further adjustment of the valve is necessary.

If everything else is kept constant, Equation (2-6) shows that a change in the charge pressure will change the position of the diaphragm and thereby the mass flow through the valve and in the end the superheat at the evaporator exit. In the following an example will be given where the variation in superheat as a variation of bulb pressure is

quantified. It has to be stressed that the numbers in the example are not taken from real data. But the example gives a general feeling of orders of magnitude and shows some general trends.

In the example following has been assumed:

Bulb volume: 7 cm3
Charge: R125
Refrigerant: R410A
Mass of charge: 2000 mg
Nitrogen pressure: 0,8 bar at 25ºC
Pressure from spring force: 0,5 bar

The pressure curves for the bulb and the refrigerant side are shown in Figure 4-8. In the calculation an uncertainty of 0,05 bar has been estimated for the charge pressure. The resulting superheat is shown in Figure 4-9. The line represents the value whereas the vertical lines indicate the uncertainty in superheat due to the uncertainty in the charge pressure.

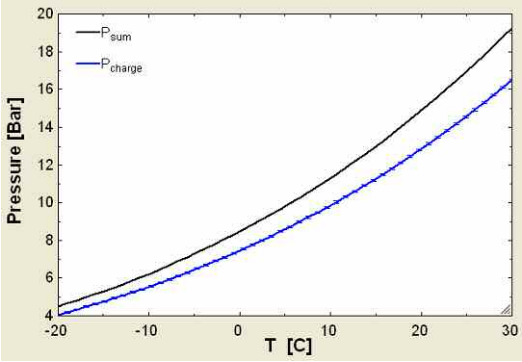

Figure 4-8: Pressure curves for refrigerant side and bulb

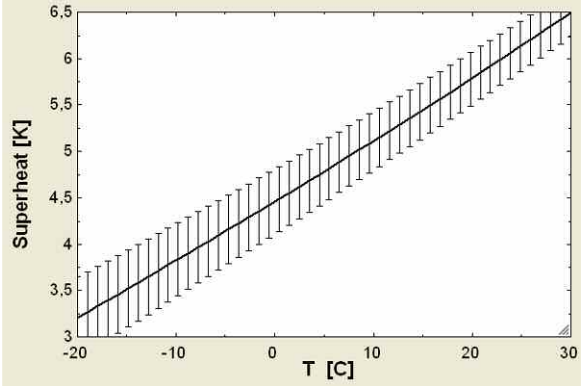

Figure 4-9: Superheat curve with uncertainty

The example shows that a variation of 0,05 bar in the charge pressure gives a variation of app. 0,25 K in superheat setting. Taken into account that Danfoss delivers valves that are adjusted with an accuracy of 0,25 K, it can be concluded that the charge pressure in this particular example is not allowed to vary more than 0,05 bar after adjustment of the valve.
Again it has to be stressed, that the numbers in the example change from application to application, but it gives a feeling of how much variation in the charge pressure can be accepted.

5 Charges for thermostatic expansion valves

The preceding three chapters have given an introduction to TXV's in general and to the charge more specifically. This page will sum up the essentials of these chapters.

Function of the TXV: Creates a pressure drop to initiate the evaporation and meters the flow into the evaporator in order to remain a certain superheat of the refrigerant leaving the evaporator.

Definition of charge for TXV: The content of the closed system (capsule, capillary tube and bulb) which converts the temperature signal into a pressure signal. The bulb senses the temperature of the evaporator outlet and the charge generates a pressure according to that temperature.

The superheat throughout the application range of temperatures depends on the temperature/ pressure curve of the charge and the sum curve for the valve. Figure 5-1 and Figure 5-2 show these curves for different types of charges.

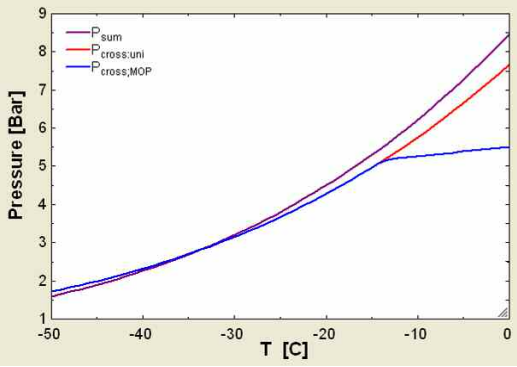

Figure 5-1: Temperature/ pressure relationship for MOP and UNI charges

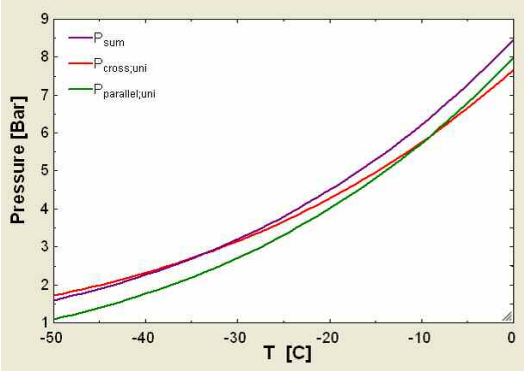

Figure 5-2: Temperature/ pressure relationship for Cross and parallel charges

The job of the TXV is to maintain the desired degree of superheat of the refrigerant leaving the evaporator. The temperature/ pressure relationship for the charge is an important parameter for the superheat. Therefore this relationship has to be known. Figure 5-3 shows the difference in the superheat for a range of evaporation temperatures for parallel charge, cross charge and MOP cross charge. The superheat is kept more constant with a cross charge.

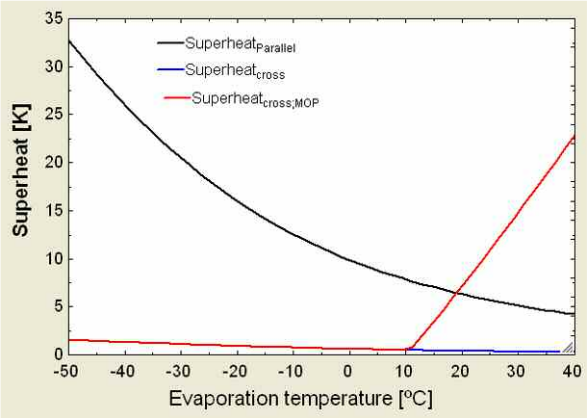

Figure 5-3: Superheat curve for parallel charge, cross chargeand MOP cross charge under similar conditions

6 Dynamic model for charges for TXV's

The charge for a TXV can in the very simple stationary case be modeled by a temperature/ pressure relationship, which is the saturation curve for the charge media. The temperature is the evaporation temperature of the system.
In the dynamic case a time constant has to be estimated as well.
This model will work for simulations where the user wants to identify some trends and some rough estimates.
However, going a bit deeper and wanting to optimize a charge for a certain application, a more detailed dynamic model is needed.

6.1 Strategy of modeling

Before starting the modelling the following has to be defined:

- Purpose of the model
- User group
- Expected output
- Strategy for input
- Choice of software

6.2 Purpose of the model

The purpose of the model is to have a model that can describe the dynamic behaviour of a charge of a TXV. The model needed should be able to represent the following charges:

- Universal charges
- MOP charges
- Charges with nitrogen (namely cross charges)
- (Charges with thermal ballast)

For any type of charge, the model should also take the dynamics of the heat transfer from the evaporator to the bulb into account. The structure of the model is shown graphically in Figure 6-1. Calculating charges with thermal ballast is an important feature, but time has not allowed covering this issue during this work.

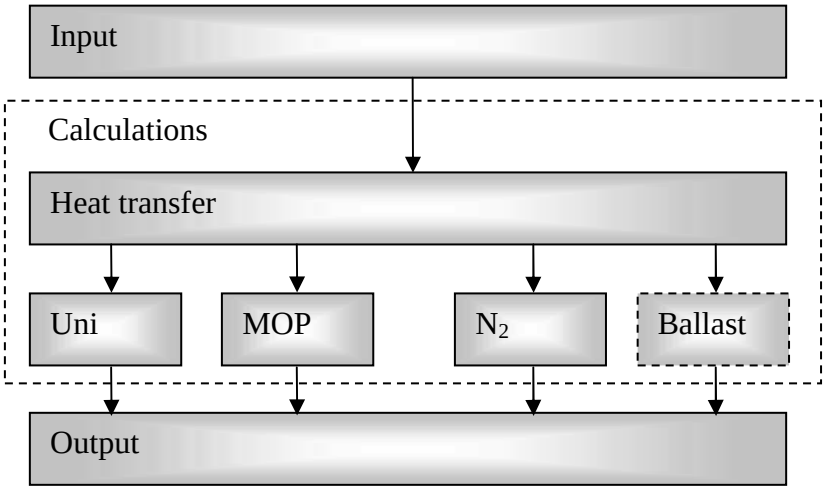

Figure 6-1: Structure of the model

6.2.1 User group

The user group for the model presented in this thesis is the R&D department of Danfoss A/S Automatic Controls. The model is supposed to be combined with models for other parts of the TXV and thereby form a complete model for TXV's.

6.2.2 Expected output

Thinking of this model as a part of a full TXV model the only important output of the model is the pressure of the capsule at each time step. However, for investigation of charges it might be interesting to look at various outputs in order to get an understanding of the value of the pressure. Therefore the model should be able to provide various outputs.

6.2.3 Strategy for input

In order to keep the model as general as possible, the strategy regarding input parameters has been to use input that are available in the specifications for the TXV and the charge, i.e. information that anyone within the Danfoss R&D department can find.
However, some of the inputs cannot be found in the specifications. These will be pointed out in the model description and it will be explained in more detail how to set these.

6.2.4 Choice of software for the model

Building a simulation model like the one presented in this thesis can be done in many different environments. The final choice often depends on some specific needs and the availability of both software and support to get started. The software chosen for this project is WinDali which is a modelling and simulation program where the models can be created in any programming language. The model presented here has been created in Borland Pascal code. WinDali covers the basic needs for this project:

- Dynamic model.
  - Since the state of the system depends on what happened before, the model has to be dynamic.
- Built in equations of state for a wide range of refrigerants.
  - The build in equations give the possibility to call any properties of refrigerants, without having to programme equations of states first.
- Handles state shifts.
  - The state shifts are determined as they appear and the model uses the set of equations specified for the actual state.
- WinDali comes with a graphical interface where parameters can be set and the results are plotted as a function of time.

For more information about WinDali, please refer to the documentation [16].

7 Heat transfer from refrigerant to charge

Modelling the dynamics of the charged system of a TXV can roughly be divided in two parts (Figure 6-1). On of them being the thermal contact between refrigerant flowing through the evaporator outlet and the charge inside the bulb, the other part being different internal phenomena inside the charged system. The thermal contact between the refrigerant and the charge depends on several parameters related to geometries, materials and the way of mounting the bulb.
In this chapter a model that describes this thermal contact will be presented. The model is limited to calculate on cylindrical bulbs because the new bulbs on the TXV's made by Danfoss are cylindrical. The shape of bulbs has changed a few times during the years. The first Danfoss bulbs were of cylindrical shape and somewhat longer than today. But the problem was that the theoretical contact line turned into either one or more points of contact, and thereby a very small contact area. In 1967 Danfoss invented and patented [17] the so called "double contact", whose purpose it was to make it easier to align the bulb on the pipe and thereby get a theoretical two line contact. In practice this also just gives some points of contact, but at least not less than two, and the alignment was easier. Recently the cylindrical bulb has been taken into use again. They are shorter and the wide strap secures a proper alignment. Therefore this project will focus on the cylindrical bulb.

7.1 Modelling

In this section it will be shown how the heat transfer from the refrigerant in the evaporator outlet to the charge in the bulb is modelled.

First of all some general definitions will be given.
The system investigated consists of a cylindrical stainless steel bulb mounted on a copper tube with a copper strap.

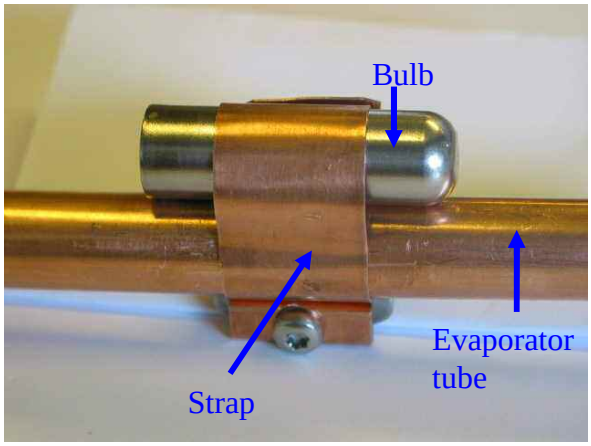

Figure 7-1: Bulb mounted on tube

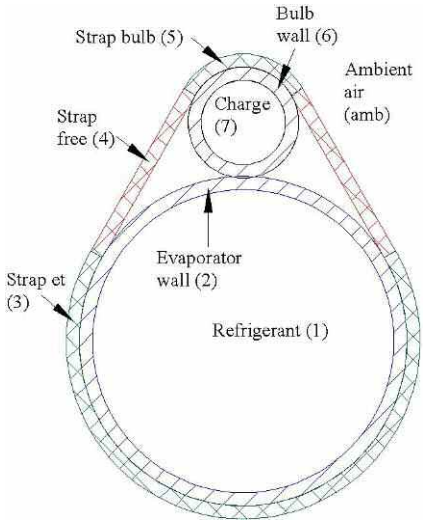

Figure 7-2: Numbering of parts in the system

Figure 7-1 shows the bulb connected to the evaporator tube with a strap. The numbers in Figure 7-2 refer to the parts in the system:

1. Refrigerant in the evaporator tube
2. Evaporator tube wall
3. Strap around evaporator tube
4. Free strap
5. Strap around bulb
6. Bulb wall
7. Charge

Amb. Ambient air

The heat fluxes in the above system are shown in Figure 7-3.

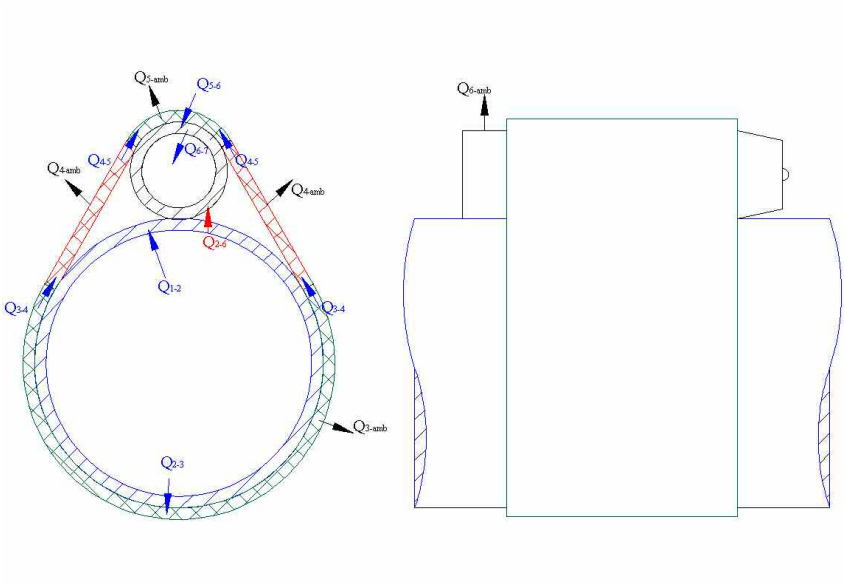

Figure 7-3: Heat fluxes in the system

The interest here is to understand how heat is exchanged between the refrigerant (1) and the charge (7).

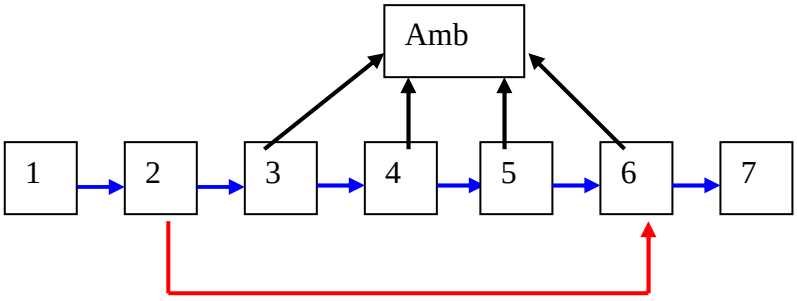

Figure 7-4: Heat fluxes in the system

From Figure 7-4 it can be seen that the temperature of the charge is a result of two different series of heat fluxes in the system. They are:

Contact 1: Refrigerant (1) ⇒ Evaporator tube wall (2) ⇒ bulb wall (6) ⇒ Charge (7)

Contact 2: Refrigerant (1) ⇒ Evaporator tube wall (2) ⇒Strap et (3) ⇒Free strap (4) ⇒Strap bulb (5) ⇒ bulb wall (6) ⇒ Charge (7)

Therefore the following will concentrate on the understanding of these two ways of heat transfer. In order to model the system some assumptions will be made.

Assumptions
In order to simplify the modeling, following assumptions are made:

Lumped mass model
No temperature profile through or along the perimeters of walls.
Strap has no mass

Looking at Figure 7-3 and Figure 7-4 there are several heat fluxes that need to be defined.
The heat flux from the refrigerant to the inner wall of the evaporator, from the bulb inner wall to the charge and from alle free surfaces to the ambient air are modeled as convective heat fluxes defined by (7-1)-(7-5).

$$\dot{Q}_{1-2} = h_{ref} \cdot A_{et\_i} \cdot \Delta T_{1-2} \quad \textbf{(7-1)}$$

$$\dot{Q}_{6-7} = h_{charge} \cdot A_{b\_i} \cdot \Delta T_{6-7} \quad \textbf{(7-2)}$$

$$\dot{Q}_{2-amb} = h_{air} \cdot A_{et\_strap} \cdot \Delta T_{2-amb} \quad \textbf{(7-3)}$$

$$\dot{Q}_{5-amb} = h_{air} \cdot A_{b\_strap} \cdot \Delta T_{5-amb} \quad \textbf{(7-4)}$$

$$\dot{Q}_{6-amb} = h_{air} \cdot A_{b\_free\_amb} \cdot \Delta T_{6-amb} \quad \textbf{(7-5)}$$

The conductive heat flux between the evaporator tube and the bulb (7-6), the evaporator tube and the strap (7-7) and between the strap and the bulb (7-8) are defined by thermal contact resistances which will be evaluated later.

$$\dot{Q}_{2-6} = \frac{1}{R_{c_{2-6}}} \cdot \Delta T_{2-6} \quad \textbf{(7-6)}$$

$$\dot{Q}_{2-3} = \frac{1}{R_{c_{2-3}}} \cdot \Delta T_{2-6} \quad \textbf{(7-7)}$$

$$\dot{Q}_{5-6} = \frac{1}{R_{c_{5-6}}} \cdot \Delta T_{5-6} \quad \textbf{(7-8)}$$

The strap is modelled as a fin where the temperatures at the endpoints are known. [5]

$$\dot{Q}_{3-4} = 2 \cdot M \cdot \frac{\cosh(m \cdot L_{strap\_free}) - \frac{\theta_l}{\theta_b}}{\sinh(m \cdot L_{strap\_free})} \quad \textbf{(7-9)}$$

$$\dot{Q}_{4-5} = 2 \cdot M \cdot \frac{\frac{\theta_l}{\theta_b}\cosh(m \cdot L_{strap\_free}) - 1}{\sinh(m \cdot L_{strap\_free})} \quad \textbf{(7-10)}$$

where:

$$\theta_l = T_5 - T_{amb} \quad \textbf{(7-11)}$$

$$\theta_b = T_3 - T_{amb} \quad \textbf{(7-12)}$$

$$m^2 = \frac{h_{air} \cdot P_{strap}}{\lambda_{strap} \cdot A_{strap\_cross}} \quad \textbf{(7-13)}$$

$$M = \sqrt{h_{air} \cdot P_{strap} \cdot \lambda_{strap} \cdot A_{strap\_cross}} \cdot (T_2 - T_{amb}) \quad \textbf{(7-14)}$$

The conservation of energy implies that:

$$\dot{Q}_{2-3} = \dot{Q}_{3-amb} + \dot{Q}_{3-4} \quad \textbf{(7-15)}$$

$$\dot{Q}_{4-5} = \dot{Q}_{5-amb} + \dot{Q}_{5-6} \quad \textbf{(7-16)}$$

$$\dot{Q}_{4-amb} = \dot{Q}_{3-4} - \dot{Q}_{4-5} \quad \textbf{(7-17)}$$

Equations (7-18)-(7-25) show the calculation of different length and areas used for the above calculation and calculated from the input of the model.

$$L_{strap\_free} = (r_{et} + r_b) \cdot \sin\left(\frac{\beta}{2}\right) \quad \textbf{(7-18)}$$

$$A_{et\_i} = 2\pi r_{et\_i} l_{bulb} \quad \textbf{(7-19)}$$

$$A_{b\_i} = 2\pi r_{b\_i} l_{bulb} \quad \textbf{(7-20)}$$

$$A_{b\_strap} = \frac{\beta}{360^o} \cdot 2\pi r_b \cdot strap_{width} \quad \textbf{(7-21)}$$

$$A_{et\_strap} = \frac{\beta}{360^o} \cdot 2\pi r_{et} strap_{width} \quad \textbf{(7-22)}$$

$$A_{b\_free\_amb} = 2\pi r_b (l_{bulb} - strap_{width}) \quad \textbf{(7-23)}$$

$$A_{strap\_cross} = strap_{width} \cdot L_{t\_strap} \quad \textbf{(7-24)}$$

where:

$$\beta = 2 \cdot A\cos\left(\frac{2(r_{et} - r_b)}{r_{et} + r_b}\right) \quad \textbf{(7-25)}$$

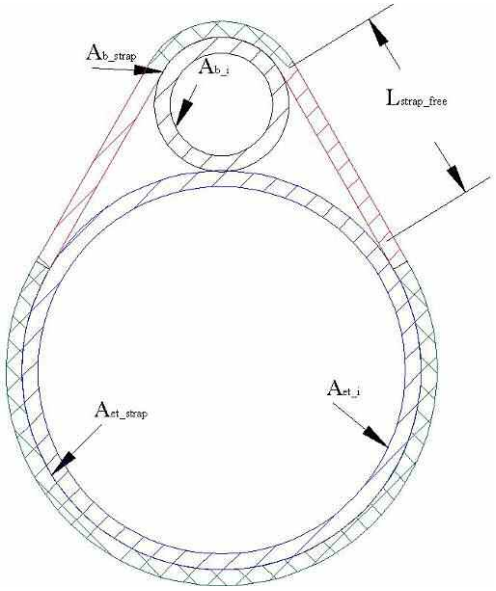

Figure 7-5: Definition of areas

Combining these heat fluxes to describe the three ways the bulb is affected, results in following equation system:

$$m_2 \cdot c_{p2} \frac{dT_2}{dt} = \dot{Q}_{1-2} - \dot{Q}_{2-3} - \dot{Q}_{2-6} \quad \textbf{(7-26)}$$

$$m_6 \cdot c_{p6} \frac{dT_6}{dt} = \dot{Q}_{2-6} + \dot{Q}_{5-6} - \dot{Q}_{6-7} - \dot{Q}_{6-amb} \quad \textbf{(7-27)}$$

$$\frac{dU}{dt} = \dot{Q}_{6-7} \quad \textbf{(7-28)}$$

The total internal energy can be expressed as the sum of the internal energy for liquid and the internal energy for gas.

$$U = m_{LIQ} \cdot u_{LIQ} + m_{GAS} \cdot u_{GAS} \quad \textbf{(7-29)}$$

Using the quality x (7-29) can be expressed as

$$U = m \cdot \left(u_{LIQ} + (u_{GAS} - u_{LIQ}) \cdot x\right) \quad \textbf{(7-30)}$$

A change in internal energy due to temperature changes can therefore be expressed as:

$$\frac{dU}{dt} = m \cdot \left(\frac{du_{LIQ}}{dt} + \frac{d((u_{GAS} - u_{LIQ}) \cdot x)}{dt} \right) \quad \textbf{(7-31)}$$

Rewriting (7-31)

$$\frac{dU}{dt} = m \cdot \left(\frac{du_{LIQ}}{dt} + x \cdot \frac{d(u_{GAS} - u_{LIQ})}{dt} + (u_{GAS} - u_{LIQ}) \cdot \frac{dx}{dt} \right) \quad \textbf{(7-32)}$$

$$\frac{dU}{dt} = m \cdot \frac{dT}{dt} \left(\frac{du_{LIQ}}{dT} + x \cdot \frac{d(u_{GAS} - u_{LIQ})}{dT} + (u_{GAS} - u_{LIQ}) \cdot \frac{dx}{dT} \right) \quad \textbf{(7-33)}$$

$\frac{dx}{dT}$ can be evaluated from the fact that the volume of the bulb and the mass in the bulb are constant. The total volume can be expressed as the sum of the gas volume and the liquid volume.

$$V = m_{LIQ} \cdot v_{LIQ} + m_{GAS} \cdot v_{GAS} \quad \textbf{(7-34)}$$

Using the quality x (7-34) can be expressed as

$$V = m \cdot \left(v_{LIQ} + (v_{GAS} - v_{LIQ}) \cdot x\right) \quad \textbf{(7-35)}$$

Thus

$$x = \frac{\frac{V}{m} - v_{LIQ}}{v_{GAS} - v_{LIQ}} \tag{7-36}$$

And

$$\frac{dx}{dT} = \frac{d}{dT}\left(\frac{\frac{V}{m} - v_{LIQ}}{v_{GAS} - v_{LIQ}} \right) \tag{7-37}$$

Inserting (7-37) into (7-33), the change in internal energy can be expressed as a function of temperature.

$$\frac{dU}{dt} = m \cdot \frac{dT}{dt}\left(\frac{du_{LIQ}}{dT} + x \cdot \frac{d(u_{GAS} - u_{LIQ})}{dT} + (u_{GAS} - u_{LIQ}) \cdot \frac{d}{dT}\left(\frac{\frac{V}{m} - v_{LIQ}}{v_{GAS} - v_{LIQ}} \right) \right) \tag{7-38}$$

Given the definitions

$$c_{v\_LIQ} = \frac{du_{LIQ}}{dT} \tag{7-39}$$

$$c_{v\_GAS} = \frac{du_{GAS}}{dT} \tag{7-40}$$

(7-38) can be written

$$\frac{dU}{dt} = m \cdot \frac{dT}{dt}\left(c_{v\_LIQ} + x \cdot (c_{v\_GAS} - c_{v\_LIQ}) + (u_{GAS} - u_{LIQ}) \cdot x \right) \tag{7-41}$$

Combining (7-28) and (7-41) the heat flux $Q_{6\text{-}7}$ becomes

$$Q_{6-7} = m_7 \cdot \frac{dT_7}{dt}\left(c_{v\_LIQ\_7} + x \cdot (c_{v\_GAS\_7} - c_{v\_LIQ\_7}) + (u_{GAS} - u_{LIQ}) \cdot x \right) \tag{7-42}$$

The temperature response of the charged system is determined by the thermal masses, material properties, thermodynamic properties of the charge and the properties of the thermal contacts between the contact faces. Thermal masses, material properties and thermodynamic properties of the charge are known, while the properties of the contact faces will be subject to research.

The heat flows through two different contact faces. Both of them need to be characterized with a thermal contact resistance. These have been evaluated using experimental testing and finite element calculations. In order to determine one without influence from the other, both techniques have been applied where one of the contacts is inactive (insulated) while the other is active.

7.2 Determination of thermal contact resistances

The thermal contact resistances have been evaluated from a finite element (FE) model which has been calibrated with experimental test results. The values found have been used in an analytical model built on the equations presented in this chapter. The results from the analytical model have been compared to measurements on charged bulbs.

The procedure has been the following:

- Experimental evaluation of the temperature distribution in empty bulb
- Finite element model used to find contact properties
- Contact properties transferred to contact resistances for use in the analytical model
- Tests with charged bulbs.

7.3 Experimental measurements

All measurements described in this report, are measurements where the bulb is mounted on a copper tube whose outer temperature can be changed a few degrees almost like a step function. The apparatus used is basically a copper tube that is connected to two bathes at two different temperatures. If the media flowing through the tube is taken from bath one the tube has the same temperature as bath one. By closing some valves and opening others the media can be taken from bath two instead. This will change the temperature of the tube to the temperature of bath one. In order to control the ambient, the tube is put into an insulated chamber (A rebuild household freezer). The chamber can be cooled and heated in order to maintain the desired temperature.
The uncertainty of the measurements is assumed to be within 5 to 10 seconds on the time constant. The assumption is based on previous studies at Danfoss.

Figure 7-6: Test apparatus

Figure 7-7: Copper tube inside the chamber. Upper: with bulbs mounted, Lower: Without bulbs

Schematically the setup looks like Figure 7-8.

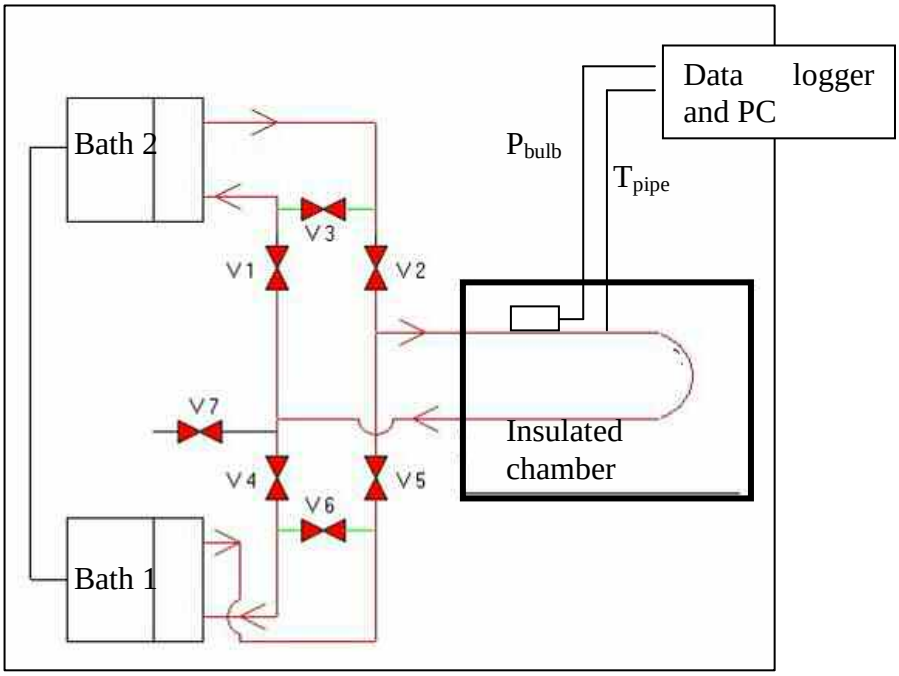

Figure 7-8: Test setup

The bulb is mounted on the pipe in the insulated chamber. The temperature of the pipe depends on the temperature of the fluid flowing through it. By switching the flow from one bath to the other, the temperature of the pipe will change with a time constant of 3 s (Figure 7-9).

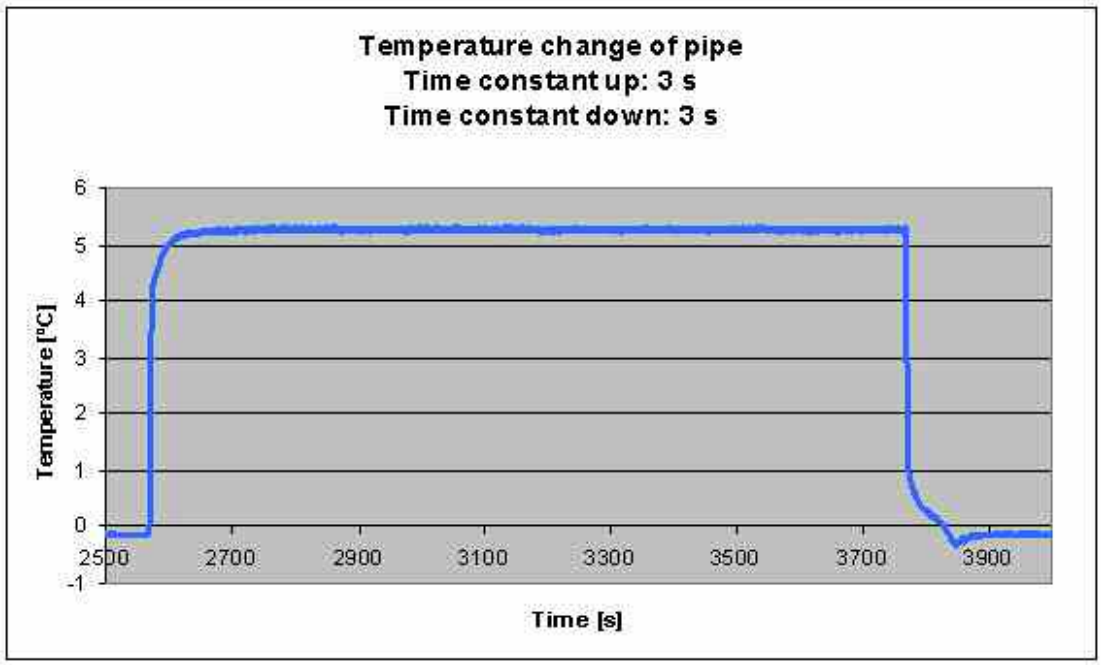

Figure 7-9: Temperature curve for the outer wall of the test rig during a step

The bulb however, will change its temperature depending on the contact with the pipe. The outcome of the measurement is the temperature as a function of time from which the time constant can be determined.

7.4 Experimental evaluation of the temperature distribution in empty bulb

In the simulations, the contact resistances will be the unknown values to determine. Therefore the temperature distribution in the bulb wall needs to be known.
This has been done experimentally by measuring the temperature at four places inside an empty bulb. The temperature was measured at four places as shown in the figure.
The measured temperature curves have been used to calibrate the FE model.

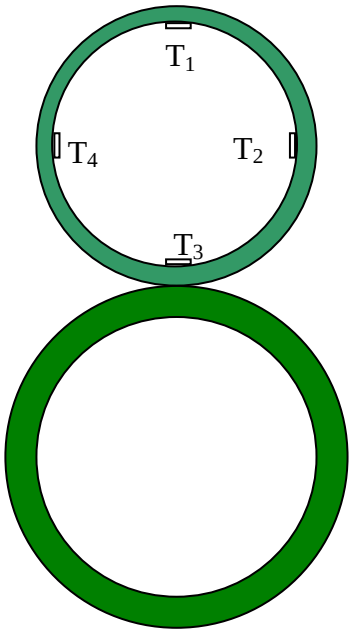

Figure 7-10:Location of measurement

7.5 Test series:

The test series covers tests of the two contacts individually and a combined.
Three tests were performed with conditions as shown in Table 7-1.

	Pipe contact	Strap contact
Test 1	X	
Test 2		X
Test 3	X	X

Table 7-1: Tests performed on bulb with temperature sensors

The tests show the temperature distribution in the bulb.

7.5.1 Results:

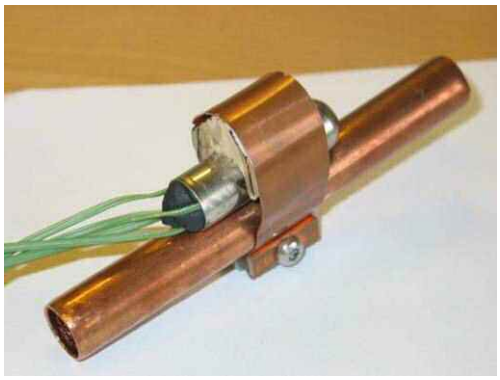

Figure 7-11: Wooden brick as insulation between strap and bulb

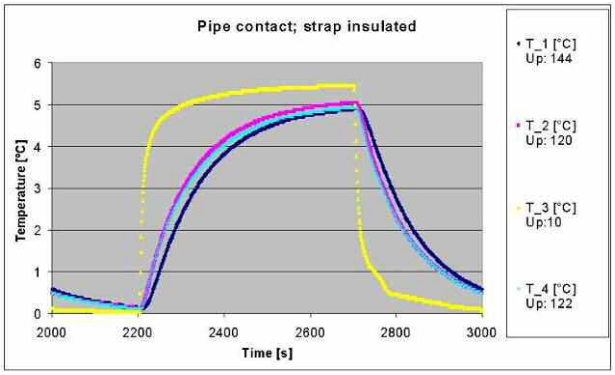

Figure 7-12: Temperature curves for the four sensors. Numbering as shown in Figure 7-10.

Figure 7-13: Wooden brick as insulation between pipe and bulb

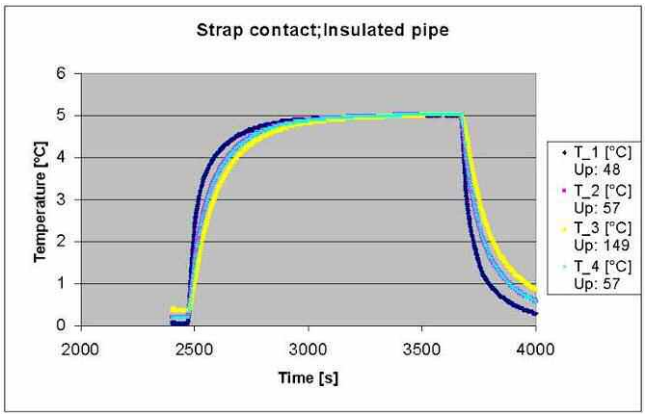

Figure 7-14: Temperature curves for the four sensors. Numbering as shown in Figure 7-10.

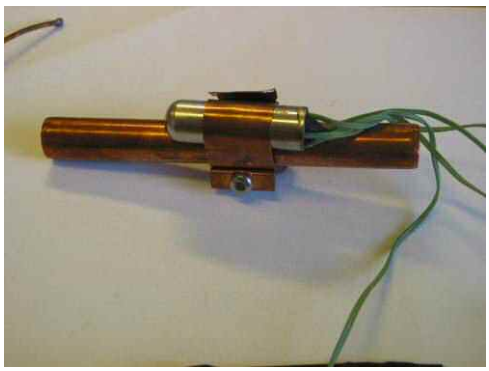

Figure 7-15: Full contact

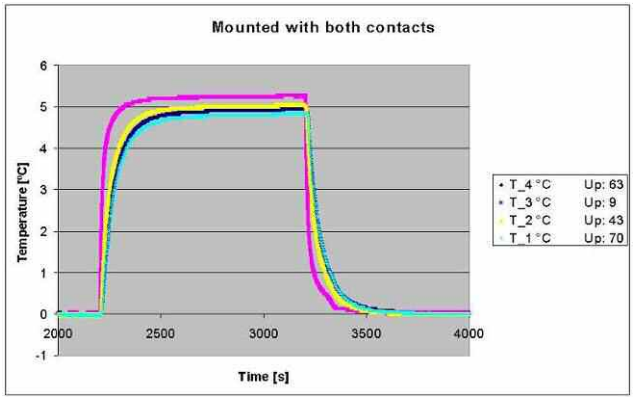

Figure 7-16: Temperature curves for the four sensors. Numbering as shown in Figure 7-10.

The temperature curves show the temperature distribution on the inside of the bulb wall. This information will be used to construct a FE model.

7.6 The Finite element model

FE software used for this investigation is SORPAS®, which is developed and mostly used for resistance welding. The analogy between this problem and resistance welding is that two bodies are squeezed together and a heat transfer is taking place. For resistance welding a current is applied, but this part is not used in this investigation.
For simplicity the problem is modelled as a 2- dimensional problem. Figure 7-17 and Figure 7-18 show the real system and the modelled section respectively.

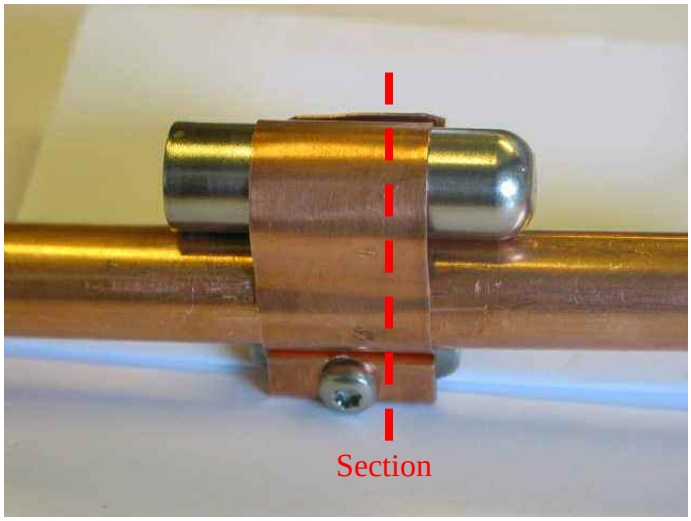

Figure 7-17: Real system

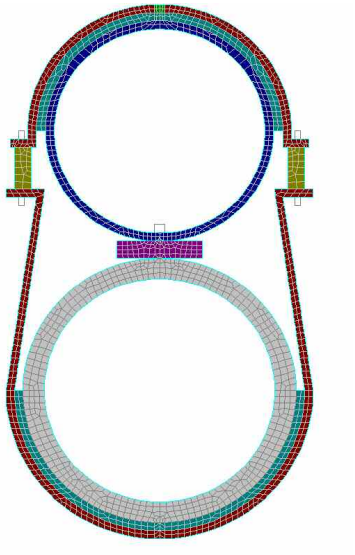

Figure 7-18: Modeled section

The FE model looks slightly different than the real model. The differences are partly caused by modeling limitations and partly due to numerical issues.
Figure 7-19 shows the parts of the model, and each part is explained in more detail in Table 7-2.

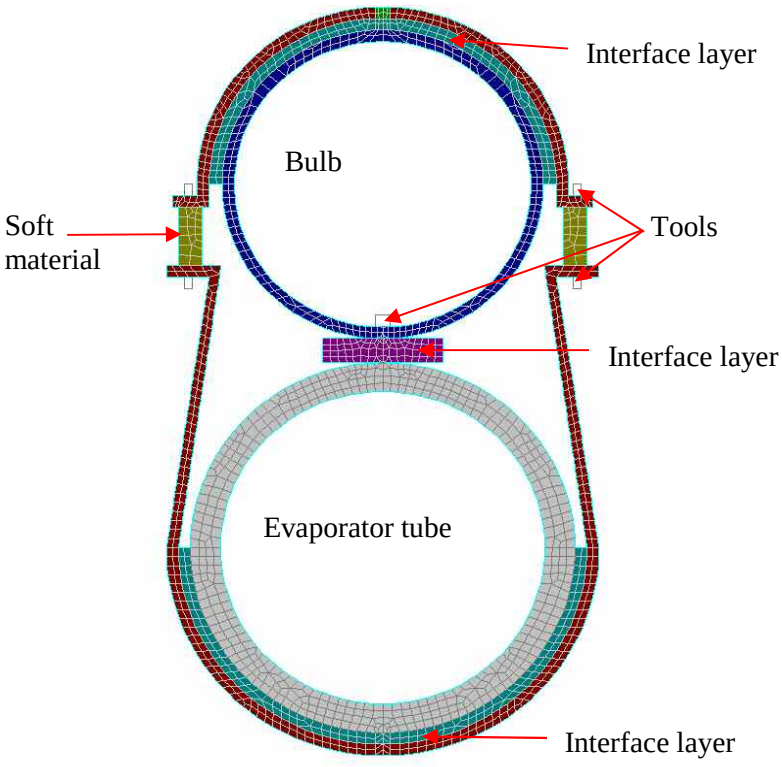

Figure 7-19: Finite element model

Part	Description
Bulb	Modeled with the actual dimensions and material properties.
Evaporator tube	Modeled with typical dimensions (Same as on test rig) Material: Copper.
Interface layer	A material where the conductivity can be adjusted in order to fit the model to the test results. The heat capacity is set to 1 J/kg/K in order not to add thermal mass. The purpose of this layer is to represent a thermal resistance.
Tools	Fictive material where boundary conditions can be applied
Soft material	Connection piece between the strap ends in order to avoid numerical problems with nodes going in contact during the squeeze.
Number of elements	770

Table 7-2: Details of model

7.6.1 Boundary conditions:

For a SORPAS® model it is required to model tools where the mechanical boundary conditions can be applied. The mechanical boundary condition for this model is an initial movement of the bulb towards the pipe. In the Danfoss refrigeration laboratory it has become common practice to tighten the strap until the bulb has moved 1 mm into the pipe, which results in a deformation of the copper tube.
The thermal boundary condition is that the copper tube keeps its temperature constant during the simulation. It has been chosen to set the temperature of the copper tube to 0ºC while all other parts have an initial temperature of 5ºC. Ambient temperature is set to 5ºC but the model is considered as being insulated from the ambient.
A complete description of the boundary conditions is given in Table 7-3.

Boundary conditions		
Boundary condition	Applied	Value
Initial squeeze	On the clamping faces of the strap	1 mm movement during the first 100 ms. (In reality this squeeze happens before heat transfer, but this is not possible in SORPAS®. But 0,1 s can be considered as instantly compared to the time constant of the whole system.
No movement of bulb	On bulb	The bulb is not allowed to deform. In reality the bulb has endplates and is therefore much stiffer than is a sectional view.
Ambient temperature	Can be entered directly	5ºC
Temperature of pipe	For the whole pipe	0ºC

Table 7-3: Boundary conditions

7.6.2 Modeling details:

In order to accommodate the above demands for boundary conditions, some modeling workarounds had to be used. The following table will show how these obstacles are overcome.

Reality	Model	Deviation from reality	Consequence for the results
The force is applied by tightening the strap.	The tools on Figure 7-19 move towards each other during the clamping phase. In order to avoid numerical difficulties with free surfaces going into contact, a very soft material is placed between the tools. This material has the same conductivity as copper and zero heat capacity.	The contact at the clamping surfaces might be better than the real situation.	This might make the contribution of the strap bigger. If it turns out to be a problem, the conductivity of that material can be changed accordingly.
The bulb does not deform	Tool is placed on the inside of the bulb	In reality the bulb is much stiffer because it is closed with endplates. This cannot be shown in a 2D sectional view.	The deformation figure becomes more like the reality.
Copper tube has constant temperature.	The material properties for the tube wall are changed. The heat capacity is given an unrealistically high value (106 J/kg/K).	In this context, none.	None.
The contacts between bulb/pipe, bulb/strap and pipe/strap are not perfect.	Interface layers are modelled between the contact areas. The thermal resistances of these layers can be varied.	The thermal resistances of the layers will be the variable parameter to fit the model to experimental results.	
Bulb is insulated from ambient	Heat transfer coefficient is set to 1 W/m2/K. (Value of 0 is not numerically possible)	There will be a small heat exchange with the ambient. But the insulation on the real model cannot be perfect either.	This could be a parameter to vary. But if the insulation in the test is sufficient, this model will give same results as the test.

Table 7-4: Modelling details

7.6.3 Deformation

Looking at the deformation figure, gives an idea, whether or not the model with its boundary conditions reacts like the real system in known situations.
In this case it is important to ensure that the deformation takes place on the evaporator tube and not on the bulb.

As it can be seen on Figure 7-20 and Figure 7-21 the deformation is taking place on the evaporator tube and of course the soft material in between the clamping devices of the strap.
After deformation, the contact area becomes 7,40E-5 m2.

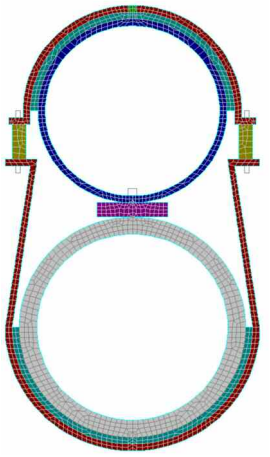

Figure 7-20: Before deformation

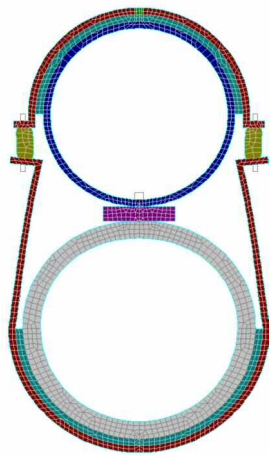

Figure 7-21: After deformation

7.6.4 Calculations:

The contact between two parts will never be as perfect in reality as it can be modelled theoretically. In order to compensate for this difference, interface layers are used. The interface layer is a material with a given conductivity and with very low heat capacity which is put in between the real contact faces. The thickness and conductivity of the interface layer will determine the heat flow between the two parts.
Basically this model needs two different interface layers, one between the strap and the bulb and one between the bulb and the pipe. The thickness of both has been set to 0,5 mm. In order to find the conductivity of them following procedure was used.
Initially a number of calculations for different conductivities of the interface layers were performed. The conductivity of one interface is varied while the other is set to 0,001 W/m/k. These analyses are comparable with the experimental results where one contact is insulated while the other is not.

7.6.5 Results:

For contact 1, it was found that a conductivity of 0,75 W/m/K for interface the layer gave the results closest to the experimental results. Whereas for contact 2 it was found that a conductivity of 0,075 W/m/K gave the closest results.
Table 7-5 shows the results obtained.

	Measured	FEM	Deviation	Deviation in %
Contact 1				
Sensor 1	144	167	23	16
Sensor 2	120	117	-3	-2,5
Sensor 3	10	10	0	0
Contact 2				
Sensor 1	48	45	-3	-6
Sensor 2	57	65	8	14
Sensor 3	149	110	-39	-26

Table 7-5: Comparison of time constants [s] for increasing temperature

7.6.6 Thermal resistance

The thermal resistance R is defined as:

$$R = \frac{l}{\lambda \cdot A} \cdot t \qquad \textbf{(7-43)}$$

Thus the thermal resistances are:

Contact	A [m2]	λ [W/m/K]	t [m]	R [K/W]
Bulb/pipe	7,40E-5	0,75	0,0005	9
Strap/bulb	4,787E-4	0,075	0,0005	13,9
Strap/evaporator tube	5,721E-4	0,075	0,0005	11,6

Table 7-6: Thermal contact resistances

7.6.7 Conclusion on the finite element simulations

The finite element calculations have given an estimate of the thermal resistances of the two contacts. These can now be used in the analytical lumped mass model. For further verification, the results from the analytical model have been compared to experiments with charged bulbs where the pressure of the bulb was measured.

7.7 Test on charged bulbs

Some tests were performed on bulbs charged with a very small amount of charge (80 mg propan). A small charge is chosen in order to limit the thermal mass of the charge. The bulbs were mounted in four different ways (Figure 7-22). Some were mounted on the top of the pipe, where the liquid charge will be close to the pipe and some underneath the pipe, where the liquid charge will be close to the strap.

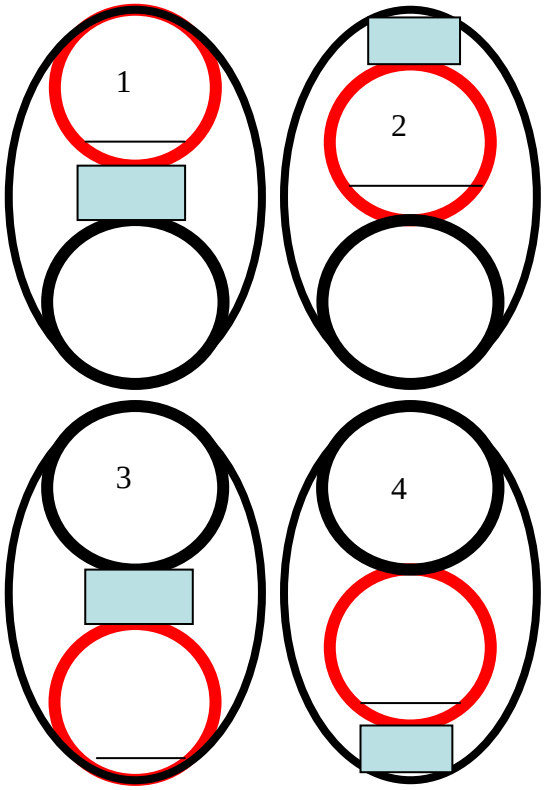

Figure 7-22: Test on charged bulbs

The bulbs are mounted differently in order to have the liquid part of the charge once close to the contact and once away from the contact. Figure 7-22 and Table 7-7 shows how each bulb is mounted.

	Mounted on top	Mounted underneath	Strap insulated	Pipe insulated
Bulb 1	X			X
Bulb 2	X		X	
Bulb 3		X	X	
Bulb 4		X		X

Table 7-7: Mounting of the four bulbs

The time constants measured for the four bulbs are shown in Table 7-8.

	Time constant up	Time constant down
Bulb 1	245	122
Bulb 2	75	15
Bulb 3	219	103
Bulb 4	127	33

Table 7-8: Time constants for the four bulbs

The right comparison for the time constant going upwards can be made between bulb 2 for Contact 1 and bulb 3 for contact 2. For the time constant going downwards on the other hand, the right comparison can be made between bulb 1 for insulated pipe and bulb 4 for insulated strap.

	Strap insulated	Pipe insulated
Time constant up	75	219
Time constant down	33	122

Table 7-9: Comparable time constants for the two contact interfaces

7.8 The analytical model

The contact resistances can be inserted in the modelled lumped mass model of the charged system based on the equations presented in this chapter.

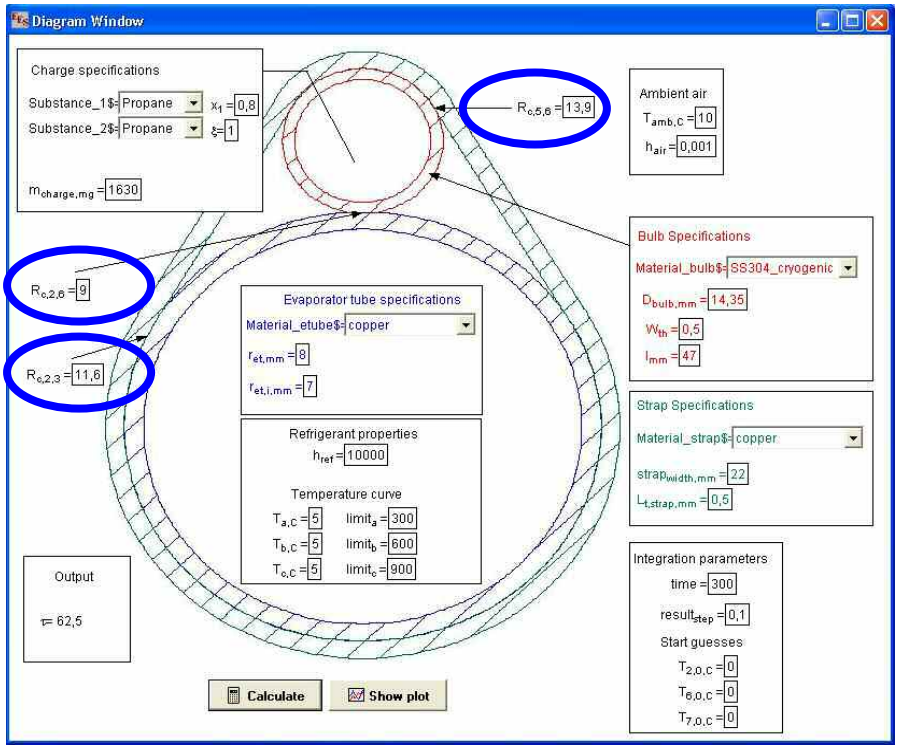

Figure 7-23: Test on charged bulbs

Inserting the given conditions, the model should be able to predict the time constants as measured on the charged bulbs. In order to see the effect of each of the two contacts, three comparisons are made. One for pipe contact only (insulated strap), one for strap contact only (insulated pipe), and one in which both contacts are active.
Furthermore one comparison is made for a larger amount of charge also with both contacts active.

7.8.1 Results:

	Test	Calculation	Deviation in %
R290 80 mg, strap contact (insulated pipe)	219	232	6
R290 80 mg, only pipe contact (insulated strap)	75	78	4
R290 80 mg (both contacts)	52	59	13
R290 1630 mg (both contacts)	62	63	2

Table 7-10: Time constants. Calculated and measured

Table 7-10 shows the measured and the calculated time constant for different mounted and charged bulbs. The deviations are probably due different mounting of the bulb. Although it has been tried to mount the bulb equally, one bulb can get a better contact than the other.
An often asked question is how much of the heat is actually transferred through the strap and how much through the direct bulb contact. This information can be extracted from the numbers in Table 7-10. The calculated time constant for the case where the pipe is insulated is about four times larger than the calculated time constant for the case where both contacts are active. This means that about 25% of the heat is transferred through the strap and the remaining 75% is transferred through the direct contact. For the test results these numbers are 23% for the strap and 70% for the direct contact. The percentages do not add to 100 because of uncertainties in the measurements.

7.8.2 Test at different ambient temperatures

In all the above tests the bulbs were insulated from ambient. Also in the calculations, the heat transfer rate to the ambient air was set to 0,001 which, compared to normal values of 5-20, is close to zero.
In the following tests, the bulbs were mounted without any insulation and tests were run at different ambient temperatures. The calculations are performed as follows:
The initial values are given and the simulation is started. After some time the system reaches a constant temperature somewhere between the pipe temperature and the ambient temperature. After reaching that state, the temperature of the pipe is changed. All tests are performed on two bulbs with 1630 mg propane (R290) in the same test setup for all ambient temperatures.

Three numbers are important for comparison of measurements and tests.

- Temperature after stabilizing but before changing pipe temperature (Ts)
- Time constant for temperature change of the charge (τ)
- Temperature after temperature change (Tf)

The unknown factor in these calculations is the heat transfer rate to the ambient air (hair). Therefore it has been tried to find a value of hair which satisfies the tests at different ambient temperatures.

The test conditions are again 0 ºC for the one bath and 5 ºC for the other. The ambient temperatures that have been tested are:

- 1ºC
- 5ºC
- 10ºC
- 20ºC

7.8.3 Results:

The results of the simulations including heat exchange with ambient at different temperatures are listed in Table 7-11.

	Test	Calculation	Deviation
1ºC (hair=4 W/m2/K)			
Ts [ºC]	-0,65	0,08	-0,57
Tf [ºC]	4,26	4,67	-0,41
τ [s]	52	58,4	-6,4
5ºC (hair=4 W/m2/K)			
Ts [ºC]	-0,23	0,39	-0,62
Tf [ºC]	5	4,98	0,02
τ [s]	58	58,4	-0,4
10ºC (hair=4 W/m2/K)			
Ts [ºC]	0,73	0,77	-0,04
Tf [ºC]	5,49	5,36	0,13
τ [s]	53	58,4	-5,4
20ºC (hair=4 W/m2/K)			
Ts [ºC]	2	1,53	0,47
Tf [ºC]	6,58	6,13	0,45
τ [s]	56	58,4	-2,4

Table 7-11: Comparison of calculated and measured data for systems at different ambient temperatures.

7.8.4 Comments on Table 7-11

Some of deviations in Table 7-11 need some attention. It seems like the measured data are not right, probably due to wrong calibration. It has been assumed, that the pressure transmitters had a constant offset. Therefore the bulbs were stabilized at 5ºC pipe temperature and with 5ºC ambient. At this point the pressures were read and corrected according to the known saturation pressure at 5ºC. This offset for each pressure transmitter was used for all data in the above test. But obviously this was not good enough, since the temperature can go below 0ºC even though the pipe is at 0ºC and the ambient is at 1ºC/5ºC.

7.9 Conclusion on the model for the heat transfer from the system refrigerant to the charge

The model presented in this chapter calculates the heat transfer between the refrigerant leaving the evaporator and the charge inside the bulb. With the input of geometrical data and material parameters the model calculates the temperature development of the charge over time. Having the temperature over time curve, the time constant can be evaluated. The model results correlate with experimental data for different charges. Furthermore it can be noted that the heat transfer through the strap equals about 20-30 % of the total heat transfer whereas the remaining 70-80% is transferred through the direct contact.

8 Charge model

The charge model has been changed and improved throughout the whole work, in order to find the most simple that works. Therefore, before presenting the final model, there will be a brief description of the development of the model.
The charged system can be considered as a two bulb system. The system is charged with a charge media and possibly some nitrogen. The important signal for the valve is the pressure in the capsule, i.e., just above the diaphragm. Determining the exact pressure in the capsule requires knowledge about the distribution of charge media and nitrogen inside the charged system and also the temperatures, respectively.

8.1 Basic two-bulb system

Depending on the initial charging procedure and the history of working conditions the distribution of liquid and gas can change. The liquid phase contains the liquid charge media, while the gas phase is a mixture of nitrogen and charge media vapour.

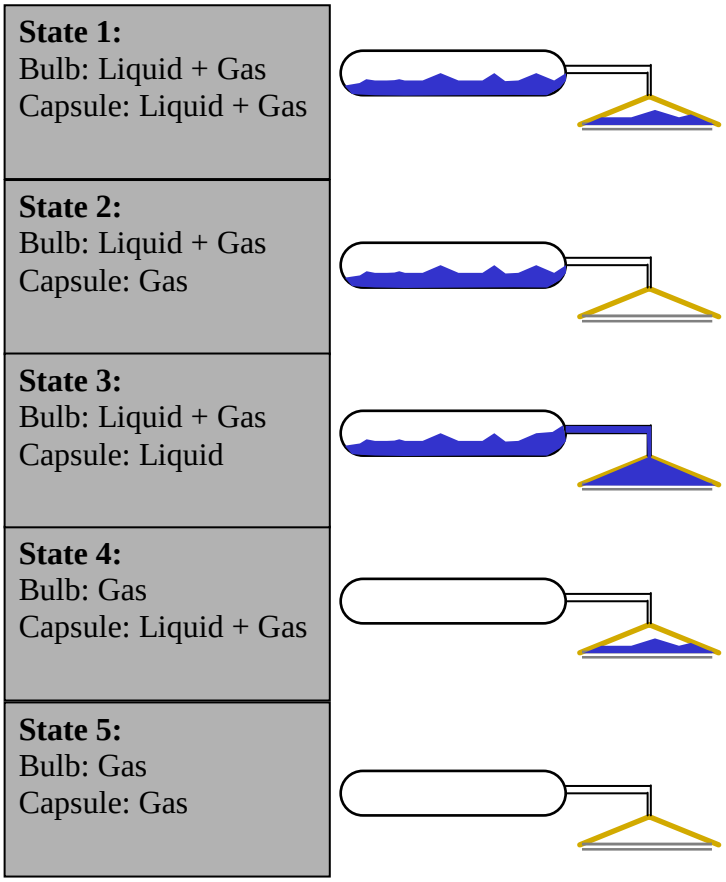

Figure 8-1: Different states of the charged system

Looking at a TXV on a refrigeration system, states 1, 2 and 3 are the three states where the valve can work properly. In states 4 and 5 there is no free liquid surface in the bulb which means that the bulb is no longer in control of the valve. State 3 can occur only for UNI charges whereas state 4 is possible only with MOP charges because of the limited

amount of charge media. The phenomenon is called charge migration and should always be avoided. But is has been included in the model in order to be able to observe this phenomenon. State 5 is where the MOP charge is above the breakpoint and the refrigeration system will feel the effect of the MOP charge i.e. the valve does not open any more for increasing temperature at the evaporator outlet. Instead the superheat increases rapidly.
The charge of a TXV will most likely shift between states 1 and either 2 or 3 while the refrigeration system runs through both on and off cycles.

8.2 The static model

The model can be shown graphically very simple. There are two volumes, the capsule and the bulb. They are connected through a capillary tube and the temperature of both of them is known.

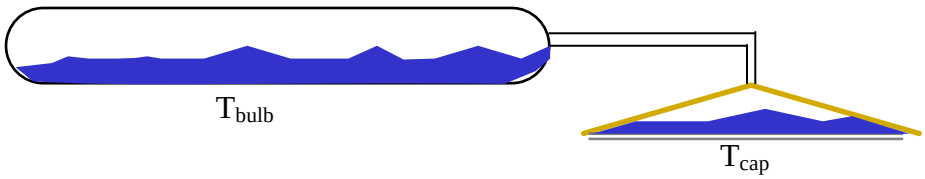

Figure 8-2: Static charge model

In order to calculate the pressure at a certain temperature, it has to be known which of the 5 states in Figure 8-1 describes the charge. For state 1 the pressure of each volume is given by:

$$P_{tot} = p_{ref} + p_{N2} \tag{8-1}$$

The partial pressure of charge is given by the saturation pressure at the corresponding temperature.

$$p_{ref} = P_{BubT}(T) \tag{8-2}$$

The partial pressure of nitrogen is given by the ideal gas law.

$$p_{N2} = \frac{m_{N2} \cdot R_{uni} \cdot T}{M \cdot V} \tag{8-3}$$

Equations (8-1) to (8-3) can be applied for both bulb and capsule. And since the system is a closed system the total mass of nitrogen is constant.

$$m_{N2\_tot} = m_{bulb\_N2} + m_{cap\_N2} \tag{8-4}$$

The connection through the capillary tube secures the mechanically equilibrium

$$P_{bulb\_tot} = P_{cap\_tot} \quad \textbf{(8-5)}$$

Equations (8-1) to (8-5) form a set of equations that determines the pressure of the system shown in Figure 8-2, assuming that the system is in state 1.

Experimental tests:

In order to test this calculation an experimental test was made.
A two bulb system was constructed. The bulbs are connected through a tube on which a ball valve was mounted. The pressure of each bulb is measured separately in order to verify that they are equal as stated in (8-5).

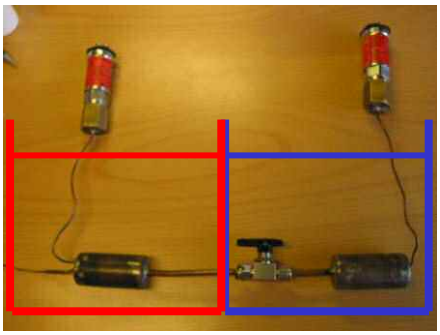

Figure 8-3: Test specimen

Figure 8-4: Test specimen in the bath

The test specimen was charged with 3010 mg propane and 0,86 bar nitrogen at 20ºC (0,003677 mol) and put in a bath where the temperature of the bath can be controlled individually for the two bulbs. Before testing, the initial mass of charge in one of the volumes has to be determined. This was done by closing the ball valve and raising the temperature of the volume that will be kept at constant temperature in the test. On the temperature pressure curve, the breakpoint of the charge can be determined and the mass of propane in that volume can be found. In this case the starting mass of the volume was 950 mg.
Initially, both baths were stabilised at 20ºC and the ball valve was opened. Then the temperature of one bath was slowly (5K/hour) decreased to 5ºC while the other was kept at 20ºC.
Figure 8-5 shows a plot of the pressure plotted as a function of the temperature of the bath that was varied. The black curve is measured, while the red curve was calculated with Equations (8-1) to (8-5).

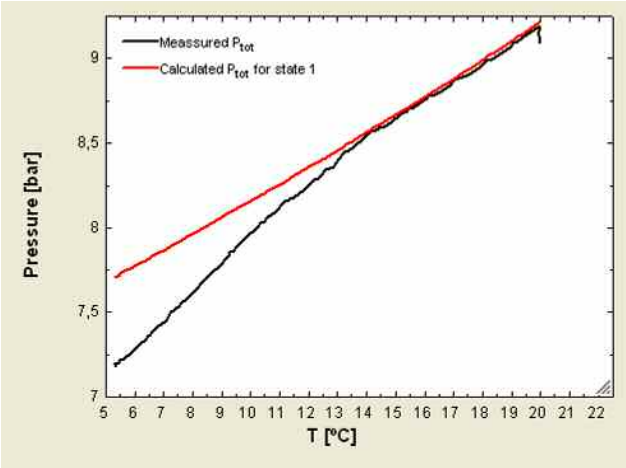

Figure 8-5: Measured and calculated pressure for two bulb system

The plot on Figure 8-5 shows that there is good agreement between calculated and measured pressure in the range from 20ºC to app. 14 ºC. Looking at the number of moles of nitrogen in the volume with varying temperature (Figure 8-6) it becomes obvious that the model does not find a physically solution, i.e. the number of nitrogen moles becomes negative at about 12,5ºC.

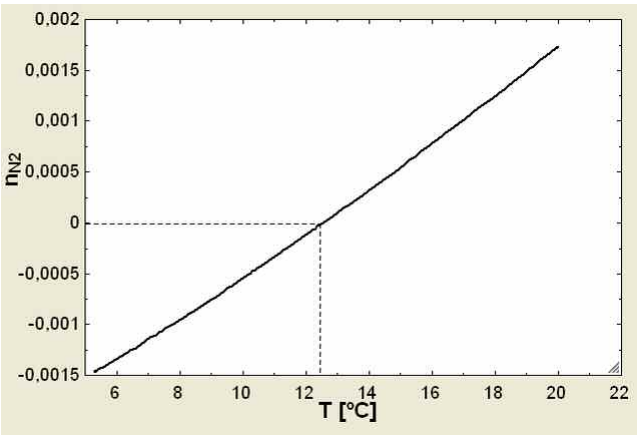

Figure 8-6: Calculated number of nitrogen moles in the volume with varying temperature

Conclusion on the test results:

The system is initially in state 1. At thermal equilibrium the pressure of propane is the same in both volumes. As soon as one volume becomes colder than the other, this will result in a lower partial pressure of propane. In order to equalize the total pressure of the volumes a small portion of a mixture of propane vapour and nitrogen will flow to the cold volume.

As the temperature difference between the volumes increases, more propane evaporates in the volume with high temperature and a mixture of propane vapour and nitrogen flows to the cold volume where the propane condenses while the nitrogen concentrates

and thereby builds up a higher partial pressure of nitrogen. This process can keep on until one of two scenarios is seen.

1. All nitrogen has moved to the cold volume
2. The last drop of propane has evaporated in the warm volume

If all nitrogen has moved to the cold volume, the last liquid has to evaporate before the system can decrease the pressure further. The point where this happens can be predicted with the model presented in Equations (8-1) to (8-5).
But if there is only a little amount of liquid in the warm volume, it is very likely that the last drop of liquid will be evaporated before all nitrogen has moved to the cold volume. In either case, the system will from that point be characterised by state 2 in Figure 8-1.
In state 2 the pressure of the volume which does not contain liquid has to be calculated differently than in state 1. The pressure is no longer the saturation pressure, but the pressure of a superheated gas mix of nitrogen and propane gas.
For a charge model it is necessary to be able to determine the points where the system shifts from one state to another. Therefore a complete model needs to calculate the mass of propane in each volume at each temperature. This can only be realized by using a dynamic model that takes its starting point in a specified start state and thereafter keeps track of the movement of mass in the system.

8.3 The dynamic model

Again the model can be shown graphically very simple. There are two volumes, the capsule and the bulb. They are connected through a capillary tube. But this time the temperature is not specified. Instead the heat input is specified.

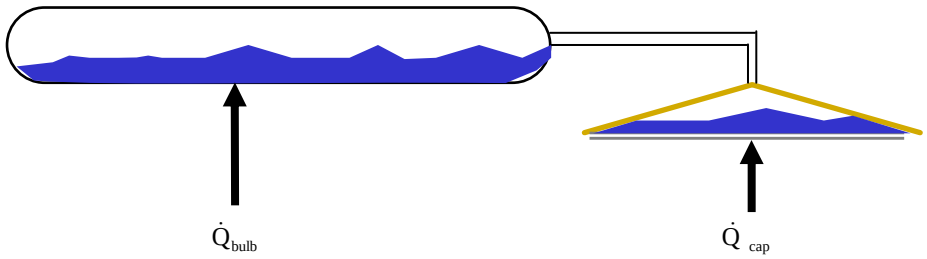

Figure 8-7: Dynamic charge model

The model starts in thermal and mechanical equilibrium and with a liquid and a gas phase in both volumes. As the temperatures of the volumes start changing, the model calculates the transport of mass and energy between the volumes.
The dynamic variables for the calculation are the masses of charge media, the masses of nitrogen and the internal energy for bulb and capsule. With known masses, volumes and internal energy, the state of the charge can be evaluated.

8.3.1 Assumptions:

The following assumptions have been made for the charge model:

1. No liquid is transported from one volume to the other.
    a. Only exception is in state 3 where only liquid is transported between the volumes.
2. The temperature is uniform throughout the whole volume.
3. The capsule volume is held constant. In reality the volume changes as the diaphragm deflects.
4. The volume of the capillary tube is not considered. (If the temperature of the capillary is the same as either bulb or capsule, the volume can be added respectively).

8.3.2 State shift

As the simulation runs, the model continuously evaluates which state describes the model. Figure 8-8 shows which state shifts are set up in the model.
The model always starts in state 1. The arrows show the possible connections between the states.

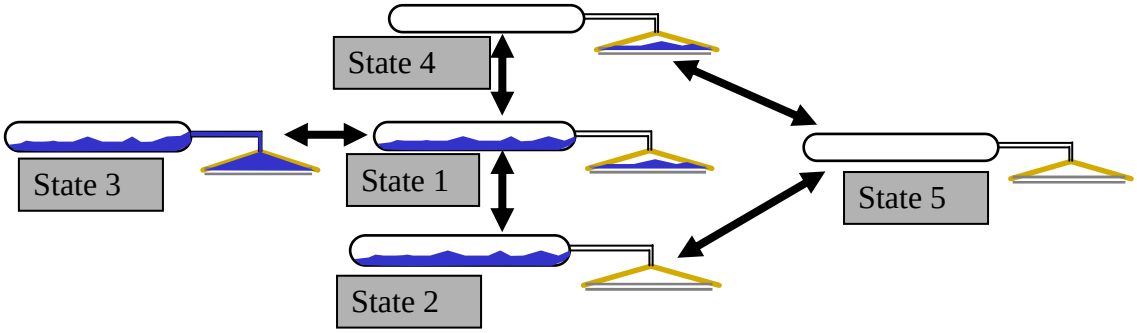

Figure 8-8: States

If the model detects a state change it has some routines to find the time for the state change more precisely. After the state change it increases the step size again. The model uses the volume fraction of liquid (fg) [13] in both bulb (8-6) and capsule (8-7) to determine state shifts.

$$fg_{bulb} = \frac{\frac{m_{bulb}}{V_{bulb}} - \rho_{GAS}(T_{bulb})}{\rho_{LIQ}(T_{bulb}) - \rho_{GAS}(T_{bulb})} \quad \textbf{(8-6)}$$

$$fg_{cap} = \frac{\frac{m_{cap}}{V_{cap}} - \rho_{GAS}(T_{cap})}{\rho_{LIQ}(T_{cap}) - \rho_{GAS}(T_{cap})} \quad \textbf{(8-7)}$$

If the volume fraction of liquid is 1, the volume is filled with liquid. If it is 0, the volume is filled with gas.

8.3.3 Model structure

In the following, the equations for situation 1 will be presented first. These equations also form basis for the other states, but some corrections need to be made for each state. These will be explained in the next chapter.
As mentioned previously, the only parameter that is important for the opening degree of the TXV is the pressure of the capsule. The pressure of the capsule is the sum of the partial pressures for each of the components.

$$P_{cap\_tot} = P_{cap\_ref} + P_{cap\_N2} \quad \textbf{(8-8)}$$

The partial pressure of charge is given by the saturation pressure at the capsule temperature.

$$P_{cap\_ref} = P_{sat} \quad \textbf{(8-9)}$$

The partial pressure of nitrogen is given by the ideal gas law.

$$p_{cap\_N2} = \frac{R_{uni} \cdot T_{cap}}{v_{cap\_N2}} \quad \textbf{(8-10)}$$

The temperature and the specific volume have to be calculated. Therefore some more equations have to be introduced.

The internal energy can be expressed as:

$$U_{cap} = u_{cap\_LIQ} \cdot m_{cap\_LIQ} + u_{cap\_GAS} \cdot m_{cap\_GAS} + u_{cap\_N2} \cdot m_{cap\_N2} \quad \textbf{(8-11)}$$

The specific internal energies are given by (8-12) for the liquid phase, (8-13) for the propane vapour and (8-14) for the nitrogen.

$$u_{cap\_LIQ} = h_{cap\_LIQ} - P_{cap\_ref} \cdot v_{cap\_LIQ} \quad \textbf{(8-12)}$$

$$u_{cap\_GAS} = h_{cap\_GAS} - P_{cap\_ref} \cdot v_{cap\_GAS} \quad \textbf{(8-13)}$$

$$u_{cap\_N2} = h_{N2} - \frac{R_{uni} \cdot T_{cap}}{MW_{N2}} \quad \textbf{(8-14)}$$

The mass of liquid charge is given by:

$$m_{cap\_LIQ} = V_{cap\_LIQ} \cdot \rho_{cap\_LIQ} \quad \textbf{(8-15)}$$

The mass of propane vapour is given by

$$m_{cap\_GAS} = V_{cap\_GAS} \cdot \rho_{cap\_GAS} \quad \textbf{(8-16)}$$

The total mass of propane is the sum of that of the the vapour and the liquid.

$$m_{cap} = m_{cap\_LIQ} + m_{cap\_GAS} \quad \textbf{(8-17)}$$

In the same way, the volume is the sum of the volumes of vapour and liquid.

$$V_{cap} = V_{cap\_GAS} + V_{cap\_LIQ} \quad \textbf{(8-18)}$$

Equations (8-8) through (8-18) can be applied for the bulb as well.
The transport of propane between the bulb and the capsule is then determined by:

$$\frac{dm}{dt} = A_{capillary} \cdot c \cdot \sqrt{2 \cdot \rho_{GASMIX} \cdot \Delta P} \quad \textbf{(8-19)}$$

$$\frac{dm_{N2}}{dt} = \dot{m}_{bulb} \cdot x_{GAS} \quad \textbf{(8-20)}$$

$$\frac{dU}{dt} = \dot{m} \cdot h_{GASMIX} + \dot{Q} \quad \textbf{(8-21)}$$

The enthalpy and density of the gas mixture is given by equation (8-22) and (8-23) respectively.

$$h_{GASMIX} = (1 - x_{GAS}) \cdot h_{GAS} + x_{GAS} \cdot h_{N2} \quad \textbf{(8-22)}$$

$$\rho_{GASMIX} = (1 - x_{GAS}) \cdot \rho_{GAS} + x_{GAS} \cdot \left(\frac{P_{N2}}{R_{uni} \cdot T \cdot MW_{N2}} \right) \quad \textbf{(8-23)}$$

The parameter x_{bulb_GAS} is the mass fraction of nitrogen in the gas phase.

$$x_{GAS} = \left(\frac{m_{N2}}{m_{GAS} + m_{N2}} \right) \quad \textbf{(8-24)}$$

The heat supplied to the bulb is given by equation (8-25).

$$\dot{Q}_{bulb} = Q_{dot\_factor} \cdot (T_{final} - T) \quad \textbf{(8-25)}$$

Enthalpy calculations for nitrogen:
The enthalpy as a function of temperature for nitrogen has been estimated by a linear fit of data supplied by the database software Refprop [14]. Figure 8-9 shows some enthalpy/temperature curves for different pressures throughout a temperature range.

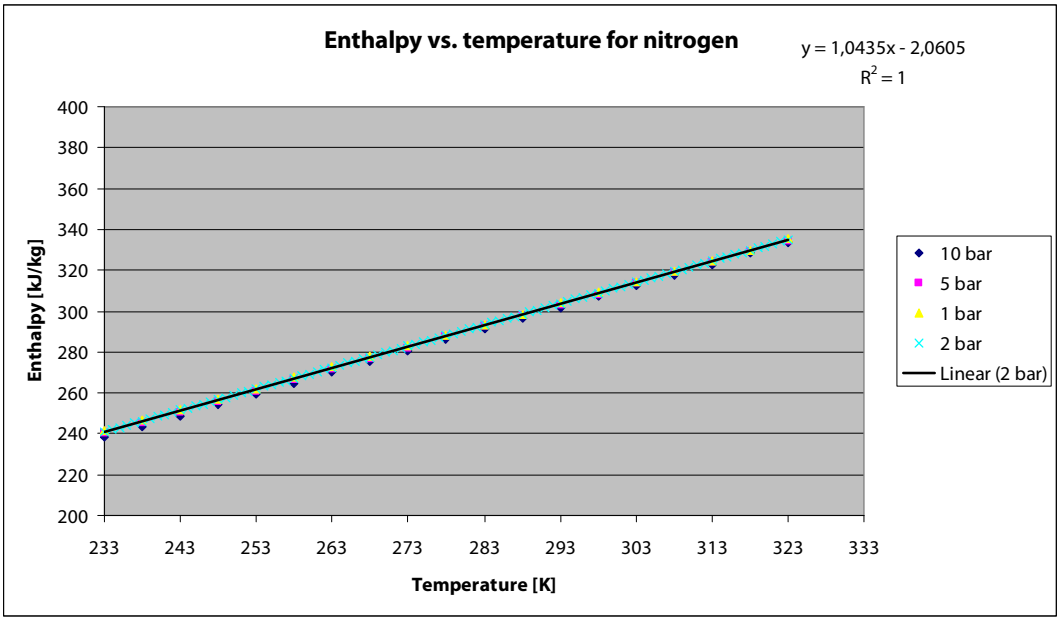

Figure 8-9: Enthalpy vs. temperature for nitrogen

From Figure 8-9 it has been assumed that the enthalpy only changes with temperature and not with pressure. In the model the enthalpy is therefore calculated from the linear fit in units as shown in Figure 8-9.

$$h_{N2} = 1{,}0435 \cdot T + 2{,}0605 \qquad \textbf{(8-26)}$$

8.3.4 Modifications of equations for state 2, 3, 4 and 5

In the previous chapter the equations for state 1 were presented. These equations also form the base for the other states. But for each state there are small differences that will be presented here.
In state 2 the bulb is calculated in the same way as in state 1. But the capsule is calculated differently. Equation (8-9) changes because the pressure of the charge media is not the saturation pressure, but the pressure of superheated gas. Also, the liquid volume and the liquid mass of the charge media can be set to zero which simplifies the calculations. In state 4 the capsule is calculated like in state 1 and the bulb is calculated with the above described changes. In state 5 both volumes contain only superheated gas and the liquid mass and volume can therefore be set to zero for both volumes.
State 3 is somehow different. Here the volume of gas in the capsule can be set to zero and the amount of nitrogen is also zero. The liquid needs to be calculated as a sub cooled liquid. Also the transport equations (8-19)-(8-21) need to be rewritten in order to transport liquid instead of gas. If the flow direction is from the capsule to the bulb the transport equations become (8-27)-(8-29).

$$\frac{dm}{dt} = A_{capillary} \cdot c \cdot \sqrt{2 \cdot \rho_{LIQ} \cdot \Delta P} \quad \textbf{(8-27)}$$

$$\frac{dm_{N2}}{dt} = 0 \quad \textbf{(8-28)}$$

$$\frac{dU}{dt} = \dot{m} \cdot h_{LIQ} + \dot{Q} \quad \textbf{(8-29)}$$

For information on the implementation of the above stated equations, please refer to the enclosure with the source code for the model.

8.3.5 Parameters

Before simulation start, some parameters need to be set. In this section the parameters will be explained. Figure 8-10 shows the parameter page in the simulation model.

The flow coefficient is the coefficient c in the transport equation (8-19).
The diameter of the capillary tube is used to calculate the flow area.
The amount of charge is the total amount of charge media for both volumes.
The initial N2 pressure is the nitrogen pressure after charging at the temperature specified below.
The above initial nitrogen pressure is only valid at this temperature.
Bulb volume is the total volume of the bulb.
Initial bulb temperature is the temperature for the bulb at simulation start.
Final temperature of the bulb is the new set point for the temperature surrounding the bulb. (8-25).
The Q_dot_bulb factor is the value that determines the heat flux for the bulb. (8-25).
Similar parameters are set up for the capsule.

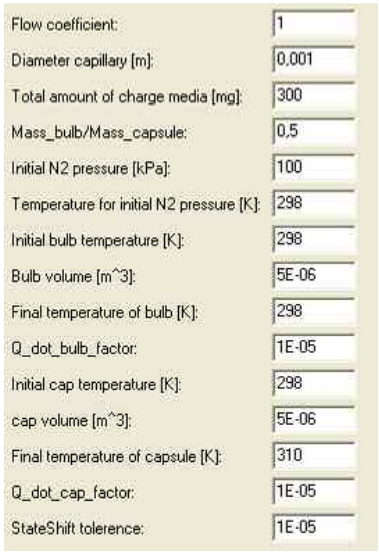

Figure 8-10: Parameters

The state shift tolerance refers to the detection of state shifts. The state shifts are determined in the way that they have to cross the boundary by the value specified here before they actually change state. Setting this value too small, the model will constantly switch between two states. Unless there is a problem with state shifts, this value should not be changed.

Having set these parameters, the model is ready for simulation. For different simulation options please refer to the WinDali documentation [16].

8.3.6 Using the model

The main purpose of the model is to see how the charge behaves under dynamic conditions. First of all it is interesting to give the model the same data as the static model presented in chapter 8.2 and compare the results with the same experiment as the static model was compared to (Figure 8-5).

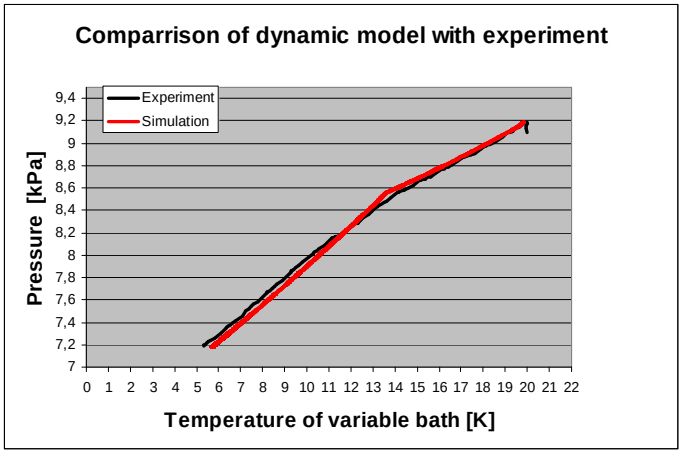

Figure 8-11: Comparison of experimental data with model results

The plot on Figure 8-11 shows the calculated and the experimental pressure of the two bulb system described in chapter 8.2. A brief reminder:
Two bulb system charged with 3010 mg propane and 0,86 bar nitrogen at 20ºC.
Both bulbs stabilized in baths at 20ºC.
Temperature of one bath decreased to 5ºC with 5 K/hour while the other bath is kept at 20ºC.

The red curve is calculated whereas the black curve is measured. The dynamic model detects the point where the last drop of liquid in the warm volume evaporates and the slope of the pressure curve changes. The same trend is seen in the experiment. But there is a difference in the transition phase from state 1 to state 2. The model detects the point of change and changes equations, whereas in the experiment the change does not happen in one point but takes place continuously from about 13ºC to 10ºC.
In the temperature range where the system changes state, there might not necessarily be thermodynamic equilibrium. The gas phase might be slightly superheated before the last drop of liquid evaporates. The phenomenon is seen in diffuse phase transitions which has been described in [8]. The model assumes thermodynamic equilibrium for each volume individually. Therefore the change of state takes place at one certain point on the curve.

8.4 New test setup

During the combined effort of testing and simulating, it was realized that a new test setup was needed in order to minimize the uncertainties. In the new setup two things were changed.

1. Each of the two bulbs can be charged individually (Figure 8-13).
2. The bulbs and the bath were made in glass in order to be able to determine the state of the system visually (Figure 8-12).

The first change implies that the connection between the bulbs can be closed and the bulbs charged individually. That way the start mass of both bulbs is known. The second change was made in order to test visually if the slope change of the pressure curve really is caused by a state shift. The new bulbs were made of glass. Therefore it was possible to see whether there was liquid in the bulbs or not. It was not possible, though, to determine the exact point were the last drop evaporates. A picture of the new test setup is shown in Figure 8-12.

Figure 8-12: New test setup with glass bulbs

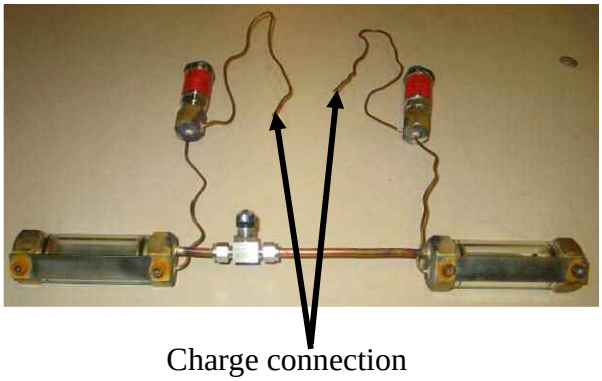

Figure 8-13: Two bulb system in glass

As long as there was relatively much liquid in the bulbs it was easy to spot. But for small amounts of liquid it was not easy to determine whether there was liquid in the bulbs or not. Figure 8-14 shows a bulb with liquid propane. In this case it is very clear that there is a liquid phase.

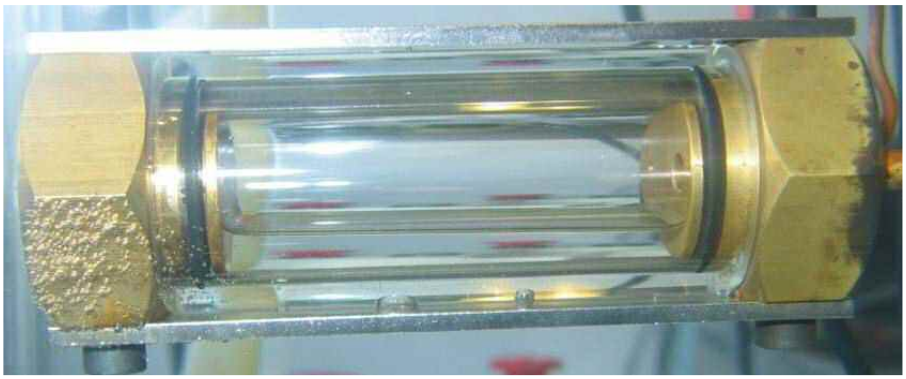

Figure 8-14: Glass bulbs with liquid propane

8.4.1 Comparison of model with new test setup

The bulbs were each charged with 1500 mg propane and an initial nitrogen pressure of 1,15 bar at 5ºC. Since the system was charged at 5ºC, the test was started at that temperature. One bath was kept at 5ºC while the other was slowly changed to 20ºC. Figure 8-15 shows the temperature/ pressure curve for the experiment (black curve). The red curve is the simulated curve.

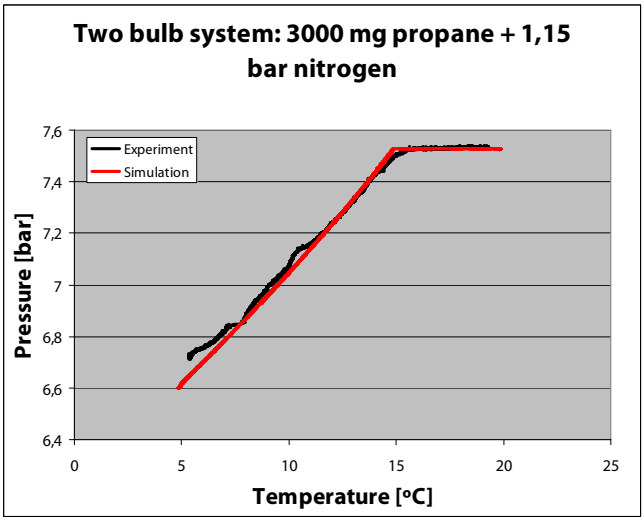

Figure 8-15: Comparison of experimental data with model results

Again it can be seen that the curve changes slope during the test. And looking at the glass bulbs it was noted that at 12 ºC there was still liquid in both bulbs whereas at 18ºC there was clearly no liquid in the bulb at high temperature. Like in Figure 8-11 the change of state is more sudden in the model than in the experiment.

8.5 Dynamic behaviour of charges in cyclic tests

It has been mentioned in the introduction, that this work was initiated by the observation of a strange observation during cyclic tests. The observation will be described in this chapter. After this, the observation will be explained using the model presented.

8.5.1 Observation

A test was made in order to find the temperature/ pressure curve for a recent developed charge. The setup was a bulb which was connected to a pressure transmitter through a capillary tube (Figure 8-16). The fitting between the capillary tube and the pressure transmitter has an internal volume of the same size as a capsule on the valve.

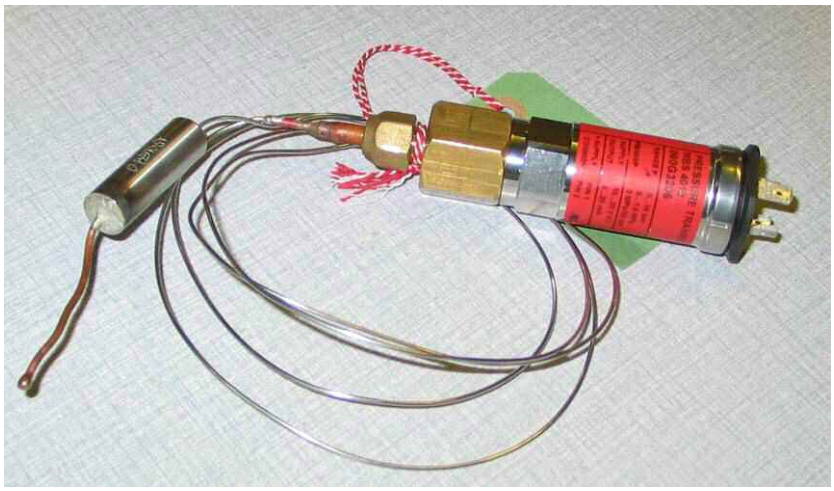

Figure 8-16: Bulb connected to pressure transmitter

The system was charged with propane and a partial pressure of nitrogen. Since the connection between the two volumes cannot be closed the distribution of propane and nitrogen after charging cannot be determined. The test was performed in the following steps:

1. The bulb was put in one bath while the pressure transmitter was held at room temperature (25ºC).
2. The temperature of the bath was decreased from 20ºC with 1 K/hour to -20ºC
3. The temperature of the bath was increased back to 20ºC with 1 K/hour

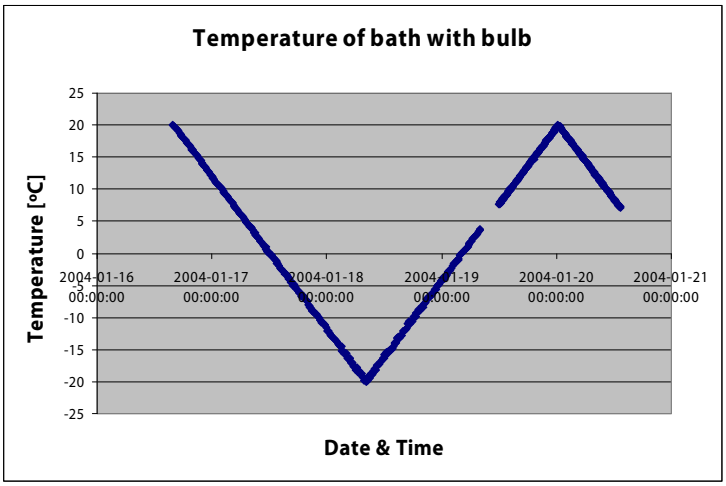

Figure 8-17: Temperature of bath with bulb over time

Plotting the pressure of the system as a function of the temperature of the bath with the bulb shows that there is no unambiguous relation between the bath temperature for the bulb and the pressure of the bulb, while keeping the capsule at room temperature (Figure 8-18).

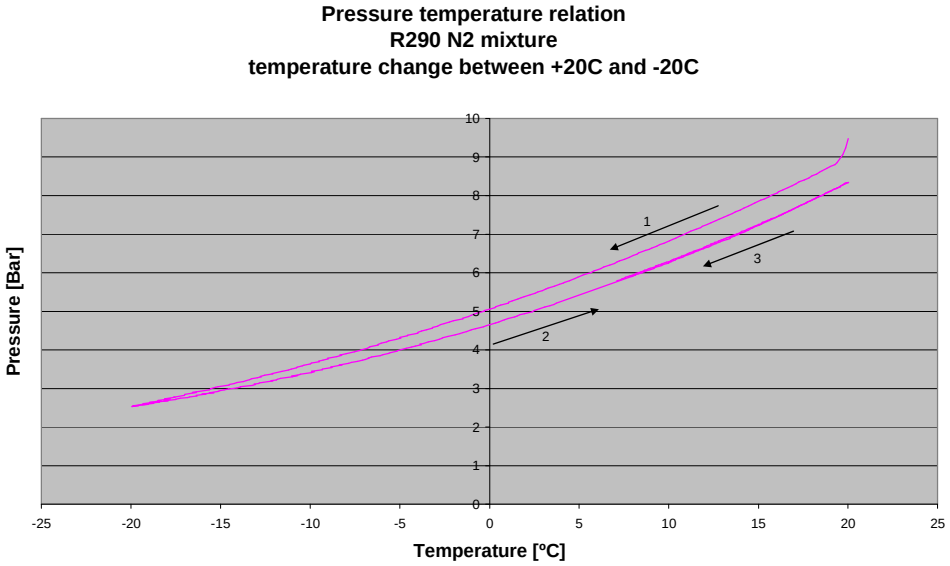

Figure 8-18: Measured temperature/pressure curve

In practice this means that the valve changes setting during operation.
The assumption was that the difference in pressure at the same temperature was due to a relocation of the nitrogen in the system.

8.6 Explanation of observations

Using the simulation model presented, it becomes clearer what happens inside the system, when the capsule is held at constant temperature while the temperature of the bulb is varied. In general there are two phenomena showing almost the same trend. One of them is as suspected the relocation of nitrogen. Another effect is the internal transport of energy that influences the temperature of both volumes. In the following, the two phenomena will be shown individually.

8.6.1 The effect of the transport of internal energy

In all experiments the temperatures of the bulb and capsule have been controlled by putting them in a bath of a certain temperature. It was assumed that the charge inside the bulb and capsule would always have the temperature of the bath they were in. In other words, the internal heat transfer was assumed to be negligible. The simulation model shows that in some cases this is true, whereas in other situations the internal heat transfer plays a significant role. The latter is especially seen where the system stays in state 1. Therefore an example will be shown where the internal heat transfer has visible influence on the system. Figure 8-19 shows the parameters chosen for this example. It has been chosen to start the simulation at 293 K with 3000 mg propane and almost no nitrogen (1 kPa) in order to eliminate the effect of the redistribution of nitrogen. With 3000 mg experience shows that the system stays fairly long in state 1. The heat transfer coefficients for both volumes are set to 0,0001. In the simulation, the temperature of the bulb is varied between 293 K and 280 K, while the temperature of the capsule is kept at 293 K. Trying to go below 280 K on the bulb temperature will result in a state shift, which is not wanted in this example.

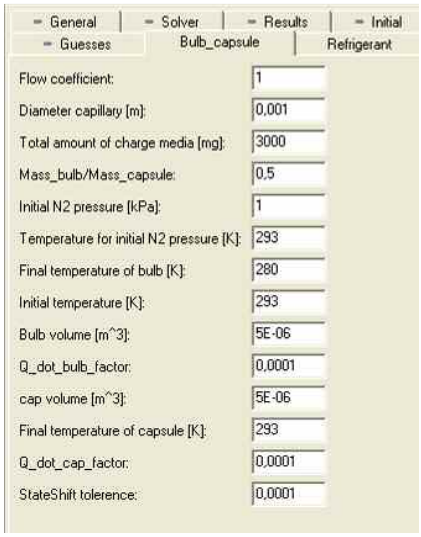

Figure 8-19: Input parameters

Figure 8-20 shows the temperatures for bulb and capsule. Even though the set point for the capsule is at 293 K, the temperature follows the bulb temperature closely. This temperature drop is caused by the internal energy transport.

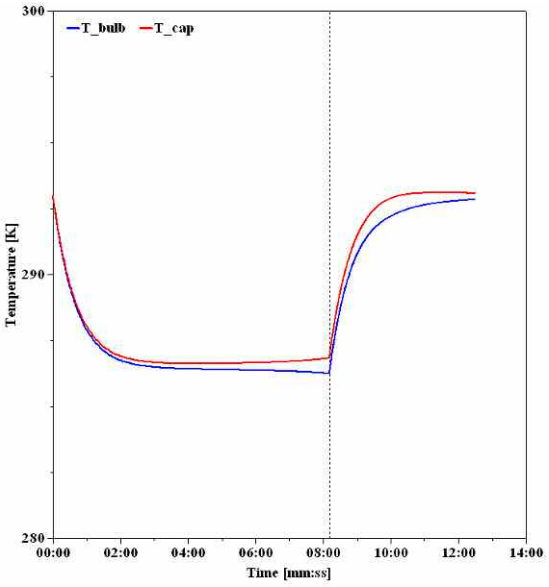

Figure 8-20: Temperature curves for bulb and capsule

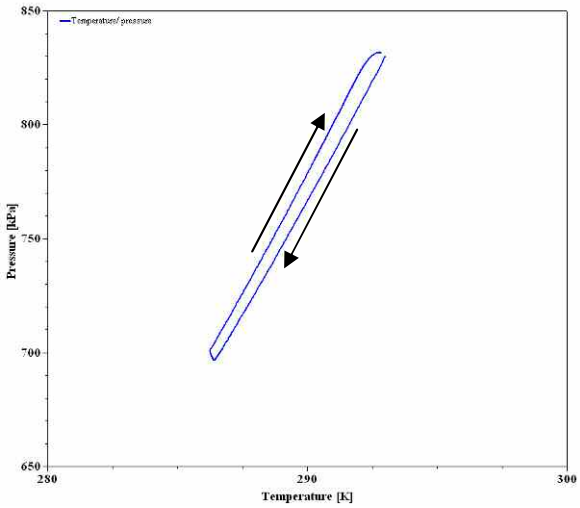

Figure 8-21: Simulated temperature/pressure curve

The temperature/ pressure curve on Figure 8-21 shows that the temperature /pressure curve is different for decreasing and increasing temperature. This is seen because the plot in Figure 8-21 does not take variation in the capsule temperature into account. This is an important point to remember during experimental testing where the temperature is measured in the bath surrounding the volume, but not inside the volume. Nevertheless, the pressure returns to the initial value after the cycle.

8.6.2 Relocation of nitrogen

In order only to see the effect of the relocation of nitrogen, it has to be ensured that the heat transfer from the outside is sufficiently larger than the internal energy transport. That way the temperature of the volumes can be controlled. To ensure that the capsule temperature does not vary due to internal energy transport, the Q_dot_cap_factor is set to 0,01 while the Q_dot_bulb_factor is set to 0,0001. All parameters set for the simulation are shown in Figure 8-22.
Figure 8-23 shows that the capsule temperature stays constant at its set point while the bulb temperature is varied.

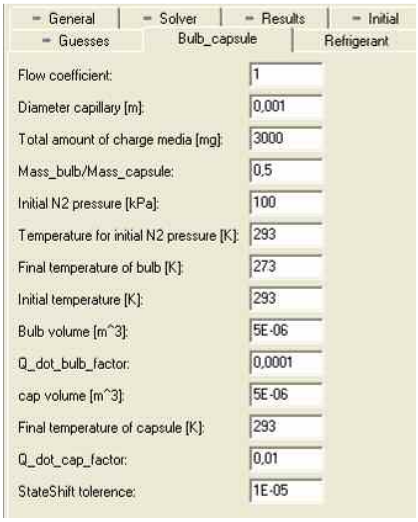

Figure 8-22: Parameters set for simulation

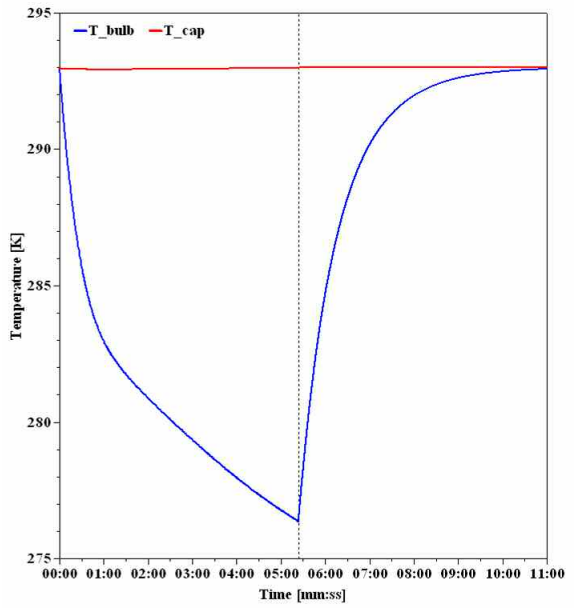

Figure 8-23: Temperature curves for bulb and capsule

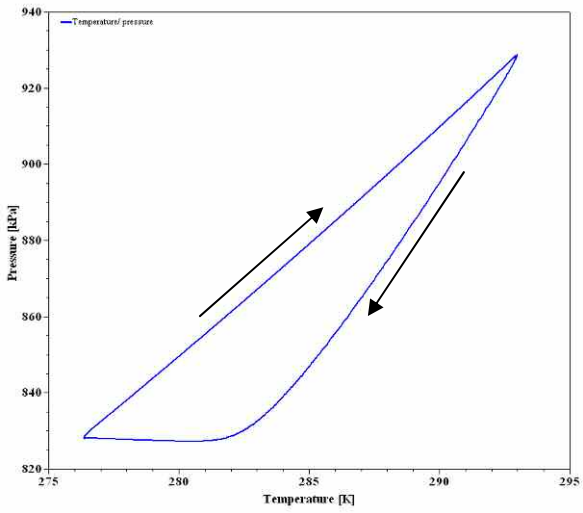

Figure 8-24: Measured temperature/pressure curve

Figure 8-24 shows a plot of the pressure as function of the temperature of the bulb. The lower part of the curve is for the decrease of temperature whereas the upper part is for

the increase of temperature. An important observation is that even though the pressure curve is different for increasing and decreasing temperature, the pressure does return to its origin as soon as the temperatures equalize.

In order to understand the difference of the two curves, it helps to looks at the movement of nitrogen in the system. Figure 8-25 shows the amount of nitrogen in the two volumes during the simulation. Figure 8-26 shows the volume fraction of the liquid phase for the bulb and the capsule.

As soon as the temperature of the bulb becomes lower than the temperature of the capsule, a small portion of a mixture of propane vapour and nitrogen flows to the bulb. The propane will condense whereas the nitrogen builds up a higher partial pressure to compensate for the lower saturation pressure of the propane. This process keeps going until no more nitrogen is left in the capsule. Thereafter the pressure cannot be decreased. The remaining process is only movement of propane from the capsule to the bulb.
For increasing temperature of the bulb, the flow changes direction. A mixture of nitrogen and vapour starts flowing to the capsule and the pressure increases. As the temperature of the bulb approaches the temperature of the capsule, the mass flow approaches zero. Equilibrium is reestablished. But it is important to notice that the amount of nitrogen does not return to its origin. This is because the partial pressure of nitrogen has to be the same in both volumes. And because of the mass flow during the process, the capsule now contains more liquid and thereby has less volume for the gas phase. Therefore it takes less nitrogen to build up the same partial pressure.

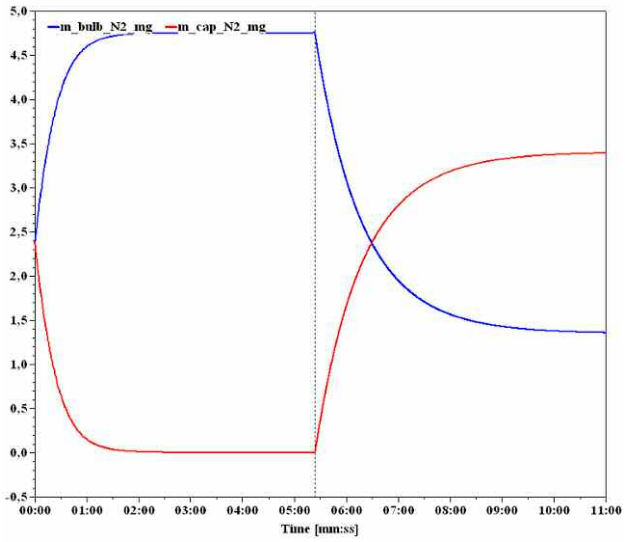

Figure 8-25: Mass of nitrogen [mg] in bulb and capsule

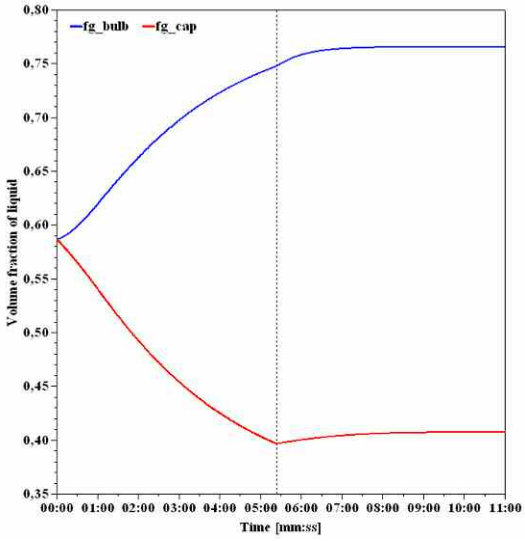

Figure 8-26: Volume fraction of liquid in bulb and capsule

Figure 8-26 shows that during the simulation, liquid has evaporated in the capsule and has condensed in the bulb. There is still liquid in both volumes but the distribution has changed.

The concluding remark on this simulation is that the distribution of nitrogen and propane has changed, but the system does return to the same pressure for equal temperatures.

In the next simulation it will be shown what happens when so much propane is transported that the liquid phase in the capsule disappears, i.e. the system changes from state 1 to state 2.

The only change in parameters shown in Figure 8-22 is that the mass of propane has been set to 300 mg instead of 3000 mg.
The temperature variation is run through three cycles in order to show the effect of the state change. The temperature curves are shown in Figure 8-27. The red dotted lines indicate a state change in the model, whereas the black dotted lines indicate a change of the bulb temperature set point. Figure 8-28 shows the state of the model during the simulation.

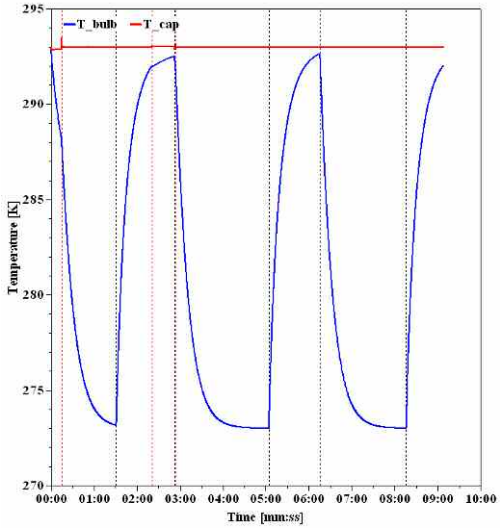

Figure 8-27: Temperature curves for bulb and capsule

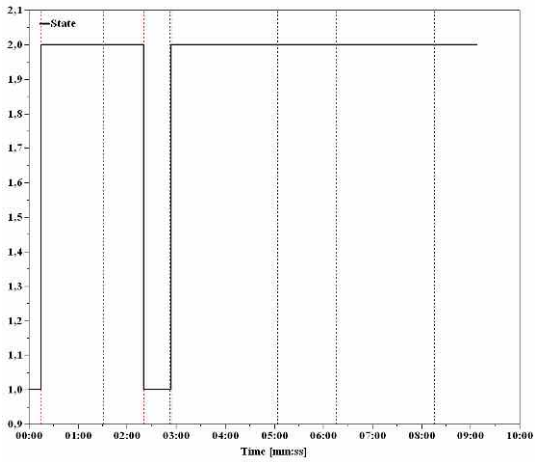

Figure 8-28: State of the model

Figure 8-28 shows that the model starts in state 1 and shifts to state 2. Later it returns shortly to state 1 before it changes to state 2 for the remaining time.

Figure 8-29 shows the bulb pressure as a function of the bulb temperature. The curve looks somewhat different than in the previous simulation (Figure 8-24). The very first part of the curve is for the system at state 1. Then it changes slope at the state change. This was already seen in Figure 8-11 where the model was compared to experimental data. The pressure increases at a lower level but returns to the original pressure. Just before that the model changed back to state 1, which means that the capsule does contain liquid again. But as soon as the temperature starts decreasing, the model changes back to state 2 and the pressure decreases at an even lower level than before. Next time the temperatures are equalized, the system is still in state 2 and the pressure does not return to its origin. This continues for the remaining cycles.

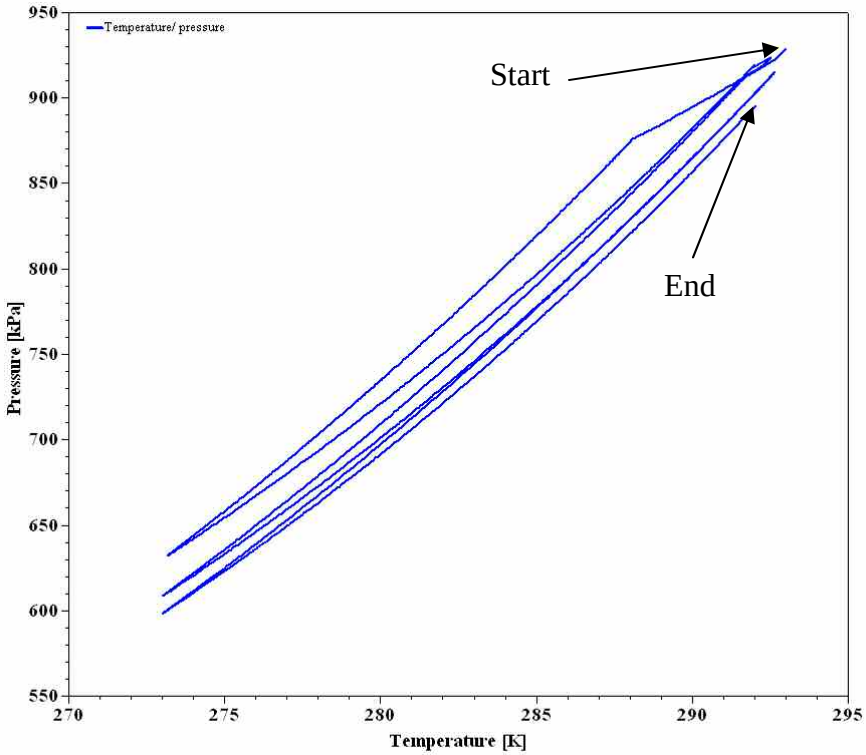

Figure 8-29: Temperature pressure curve for bulb

Figure 8-30 and Figure 8-31 show the mass of nitrogen and the volume fraction of liquid respectively.

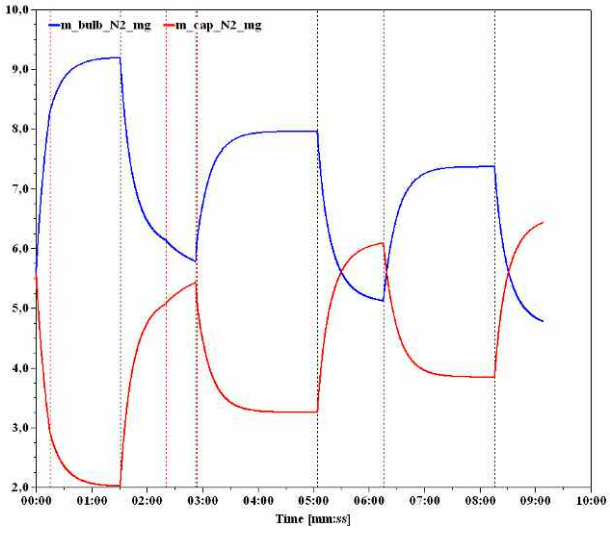

Figure 8-30: Mass of nitrogen [mg] in bulb and capsule

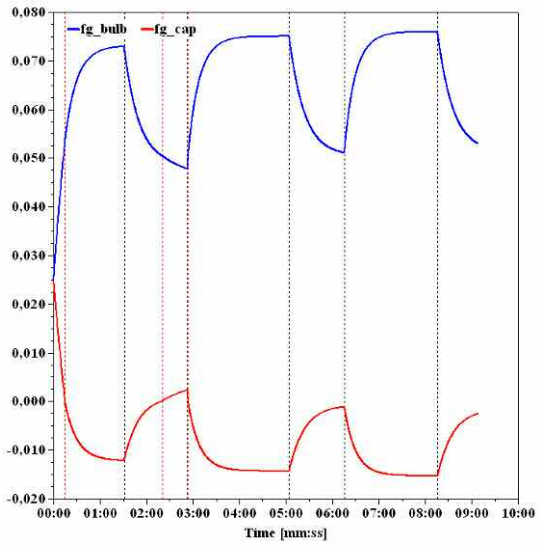

Figure 8-31: Volume fraction of liquid in bulb and capsule

Now it has been shown what most likely has caused the pressure loss in the experiment described in chapter 8.5.1 starting on page 59. The system has changed from a starting

point where both volumes contained some liquid to at state where one volume only contains vapour and nitrogen.
The above example shows that the total pressure of the system decreases during the cyclic experiment. In the next example the same test as above will be run through more cycles in order to see if the pressure level will stabilize.

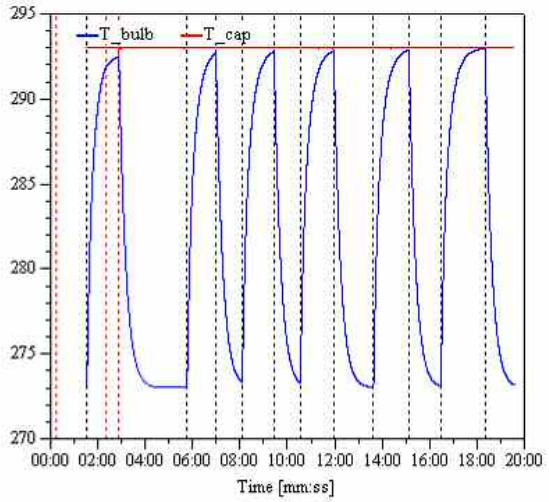

Figure 8-32: Temperature curves for bulb and capsule

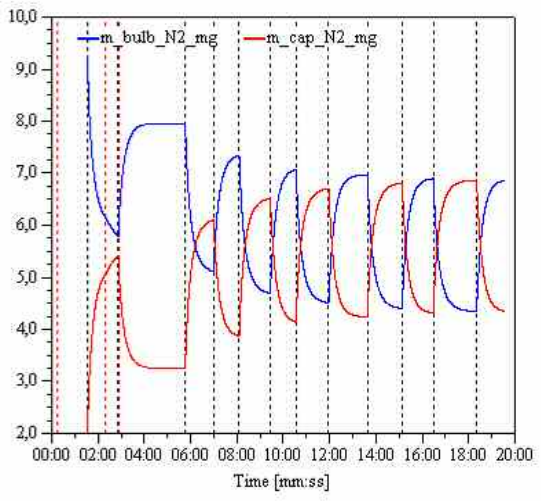

Figure 8-33: Mass of nitrogen [mg] in bulb and capsule

Figure 8-32 shows the temperature variation throughout the simulation. Figure 8-33 shows the mass of nitrogen in the bulb and capsule. Figure 8-33 shows that the mass of nitrogen at a certain temperature seems to stabilize after 5 cycles. Looking at the temperature pressure curve for the bulb in Figure 8-34 it also becomes clear that the pressure has stabilized at a lower level than the starting point. Figure 8-35 shows the variation in the partial pressure of nitrogen in the bulb.

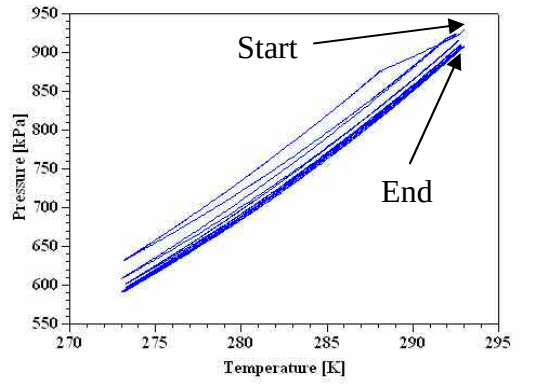

Figure 8-34: Temperature pressure curve for bulb

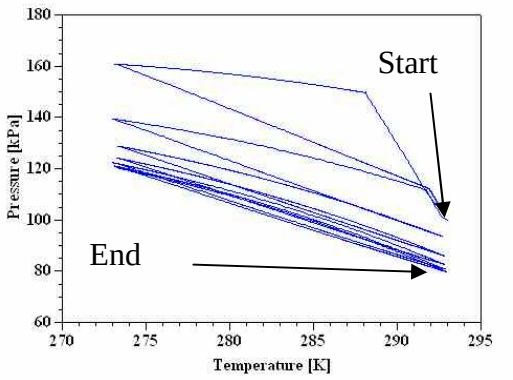

Figure 8-35: Partial pressure of nitrogen as a function of bulb temperature

The simulations show that the pressure level decreases for some cycles and stabilizes at a lower level than initially.

8.7 Discussion on the use of the model

The purpose of building the model was to get a better understanding of the two bulb system on the TXV. There had been some observations that could not really be explained and definitely not quantified. Through building and using the model, it now becomes easier to understand and even quantify the phenomenon of loosing pressure in cyclic tests.
It has been shown that the temperature/pressure curve changes for different distributions of charge media (propane in the examples) and nitrogen. One important point is that the pressure will be the same at equal temperatures of bulb and capsule as long as there exists a liquid phase in both of them, i.e. the system is in state 1. If the liquid of one volume evaporates totally during the test, the pressure will decrease. Remembering Figure 4-8 and Figure 4-9 the superheat setting of the valve will change due to this pressure decrease. The system will get back to its initial pressure as soon as there is liquid in both volumes again. This can be ensured by cooling the volume with superheated gas below temperature of the volume containing liquid. The problem with a valve on a refrigeration system is that the temperatures of bulb and capsule are not constantly monitored. Therefore, besides explaining the phenomena, the aim of using this model is also to try to find the parameters that Danfoss can change in the valve design in order to minimize this phenomenon.
Now, having understood the phenomenon it becomes obvious that minimizing it means that the fraction of nitrogen that can move to the capsule has to be minimized. This can basically be done in two ways.

1. Raise the mass of nitrogen in the system
    a. Raise the initial nitrogen pressure
    b. Increase the gas volume of the total system
2. Decrease the space available for gas in the capsule
    a. Decrease capsule volume
    b. Increase liquid phase in the capsule

Possibility 2 b cannot be realized for MOP charges. Therefore the most feasible way to minimize the phenomenon is to increase the bulb volume, decrease the capsule volume and maybe raise the initial pressure level. The latter solution requires a new setting of the valve in order to obtain the same superheat. Just to show the effect of decreasing the capsule volume, the last example has been repeated where the capsule volume has been decreased from 5 cm^3 to $1cm^3$.

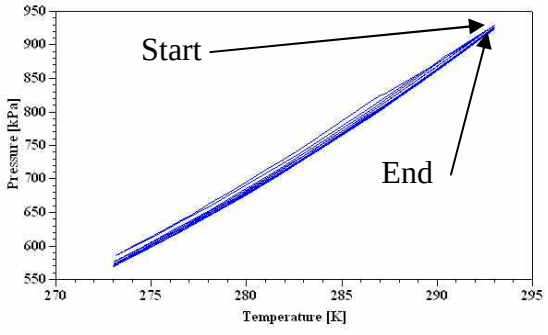

Figure 8-36: Temperature pressure curve for bulb

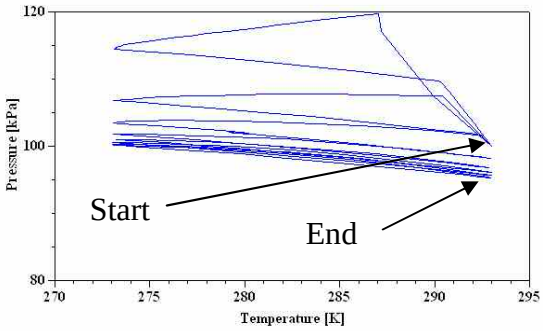

Figure 8-37: Partial pressure of nitrogen as a function of bulb temperature

Comparing Figure 8-36 with Figure 8-34 and Figure 8-37 with Figure 8-35 it can be seen that the pressure decrease is lower for the small capsule. A further decrease of the capsule will minimize the pressure decrease more. The extreme case where the capsule volume becomes only a small fraction of the total volume, the system will almost behave like a one bulb system.

9 The merged model

The two models described in chapter 7 and chapter 8 are merged to one model. Basically the output of the bulb contact model is used as input for the charge model.

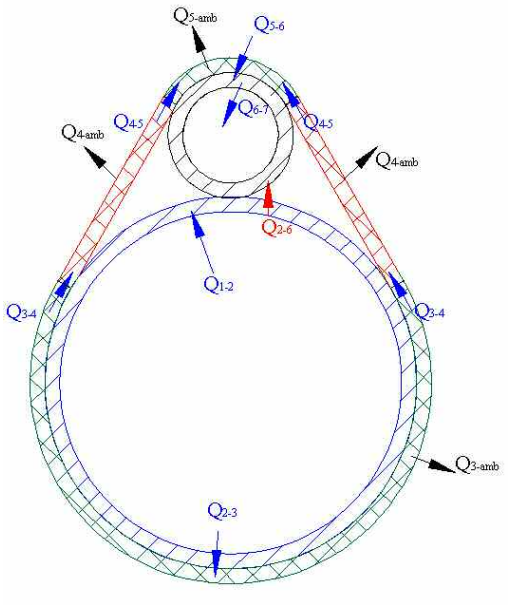

Figure 9-1: Bulb contact model

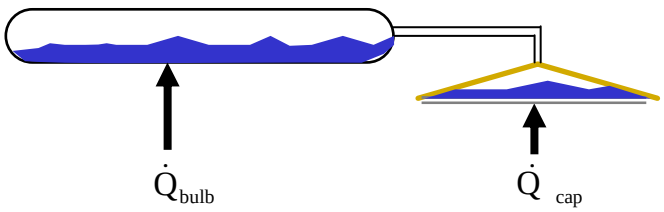

Figure 9-2: Charge model

One of the main outputs of the bulb contact model (Figure 9-1) is the heat flux $Q_{6\text{-}7}$ which is the heat flux supplied to the charge in the bulb.

In the charge model (Figure 9-2) a parameter called $\dot{Q}_{bulb}$ has to be given as input for the model. The models are combined by setting $\dot{Q}_{bulb} = Q_{6\text{-}7}$. It has also to be taken into account that $Q_{6\text{-}7}$ is dependent on the temperature inside the bulb (7-2) while the temperature inside the bulb is dependent on $Q_{6\text{-}7}$ Therefore the models can not just be coupled in series, but have to be merged into one model with a common set of equations. Figure 9-3 shows a schematic drawing of the merged model. Instead of specifying the heat flux to the bulb directly, the heat flux is now calculated based on input about geometry and materiel properties for bulb, strap and the evaporator tube.

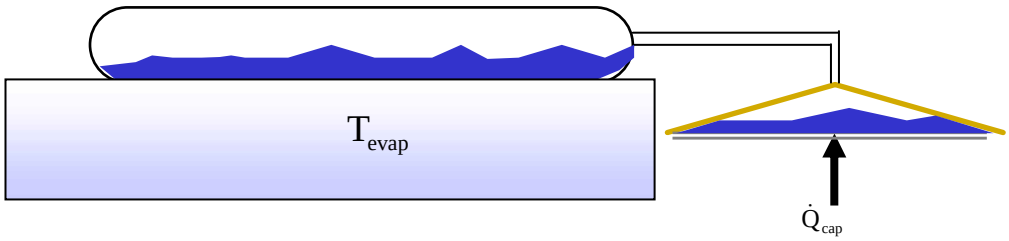

Figure 9-3: Merged model

The merged model represents more directly how the charged system of the valve is actually affected by the refrigeration system and the surroundings.

9.1 Using the merged model

The full model can be used as platform for a full TXV model. Since the main dynamics of a TXV lies in the charge, the equations for the remaining parts of the TXV can be solved statically at each time step of the merged charge model and thereby calculate the resulting opening area of the TXV.

9.1.1 Input

The input for the merged model has been spread out on 4 parameter pages.

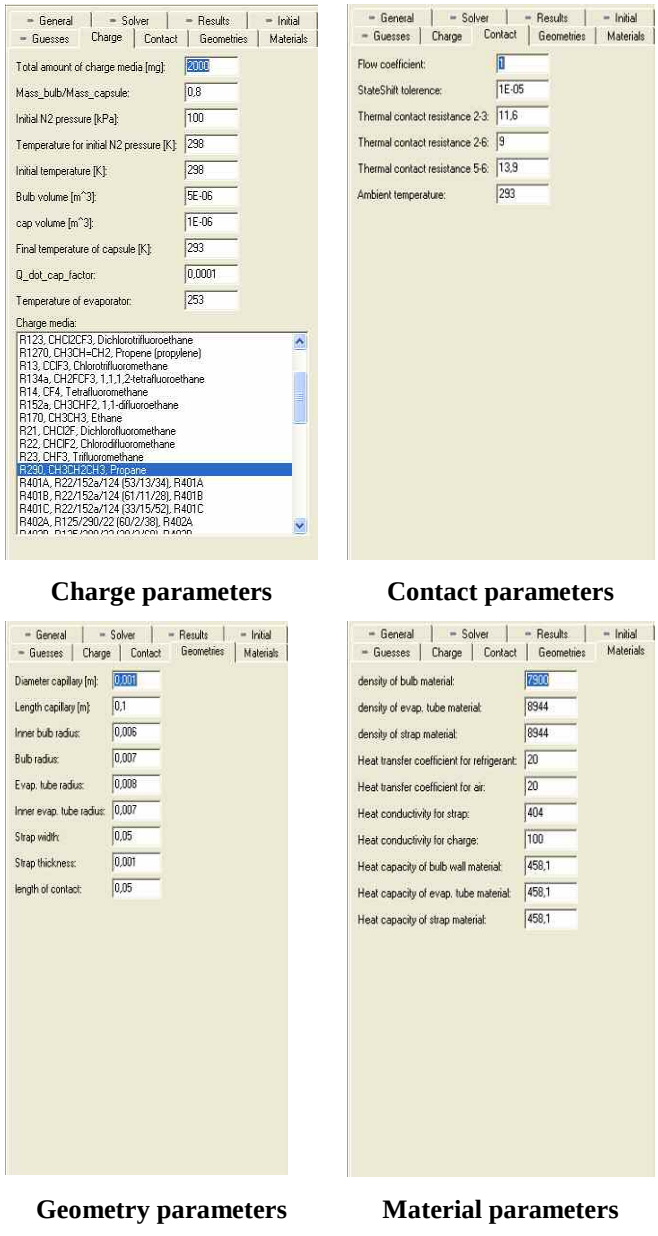

Charge parameters **Contact parameters**

Geometry parameters **Material parameters**

Figure 9-4: Input parameters for merged model

The charge parameters are almost the same as shown in Figure 8-10. The three other pages are parameters regarding the bulb contact model. And unless a different bulb or

strap design has to be evaluated, these parameters do not need to be changed. Different charges can be applied on the charge parameter page.
The Q_dot_cap_factor can only be guessed, since it is unknown. In order to avoid guessing, a model has to be developed that calculates the heat transfer to the capsule which consists of convection from the ambient and conduction from the valve body.

9.1.2 Output

The output of the model is simply any defined variable as a function of time or any other defined variable. The most interesting of course is the capsule pressure as a function of time. A typical output window is shown in Figure 9-5.

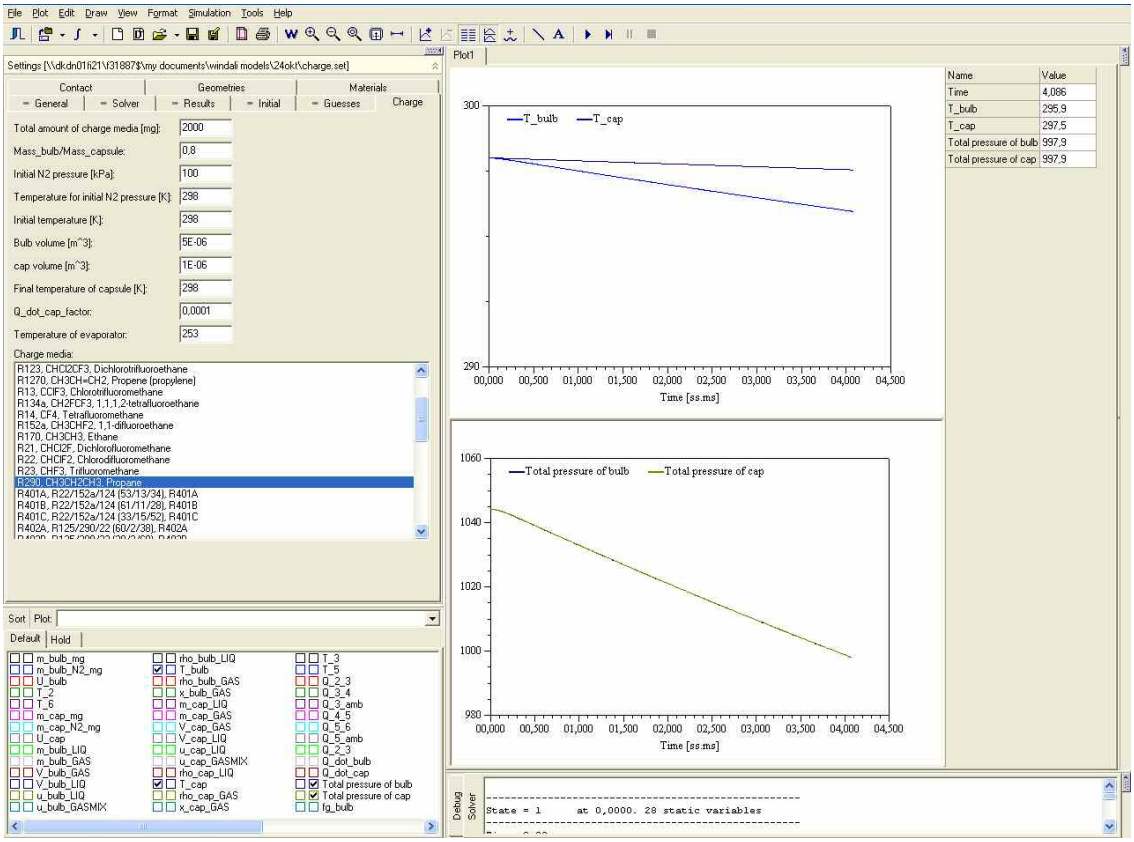

Figure 9-5: Output window for merged model

In the upper left corner the input parameters are defined. In the lower left part the variables that need to be plotted as output are selected. The middle part is the output window. The right side is a data window that is updated at every time step. All calculated data can be saved and post processed at a later time. For more information on the use of WinDali please refer to the user's manual [16].

10 Conclusions and suggestions for future work

In this thesis, a dynamic model for charges for thermostatic expansion valves has been presented. The model is able to describe phenomena that have been seen in experiments, but could not be predicted with the existing static models. The model consists of two parts. One part describes the heat transfer from the evaporator outlet to the bulb while the other describes the internal movement of mass and energy between the capsule and the bulb.
The heat transfer model calculates the temperature development over time in the charge as a result of a temperature change at the evaporator. The model can predict time constants for different charges and different geometries and materials for bulb, strap and evaporator outlet tube. The model has been verified by experiments where the time constants are predicted within an accuracy of 10 %. Furthermore it has been shown that approximately 20-30 % of the heat is transferred through the strap whereas the remaining 70-80 % is transferred through the direct contact between the bulb and the evaporator tube.
The charge model calculates the pressure of the charged system for a specified heat input. Modelling charges and keeping track of different parameters have given a better understanding of which phenomena occur in the charged system. Results that were obtained through experiments prior to this project can be explained.
It has been shown that the phenomena of loosing pressure due to the relocation of charge media and nitrogen during cyclic experiments depends strongly on the capsule volume and the bulb volume. But also other parameters like the amount of charge media and nitrogen do have some influence. Therefore the new dynamic model can be used to evaluate new combinations of bulb, capsule and charge in order to clarify whether or not the combination will be likely to loose pressure during cyclic operation.

10.1 Suggestions for future work

The very first figure of this thesis (Figure 1-1 on page 2) shows the process of the work. During development of the models presented a couple of cycles have been taken. And of course more could be taken in the future in order to improve the model further. In the following a few possible improvements will be listed.

- Use a model for capillary tubes between the two volumes instead of the pure pressure equalization in equation (8-19).
- Take into account that liquid can get into the capillary tube. Small droplets might be able to block the capillary tube and thereby limit the mass flow between the volumes.
- Calculate the heat flux from the valve body to the capsule.
- Include the thermal ballast brick that can be added to charges.
- Implement procedure for mixture charges as described in Appendix A.

Besides improving the model there is also need for effort to implement the model in a valve model and to implement the valve model in a refrigeration system model in order to be able to optimize on the whole system by changing parameters for the charge of the TXV.

11 References

1. Aguilar, J., Cäsar, R., Köhler, J., Tegethoff,W., Tischendorf, C., 2006, *Wege zur modellierung von thermostatischen Expansionsventilen*, Luft- und Kältetechnik 1-2/2006.
2. ARI standard 210/240
3. Conde, M.R., Suter, P., 1991, *A mathematical simulation model for thermostatic expansion valves*, Heat recovery systems & CHP Vol. 12, No. 3, pp271-282.
4. F-Chart software, *EES Engineering Equation solver for Microsoft Windows Operating System*, http://www.fchart.com
5. Incropera, F. P., De Witt, D. P., 1996, *Introduction to heat transfer*, John Wiley and sons, Inc., USA, 801 pages
6. James, K.A., James R.W., 1987, *Transient analysis of thermostatic expansion valves for refrigeration system evaporators using mathematical models*, Trans. Inst. M C Vol. 9 No. 4.
7. Jørgensen B., 1997, *Vedr. Blandinger af R125+R152a. Sammenligning mellem målte værdier og beregnede værdier (REFPROP)*, Danfoss internal technical report no. 97-061.
8. Kuleshov, G. G., 1984, *External interaction Equilibria in the thermodynamics of diffuse Phase Transitions of the first kind*, Russian Journal of Physical Chemistry Vol. 58, pp 2385-2396
9. Lenger, M.J., Jacobi, A.M., Hrnjak, P.S.,1998, *Superheat Stability of an evaporator and thermostatic expansion valve*, ACRC project 76.
10. Outcalt S.L., McLinden M.O., *A modified Benedict-Webb-Rubin equation of state for the thermodynamic properties of R152a (1,1- difluoroethane)*, J. Phys. Chem. Ref. Data, Vol. 25, No. 2, 1 996
11. Outcalt S.L., McLinden M.O., *Equations of state of R32 (Diflouromethane) and R125 (Pentaflouroethane)*, International journal of thermophysics, Vol. 16, No. 1, 1995
12. Patel, N. C., Teja A. S., *A new cubic equation of state for fluids and fluid mixtures*; Chemical Engineering Science Vol. 37, No. 3. pp. 463-473, 1982
13. Pedersen, J. T., 1996 *Beregning af væskevolumen som function af temperatur ved forskellige fyldningsgrader for R 160 (etylchlorid)*, Danfoss internal technical report no. 96-007
14. Raven H. F., 1995, *Automatic Control Engineering*, McGraw Hill, Singapore, 619 pages.
15. RefProp documentation, http://www.nist.gov/srd/nist23.htm
16. Skovrup M.J., *WinDali a modelling and simulation system for Microsoft window*
17. US patent No. 3,104,551, Patented Sept. 24th 1963.

A Mixture charges

In numerous applications charges are binary mixtures of substances. PVT data for these charges cannot always be found in the literature. Therefore the model preferably has to include a mixture procedure where the properties of a mixture are calculated using the pure substance properties as input. The mixture procedure presented in this appendix has been used on static models while using different software (Engineering Equation Solver (EES)) than for the final model. Therefore this procedure has to be translated from EES to WinDali before it can be implemented. The appendix is included because it shows how the mixing procedure was implemented in EES and translating it to WinDali is more or less a programming issue.
During the whole description the focus will be on the mixture of R125 (pentafluoroethane) and R152a (1,1-difluoroethane). This mixture, in different compositions, is used as charge media in numerous applications. Besides that, the method described and the software that has been developed can be used for any binary mixture and in principle be extended to mixtures of more than two components.

A.1 Property modeling

The procedure is based on the equation of state proposed by Patel and Teja [12]. The purpose is to be able to describe the properties of the mixture.

Following structure is followed:

- Fit parameters for equation of state for both of the pure substances.
- Find $Cp^0(T)$ for both substances
- Apply mixing rules to find the combined equation of state
- Calculate properties.

A.2 Fit parameters for equation of state for pure substances

In order to apply Patel and Teja's equation of state two parameters have to be calculated. In the following, these will be explained in detail.

A.2.1 The Patel/ Teja equation of state

Patel and Teja have proposed following cubic equation of state:

$$P = \frac{RT}{v-b} - \frac{a[T]}{v(v+b)+c(v-b)} \qquad \textbf{(A-1)}$$

where

$$a[T] = \Omega_a \left(\frac{R^2 T_c^2}{P_c} \right) \alpha[T_R] \qquad \textbf{(A-2)}$$

$$b = \Omega_b \left(\frac{RT_c}{P_c} \right) \quad \textbf{(A-3)}$$

$$c = \Omega_c \left(\frac{RT_c}{P_c} \right) \quad \textbf{(A-4)}$$

$$\Omega_a = 3\zeta_c^2 + 3(1-2\zeta_c)\Omega_b + \Omega_b^2 + 1 - 3\zeta_c \quad \textbf{(A-5)}$$

$$\Omega_b^3 + (2-3\zeta_c)\Omega_b^2 + 3\zeta_c^2\Omega_b - \zeta_c^3 = 0 \quad \textbf{(A-6)}$$

$$\Omega_c = 1 - 3\zeta_c \quad \textbf{(A-7)}$$

$$\alpha[T_R] = \left[1 + F(1 - T_R^{1/2})\right]^2 \quad \textbf{(A-8)}$$

F and ζ_c are determined for a large number of pure substances. But only a few of the listed substances are refrigerants. Therefore these two parameters have to be determined by fitting to experimental PVT data. Due to lack of such data, RefProp 6,0 will be used to generate these data. The data generated by RefProp are based on a 32 parameter Modified Benedict-Webb-Rubin equation of state [10] and [11], which has been fitted to an extensive set of experimental data. Therefore the benchmark for the data fitting will be the values generated by RefProp.

A.2.2 Evaluation of F and ζ_c:

In order to evaluate F and ζ_c following procedure is followed.

- Input acentricfactor, Critical temperature and critical pressure.
- ζ_c and F are initially determined using the acentricfactor ω in (A-9) and (A-10).

$$F = 0{,}452413 + 1{,}30982 \cdot \omega - 0{,}295937 \cdot \omega^2 \quad \textbf{(A-9)}$$

$$\zeta_c = 0{,}329032 - 0{,}076799 \cdot \omega + 0{,}0211947 \cdot \omega^2 \quad \textbf{(A-10)}$$

- Ω_a, Ω_b, Ω_c, a, b, c can be calculated using (A-2)- (A-8).
- At vapour/liquid equilibrium the fugacity of the vapour f^v has to be equal to the fugacity of the liquid f^l. The fugacity for both phases can be found by:

$$\ln\left(\frac{f}{P}\right) = Z - 1 - \ln(Z - B) + \frac{a}{2RTN} \ln\left(\frac{Z+M}{Z+Q}\right) \quad \textbf{(A-11)}$$

$$B = \frac{bP}{RT} \quad \textbf{(A-12)}$$

$$M = \left(\frac{b+c}{2} - N\right)\frac{P}{RT} \quad \textbf{(A-13)}$$

$$N = \left[bc + \left(\frac{b+c}{2}\right)^2\right]^{1/2} \quad \textbf{(A-14)}$$

$$Q = \left(\frac{b+c}{2} + N\right)\frac{P}{RT} \quad \textbf{(A-15)}$$

$$Z = \frac{Pv}{RT} \quad \textbf{(A-16)}$$

The calculated pressures and volumes can be compared with measured data at the particular temperature, and by running through a number of temperatures along the saturation curve and minimizing the difference between $Property_{calc}$ and $Property_{meassured}$, a value of F and ζ_c can be found.

These values can then be inserted in (A-1) and calculated data can be compared with measured data.

A.2.3 Results:

In order to validate the calculations, F and ζ_c were calculated for propane, which is one of the substances for whose F and ζ_c values are presented in [12].
Table A-1 shows the parameters calculated compared to the values given in [12] for propane.

	F	ζ_c
[12]	0,648049	0,317
Calculated	0,6451	0,3171
% deviation	-0,455	0,032

Table A-1: Calculated parameters and table values

As shown in Table A-1, there are small deviations. This could be because the calculations not are based on the exact same set of data.

A.2.4 Applying the method for R125 and R152a

Having verified that the calculations give results close to the values in [12], the calculations are now performed on the substances of interest, R125 and R152a.
Figure A-1and Figure A-2 shows the calculated (Black curve) and the experimental (Blue curve) pressure for these two substances.
Figure A-3 and Figure A-4 show the residual $res = \frac{P_{test} - P_{calc}}{P_{test}}$ for R125 and R152a respectively.

	F	ζ_c
R125	0,8206	0,3081
R152a	0,7901	0,3102

Table A-2: Calculated parameters for R125 and R152a

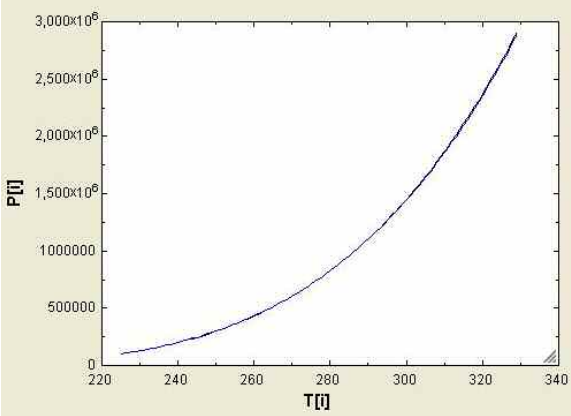

Figure A-1: Calculated and experimental pressure for R125

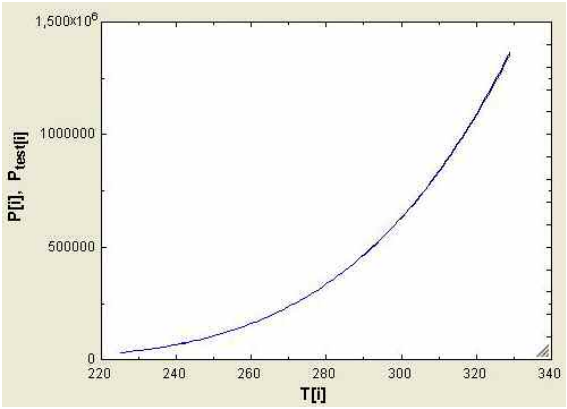

Figure A-2: Calculated and experimental pressure for R152a

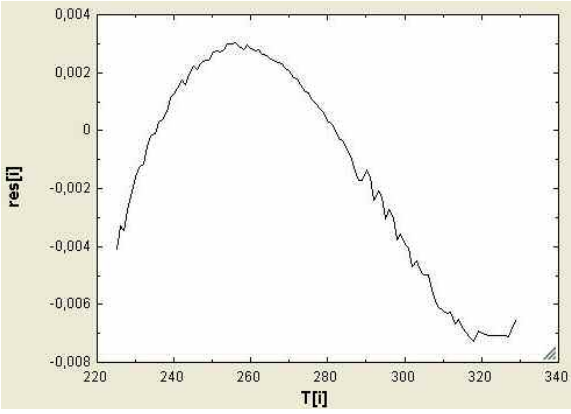

Figure A-3: Residual pressure for R125

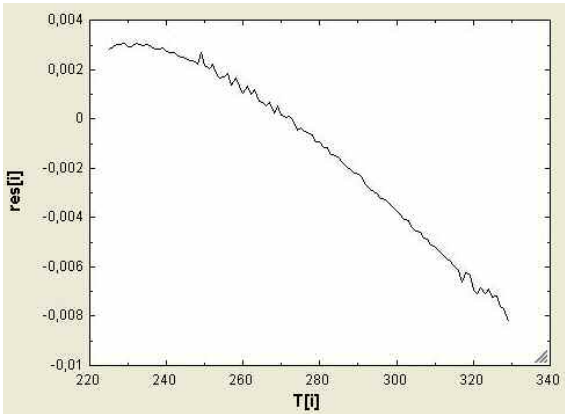

Figure A-4: Residual pressure for R152a

A.3 Mixing rules

In order to combine the two equations of state obtained, following mixing rules have to be applied.

$$a_m = \sum_i \sum_j x_i x_j a_{ij}$$
$$b_m = \sum_i x_i b_i \qquad \textbf{(A-17)}$$
$$c_m = \sum_i x_i c_i$$

$$a_{ij} = \xi_{ij}(a_{ii}a_{jj})^{1/2} \qquad \textbf{(A-18)}$$

Where i and j denote the substance number.

ξ_{ij} is the binary interaction coefficient which can only be determined by comparing calculated to measured properties. If no such data are available, ξ_{ij} is set to 1.
Having calculated a_m, b_m and c_m, these can be used in (A-1) and the equation of state applies for the mixture.

The degree of freedom for the mixture can be determined by the phase rule:

$$F = 2 - \pi + N \qquad \textbf{(A-19)}$$

Where:
π: number of phases
N: number of chemical species

For a binary mixture where two phases exist, the number of degrees of freedom is 2. This means that the state of the mixture can be determined by fixing only two independent parameters. This could typically be temperature and the composition of the liquid phase. In order to ensure equilibrium, the fugacity of each component has to be the same for both phases of the component. The fugacity of a component in a mixture can be determined by:

$$RT\ln\left(\frac{f_i}{P}\right) = -RT\ln(Z-B) + RT\left(\frac{b_i}{v-b_m}\right) - \frac{\sum x_j a_{ij}}{d}\ln\left(\frac{Q+d}{Q-d}\right)$$
$$+\frac{a(b_i+c_i)}{2(Q^2-d^2)} + \frac{a}{8d^3}\left(c_i(3b_m+c_m)+b_i(3c_m+b_m)\right)\left(\ln\left(\frac{Q+d}{Q-d}\right) - \frac{2Qd}{Q^2-d^2}\right) \qquad \textbf{(A-20)}$$

$$Z = \frac{Pv}{RT}$$
$$Q = v + \frac{b_m + c_m}{2}$$
$$B = \frac{b_m P}{RT}$$
$$d = \sqrt{b_m c_m + \frac{(b_m + c_m)^2}{4}}$$

(A-21)

A.4 Calculate properties

With the equation of state and $Cp^0(T)$ known, the thermodynamic properties such as enthalpy and entropy can be calculated. The general equations for pure substances are

$$dH = C_p dT + \left[V - T\left(\frac{\partial V}{\partial T}\right)_p \right] dP$$
$$dS = C_p dT - \left(\frac{\partial V}{\partial T}\right)_p dP$$

(A-22)

For practical use, the calculation of changes (From a defined reference state to the desired state) in enthalpy and entropy are calculated in three steps. (Figure A-5)

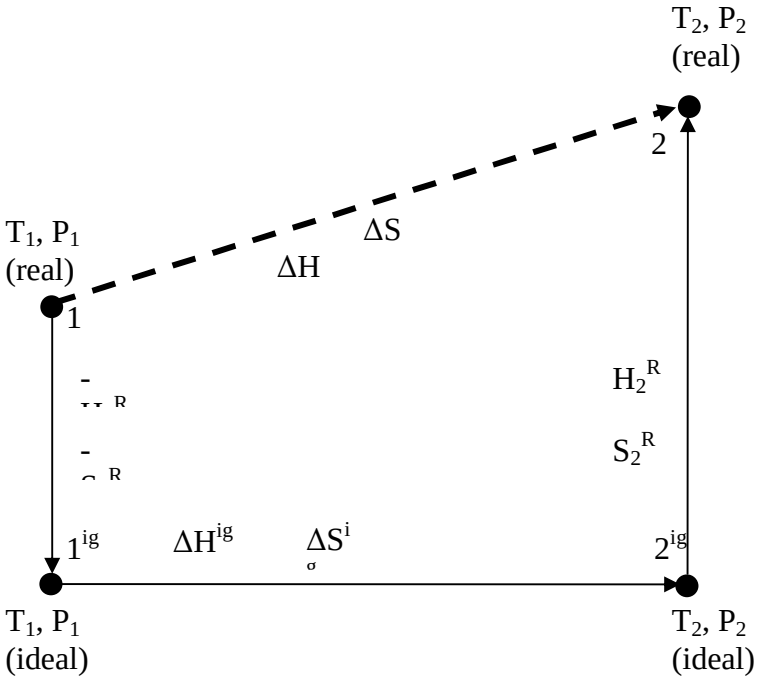

Figure A-5: The three steps for calculation of property changes

At first the substance undergoes a hypothetical process to reach an ideal gas state at the temperature of the reference state. The enthalpy and entropy difference between the

reference state and the ideal gas state are found by (A-23) and (A-24) inserting the reference conditions.

$$H - H^0 = RT(Z-1) - \left(T\frac{\partial a}{\partial T} - a \right)\left[\frac{1}{2N} \ln\left(\frac{Z+M}{Z+Q} \right) \right] \quad \textbf{(A-23)}$$

$$S - S^0 = -R \cdot \ln\left(\frac{P}{Z-B} \right) - \frac{\partial a}{\partial T}\left[\frac{1}{2N} \ln\left(\frac{Z+M}{Z+Q} \right) \right] \quad \textbf{(A-24)}$$

Next step is to bring the substance to the ideal state at the wanted temperature. For this, the ideal gas specific heat C_p^0 is needed. The temperature dependent ideal specific heat is determined by (A-25) for R152a [10] and (A-26) for R125 [11]

$$\frac{Cp^0}{R} = c_0 + c_1 T_r + c_2 T_r^2 + c_3 T_r^3$$
$$c_0 = 3{,}354951$$
$$c_1 = 4{,}245301 \quad \textbf{(A-25)}$$
$$c_2 = 3{,}735248$$
$$c_3 = -1{,}608254$$

$$\frac{Cp^0}{R} = c_0 + c_1 T_r + c_2 T_r^2 + c_3 T_r^3$$
$$c_0 = 3{,}111514$$
$$c_1 = 10{,}582115 \quad \textbf{(A-26)}$$
$$c_2 = -1{,}843797$$
$$c_3 = 0{,}019273$$

Third and last step is to determine the departure from the now reached ideal state and the final real state. Here (A-23) and (A-24) are used again, this time inserting the final state conditions.

The total property change is the sum of the changes of the three steps.

$$\Delta property = -\Delta process\,1 + \Delta process\,2 + \Delta process\,3 \quad \textbf{(A-27)}$$

The total change in enthalpy and entropy are therefore defined by (A-28) and (A-29) respectively.

$$\Delta H = -\left(RT_{ref}(Z-1) - \left(T_{ref}\frac{\partial a}{\partial T} - a \right)\left[\frac{1}{2N} \ln\left(\frac{Z+M}{Z+Q} \right) \right] \right)$$
$$+ R\left(c_0 + c_1 T_{r\_state-ref} + c_2 T_{r\_state-ref}^2 + c_3 T_{r\_state-ref}^3 \right) \quad \textbf{(A-28)}$$
$$+ \left(RT_{state}(Z-1) - \left(T_{state}\frac{\partial a}{\partial T} - a \right)\left[\frac{1}{2N} \ln\left(\frac{Z+M}{Z+Q} \right) \right] \right)$$

$$S - S^0 = R \cdot \ln\left(\frac{P}{Z-B}\right) - \frac{\partial a}{\partial T}\left[\frac{1}{2N}\ln\left(\frac{Z+M}{Z+Q}\right)\right] + R\left(c_0 + c_1 T_r + c_2 T_r^2 + c_3 T_r^3\right) - R \cdot \ln\left(\frac{P}{Z-B}\right) - \frac{\partial a}{\partial T}\left[\frac{1}{2N}\ln\left(\frac{Z+M}{Z+Q}\right)\right] \quad \textbf{(A-29)}$$

Where:

$$\frac{\partial a}{\partial T} = \Omega_a R^2 T_c \left(-1 - F + F\sqrt{\frac{T}{T_c}}\right)\frac{F}{P_c\sqrt{\frac{T}{T_c}}} \quad \textbf{(A-30)}$$

In order to determine enthalpy for binary mixtures, following method has been used:

Both pure substances undergo the two first steps mentioned above.
At ideal conditions the enthalpy of the mixture calculated as the concentration weighted sum of the pure substance enthalpies. For entropy calculations, the ideal mixing entropy S_{mix} is added. $S_{mix} = -R\left(x_1 \ln(x_1) + x_2 \ln(x_2)\right)$
The departure for the mixture between ideal and real fluid state is calculated. For binary mixtures (A-30) becomes (A-31).

$$\frac{\partial a_m}{\partial T} = -x_1^2 \omega_{a\_1} R^2 \frac{T_{c\_1}}{P_{c\_1}}\sqrt{\alpha_1}\frac{F_1}{\sqrt{\frac{T}{T_{c\_1}}}} + x_1\xi_{12}\frac{x_2}{\sqrt{\omega_{a\_1}R^4\frac{T_{c\_1}^2}{P_{c\_1}}\alpha_1\omega_{a\_2}\frac{T_{c\_2}^2}{P_{c\_2}}\alpha_2}}\left[-\omega_{a\_1}R^4\frac{T_{c\_1}}{P_{c\_1}}\sqrt{\alpha_1}\omega_{a\_2}\frac{T_{c\_2}^2}{P_{c\_2}}\alpha_2\frac{F_1}{\sqrt{\frac{T}{T_{c\_1}}}} - \omega_{a\_1}R^4\frac{T_{c\_1}^2}{P_{c\_1}}\alpha_1\omega_{a\_2}\frac{T_{c\_2}}{P_{c\_2}}\sqrt{\alpha_2}\frac{F_2}{\sqrt{\frac{T}{T_{c\_2}}}}\right] - x_2^2\omega_{a\_2}R^2\frac{T_{c\_2}}{P_{c\_2}}\sqrt{\alpha_2}\frac{F_2}{\sqrt{\frac{T}{T_{c\_2}}}} \quad \textbf{(A-31)}$$

A.5 Verification of mixture rules

In order to verify the results, the calculated saturation pressures have been compared to measurements made at Danfoss prior to this project. [7]

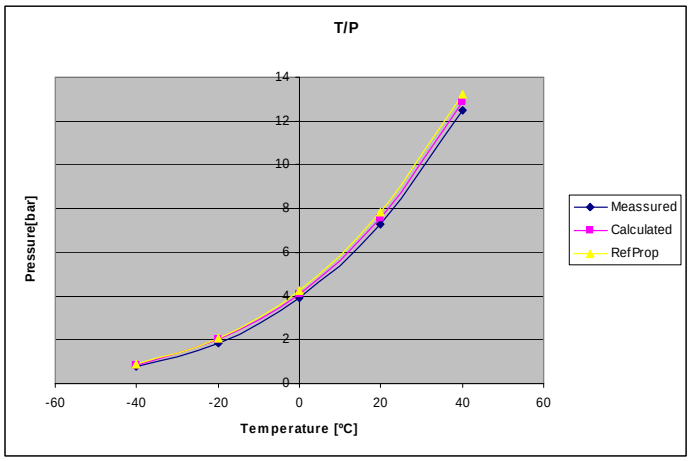

Figure A-6: Saturation pressure for 50/50 mixture of R125/R152a

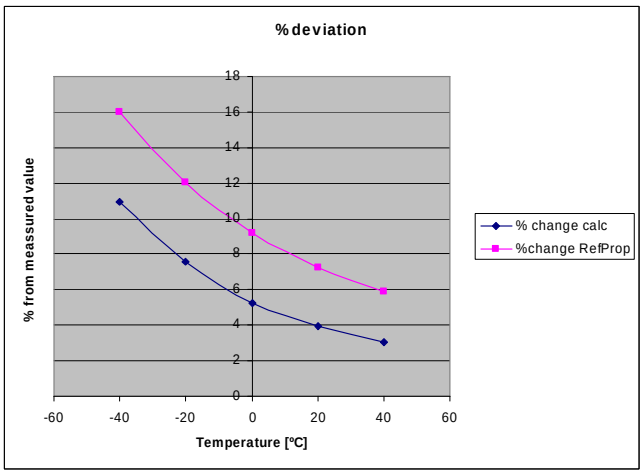

Figure A-7: Deviation between calculated and measured saturation pressures and values from RefProp for 50/50 mixture of R125/R152a

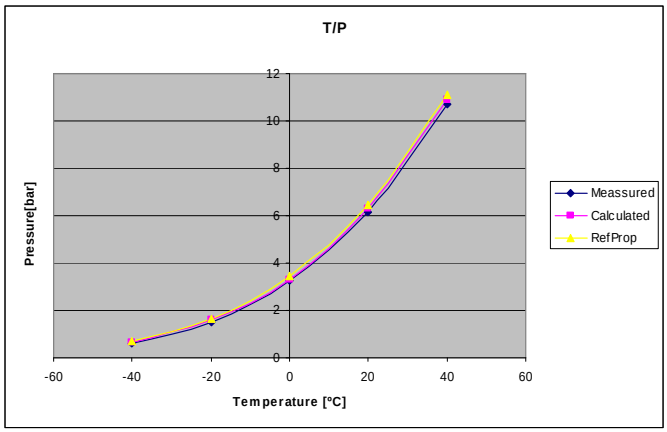

Figure A-8: Saturation pressure for 25/75 mixture of R125/R152a

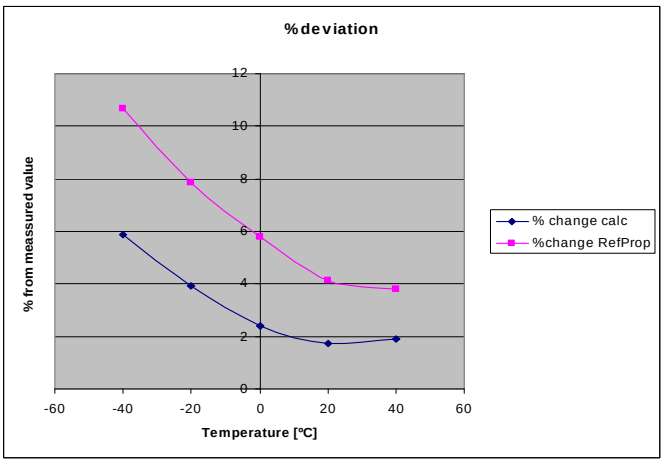

Figure A-9: Deviation between calculated and measured saturation pressures and values from RefProp for 25/75 mixture of R125/R152a

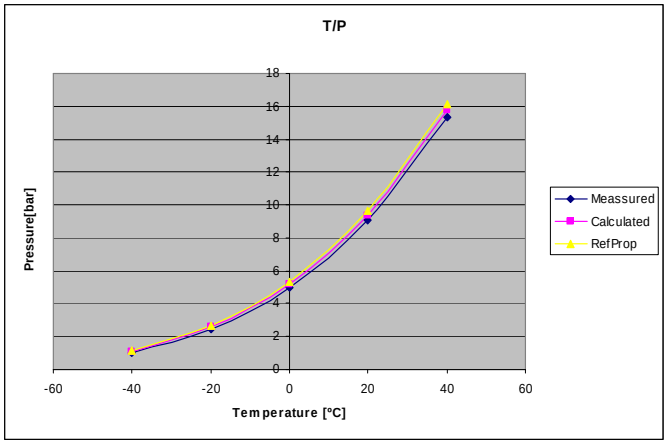

Figure A-10: Saturation pressure for 50/50 mixture of R125/R152a

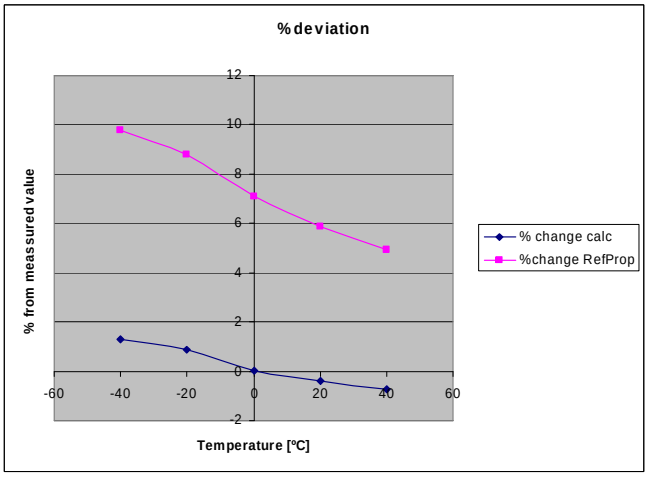

Figure A-11: Deviation between calculated and measured saturation pressures and values from RefProp for 50/50 mixture of R125/R152a

As Figure A-6 - Figure A-11 show the saturation pressures calculated by the model developed, are closer to the test results than Refprop. In all calculations the binary interaction coefficient ξ_{ij} has been set to 1. If ξ_{ij} has to be determined a more extensive test series has to be performed.

A.6 Conclusion on the modelling of mixture charges

Using the equation of state proposed by Patel and Teja [12] on the mixture of R125 and R152a the saturation pressure can be within satisfactory accuracy. Therefore, the procedure presented here should be implemented in the charge model.